



NATIONAL AND KAPODISTRIAN UNIVERSITY OF ATHENS
SCHOOL OF SCIENCE
DEPARTMENT OF CHEMISTRY
GRADUATE PROGRAM «CHEMISTRY»
SPECIALIZATION «ANALYTICAL CHEMISTRY – QUALITY ASSURANCE»

MASTER THESIS

Degradation of Cyindrospermopsin in water using Ultrasound

TOULOUPI MYRTO - FOTEINI
CHEMIST

ATHENS

JULY 2020

MASTER THESIS

Degradation of Cyindrospermopsin in water using Ultrasound

TOULOUPI MYRTO - FOTEINI

REGISTRATION NUMBER: 181214

SUPERVISING PROFESSOR:

Nikolaos S. Thomaidis, Professor NKUA

THREE-MEMBER CONSULTATIVE COMMITTEE:

Dr. Anastasia Hiskia, Research Director
Dr. Erasmia Bizani, Laboratory Teaching Staff
Nikolaos S. Thomaidis, Professor NKUA

DEFENDING DATE 14/07/20

Abstract

Cylindrospermopsin (CYN) is a cyanobacterial toxin which has been shown to be cytotoxic, dermatotoxic, genotoxic and hepatotoxic and poses a potential threat to humans and ecosystems. Therefore, the development of effective treatment processes for the degradation of CYN in surface water presents increasing scientific interest. Ultrasonication offers an alternative treatment process, involving the formation of highly Reactive Oxygen Species (ROS). The objectives of this study were a) to set-up an ultrasonication apparatus for the degradation of organic compounds in small reaction volumes, b) to optimize the operational parameters and to study their effect in the production of oxidative species using chemical dosimetry, c) to effectively degrade CYN using ultrasound and to study the kinetics of the process under various conditions, c) to develop an analytical method using HPLC-PDA in order to monitor the degradation of CYN, e) to identify the transformation products of CYN during ultrasound degradation using LC-MS/MS.

A sonolytical device operating at 850 kHz with a small-volume glass reactor was used. The position of reactor and operational parameters were optimized for the degradation of small volumes of solutions. Its optimal position was determined using 2,4-DCP as a model compound. Also, Fricke and Coumarin (COU) dosimeters were used to determine the Reactive Oxygen Species (ROS) and the hydroxyl radicals ($\text{HO}\cdot$) produced, respectively. A fast and reliable HPLC-PDA method was developed for the monitoring of CYN degradation. CYN degradation was performed under several power intensities, pH and initial concentrations. The degradation followed the first-order kinetic model with a maximum reaction rate of 0.57 mM s^{-1} observed at the highest power intensity and pH 5.8. The effect of the presence of inorganic ions (as bottled water) and organic matter (as humic acids) was also examined and they induced minimum hindrance on the degradation. A volatile (tert-butyl alcohol, TBA) and an ionic (terephthalate, TA) scavenger were used to determine the location of CYN degradation in the mixture of sonolytically-produced bubbles and bulk solution. 58 % of CYN is degraded in the bulk solution, 21% in the surface of the bubbles and 21% was attributed to pyrolysis/hydrolysis. Finally, the transformation products (TPs) of CYN were determined using an LC-MS/MS method. 20 TPs were identified.

SUBJECT AREA: Analytical Chemistry, Degradation of water pollutants

KEYWORDS: Cylindrospermopsin, Ultrasonication, Transformation Products, HPLC-PDA, LC-MS/MS

Περίληψη

Η κυλινδροσπερμωψίνη (CYN) είναι μία κυανοτοξίνη με δερματοτοξική, κυτταροτοξική και ηπατοτοξική δράση και αποτελεί πιθανή απειλή για τον άνθρωπο και τα οικοσυστήματα. Η ανάπτυξη αποτελεσματικών διεργασιών επεξεργασίας για τη διάσπαση της CYN στα επιφανειακά ύδατα παρουσιάζει αυξανόμενο επιστημονικό ενδιαφέρον. Η ηχόλυση αποτελεί μια εναλλακτική διαδικασία επεξεργασίας για την αποικοδόμηση των οργανικών ρύπων, που περιλαμβάνει τον σχηματισμό δραστικών μορφών οξυγόνου (ROS). Οι στόχοι αυτής της μελέτης ήταν α) η εγκατάσταση μιας συσκευής υπερήχων για την αποικοδόμηση των οργανικών ενώσεων σε μικρούς όγκους αντίδρασης, β) η βελτιστοποίηση των λειτουργικών παραμέτρων της συσκευής και η μελέτη της επίδρασής τους στην παραγωγή οξειδωτικών ειδών χρησιμοποιώντας χημική δοσιμετρία, γ) η αποτελεσματική διάσπαση της CYN χρησιμοποιώντας υπερήχους, η μελέτη της κινητικής και η βελτιστοποίηση της διεργασίας κάτω από διαφορετικές συνθήκες, δ) η ανάπτυξη αναλυτικής μεθόδου σε HPLC-PDA για την παρακολούθηση της διάσπασης της CYN, ε) η ανίχνευση των προϊόντων μετασχηματισμού της CYN χρησιμοποιώντας LC-MS/MS.

Μια πειραματική συσκευή υπερήχων με αντιδραστήρα γυαλιού μικρού όγκου συναρμολογήθηκε και χρησιμοποιήθηκε. Η θέση του αντιδραστήρα και οι λειτουργικές παράμετροι της συσκευής βελτιστοποιήθηκαν για την επεξεργασία μικρού όγκου διαλυμάτων. Η βέλτιστη θέση του αντιδραστήρα προσδιορίστηκε χρησιμοποιώντας την 2,4-DCP ως ένωση πρότυπο. Επίσης, χρησιμοποιήθηκε χημική δοσιμετρία με Fricke όπως και με κουμαρίνη (COU). Επιπλέον, αναπτύχθηκε μια γρήγορη και αξιόπιστη μέθοδος HPLC-PDA για την παρακολούθηση της διάσπασης της CYN. Η αποικοδόμηση της CYN πραγματοποιήθηκε υπό διάφορες εντάσεις ισχύος, pH και αρχικές συγκεντρώσεις. Η κινητική της διάσπασης ακολούθησε τον μοντέλο πρώτης τάξης. Ο μέγιστος ρυθμός διάσπασης ήταν 0.57 mM s^{-1} στην υψηλότερη ισχύ λειτουργίας και pH 5.8. Προσδιορίστηκε η περιοχή της αποικοδόμησης CYN στο μίγμα ηχολυτικά παραγόμενων φυσαλίδων και διαλύματος. 58% της CYN αποδομείται στο διάλυμα, 21% στην επιφάνεια των φυσαλίδων και 21% αποδόθηκε σε πυρόλυση / υδρόλυση. Πραγματοποιήθηκε μελέτη προσδιορισμού των προϊόντων μετασχηματισμού (TPs) της CYN με τη μέθοδο LC-MS/MS, και ταυτοποιήθηκαν 20 εξ αυτών.

ΘΕΜΑΤΙΚΗ ΠΕΡΙΟΧΗ: Αναλυτική Χημεία, Διάσπαση ρύπων

ΛΕΞΕΙΣ ΚΛΕΙΔΙ: Κυλινδροσπερμωψίνη, Ηχόλυση, Προϊόντα διάσπασης, HPLC-PDA, LC-MS/MS

*'To my schooldays
chemistry teachers'*

Acknowledgements

I would like to express my deep gratitude to Professor N. S. Thomaidis, my supervisor from Analytical Chemistry Lab, NKUA for giving me the opportunity to complete this master thesis at the NCSR Demokritos and to Dr A. Hiskia, my research supervisor from Laboratory of Photo-Catalytic Processes and Environmental Chemistry , INN, NCSR Demokritos, for the selection of the topic and the insightful guidance, enthusiastic encouragement and useful comments and input to this research work. I would also like to thank Dr. T. Kaloudis from EYDAP S.A. for his valuable and constructive suggestions during the development of this work.

My special thanks are for my co-supervisors, Dr. E. Bizani from NKUA and Dr. C. Christoforidis from NCSR Demokritos for their guidance, support and their willingness to give their time so generously throughout the planning and development of this master thesis.

I would also like to extend my thanks to all of the lab members of the Laboratory of Photo-Catalytic Processes and Environmental Chemistry, INN NCSR Demokritos for their support and their friendship.

Finally, I wish to thank my parents and my brother for their support and encouragement throughout my study.

Contents

Abstract	7
Περίληψη	8
Acknowledgements	10
Contents	11
List of Figures	15
List of Tables	18
List of Chromatograms	19
1 Cyanotoxins	21
1.1 Introduction	21
1.2 Cyanobacterial blooms	21
1.2.1 Occurrence	21
1.2.2 Traits involved in blooms development.....	22
1.2.3 Problems caused by blooms.....	22
1.3 Cyanotoxins.....	23
1.3.1 Microcystins and Nodularins	26
1.3.2 Saxitoxins.....	26
1.4 Cylindrospermopsin	26
1.4.1 Chemistry.....	27
1.4.2 Toxicity.....	29
1.4.3 Global levels of CYN in water.....	29
1.4.4 International legislation and guidelines	31
2 Removal of CYN using oxidative degradation	33
2.1 Introduction	33
2.2 Advanced oxidation processes (AOPs).....	33

2.2.1	Radiation	33
2.2.2	Photolysis and Photocatalysis	34
2.2.3	Fenton reactions	36
2.2.4	Ozonation	36
2.2.5	Sonolysis	37
2.3	Previous studies on CYN degradation using AOPs	37
2.4	Transformation Products of CYN using AOPs	39
3	Sonolysis	43
3.1	Introduction	43
3.2	Principle of the method	44
3.3	Reaction zones.....	46
3.4	Parameters affecting production of reactive species.....	47
3.4.1	Bubble Dynamics.....	47
3.4.2	Sonication Power	47
3.4.3	Ultrasonic Frequency	47
3.4.4	Dissolved Gasses	48
3.4.5	Ambient Temperature	48
3.4.6	Ambient Pressure	49
3.4.7	Solvent	49
3.5	Types of Reactors.....	49
3.6	Advantages and applications of sonolysis.....	50
3.7	Dosimetry of the ROS-producing system	51
3.7.1	Coumarin.....	52
3.7.2	Fricke solution	52
3.7.3	Terephthalic Acid.....	53
4	Analytical methods for the determination of CYN and its TPs	55

4.1	High performance Liquid Chromatography (HPLC)	55
4.1.1	Principle of the method	55
4.1.2	Liquid Chromatography types	55
4.1.3	System components	56
4.2	Mass Spectrometry	59
4.2.1	General information on mass spectrometric techniques	59
4.2.2	Instrumentation	60
4.2.3	Tandem Mass Spectrometry (MS/MS)	62
4.3	Analytical Determination of CYN	62
5	Scope of this study	63
6	Experimental procedure	65
6.1	Materials and methods	65
6.1.1	Reagents	65
6.1.2	Apparatus and Devices	65
6.1.3	Instrumentation	66
6.2	Standard solutions preparation	67
6.3	Analytical Method Development	67
6.3.1	Calibration curve	68
6.3.2	Repeatability	68
6.3.3	Limit of Detection & Limit of Quantitation	68
6.4	Sonolytical device description	69
6.4.1	Full extent and small-scale device	69
6.5	Optimization of Ultrasonic Reactor	69
6.5.1	Initial operation check	69
6.5.2	Dosimetry	70
6.6	Experiments of CYN degradation	71

6.6.1	Kinetics of CYN degradation.....	71
6.6.2	Localization.....	71
6.7	Determination of CYN.....	72
6.7.1	Chromatographic conditions for degradation monitoring.....	72
6.7.2	Mass spectrometry parameters for determination of transformation products	72
7	Results and Discussion	73
7.1	Method development for the chromatographic determination of CYN	73
7.1.1	Column Selection.....	73
7.1.2	Calibration Curve.....	78
7.1.3	Repeatability	79
7.1.4	LOD-LOQ.....	80
7.2	Optimization of Ultrasonic Reactor	81
7.2.1	Initial operation check.....	81
7.2.2	Chemical Dosimetry	83
7.3	CYN sonolytic degradation.....	88
7.3.1	Effect of ultrasonication power.....	88
7.3.2	pH effect.....	90
7.3.3	Effect of CYN initial concentration.....	91
7.3.4	Application in real water matrices	92
7.3.5	Presence of Humic Acids.....	93
7.4	Localization of CYN reaction in the sonication solution.....	96
7.5	Detection and structure elucidation of transformation products using Mass Spectrometry	98
8	Conclusions	113
	Appendix	117
9	References	125

List of Figures

Figure 1-1: Chemical structures of CYN (A), 7-deoxy-CYN (B) and 7-epi-CYN.	27
Figure 1-2: CYN's dominant form at pH 9.	28
Figure 2-1: Photoinduced process on semiconductors surfaces [73].	35
Figure 3-1: Sound frequencies Spectrum [89].	43
Figure 3-2: Schematic presentation of cavitation [94].	45
Figure 3-3: Bubble zones.	46
Figure 3-4: Type of reactors [94]. Type of reactors [94] A) bath system for indirect sonicationB) bath system for direct sonicationC) probe system.	50
Figure 3-5: Terephthalic Acid distribution.	53
Figure 4-1: HPLC basic equipment [146].	56
Figure 4-2: UV-vis reactor layout [145].	58
Figure 4-3: Layout of a PDA detector [150].	59
Figure 4-4: Layout of a Quadrupole (Q) [147].	61
Figure 6-1: CYN's spectrum.	67
Figure 6-2: Apparatus used for experimental procedure.	69
Figure 7-1: Calibration curve with concentrations range from 50 to 1000 $\mu\text{g L}^{-1}$	78
Figure 7-2: Degradation of 2,4-DCP in relation to irradiation time at different distances from the transducer ($C_0=1$ mM, 5 mL volume & 250 mL surrounding water. Acoustic power 100% of the nominal).....	82

Figure 7-3: Degradation of 2,4-DCP after several irradiation time at different horizontal positions (Co=1 mM, 5 mL volume & 250 mL surrounding water. Acoustic power 100% of the nominal).	82
Figure 7-4: Concentration of Fe ³⁺ produced under different operation sonication powers (5mL solution volume & 250 mL surrounding water, 1 cm distance from the transducer). ...	84
Figure 7-5: Produced Fe ³⁺ under different sonication power after 15 minutes of sonication (5 mL solution volume & 250 mL surrounding water, 1 cm distance from the transducer).....	84
Figure 7-6: Effect of the volume of water on the amount of Fe ³⁺ produced (5 mL solution volume , 100% nominal acoustic power, 1 cm distance from the transducer).....	85
Figure 7-7: Effect of the distance from the transducer (5 mL solution volume & 250 mL surrounding water, 100% nominal acoustic power).	86
Figure 7-8: Concentration of the produced 7-OH-COU vs concentration of the COU degraded.	88
Figure 7-9: Effect of power intensity on CYN's degradation (5 mL CYN 1 mg/L, surrounding water 250 mL, pH=5.8).....	89
Figure 7-10: pH effect on CYN's degradation (5 mL CYN 1mg L ⁻¹ , 250 mL surrounding water, 100% nominal sonication power).	90
Figure 7-11: CYN's microspecies distribution under different pH values.....	91
Figure 7-12: Initial concentration Effect during CYN's degradation (5 mL CYN, 250 mL surrounding water, 100% nominal sonication power)..	91
Figure 7-13: CYN's degradation under different water matrices (5 mL CYN 1mg L ⁻¹ , 250 mL surrounding water, 100% nominal sonication power).....	92
Figure 7-14: Degradation of CYN in presence of Humic Acids (5 mL CYN 1 mg L ⁻¹ , 250 mL surrounding water, 100% nominal sonication power).	94
Figure 7-15: Degradation of CYN in presence of TA and TBA (5mL CYN 1mg L ⁻¹ , 250 mL surrounding water, 100% nominal sonication power).	96
Figure 7-16: Reaction zones.	97
Figure 7-17: TPs formation (higher concentrations).	106
Figure 7-18: TPs formation (lower concentrations).....	106

Figure A-8-1: Spectrum of the produced Fe^{3+} after several sonication times (5 mL Fricke solution, 250 mL surrounding water, 100% nominal sonication power)..... 117

Figure A-2: Spectrum of the produced 7-OH-COU after several sonication times (1 mM COU 5 mL, 250 mL surrounding water, 100% nominal sonication power)..... 117

Figure A-3: Spectrum of the degraded COU after several sonication times (1 mM COU 5 mL, 250 mL surrounding water, 100% nominal sonication power)..... 118

List of Tables

Table 1-1: Known Categories of Cyanotoxins, their structure, mode of action and the genera known to produce them [13].	24
Table 1-2: CYN's physicochemical properties.	28
Table 2-1: AOPs previously employed for CYN's degradation.	37
Table 2-2: Previously identified CYN's transformation products.	40
Table 7-1: Columns examined for CYN determination.	73
Table 7-2: Method Repeatability	80
Table 7-3: LOD & LOQ determination.	81
Table 7-4: Rate of production of Fe^{3+} and 7-OH-COU	87
Table 7-5: Chemical Analysis of Selected bottled Waters.	92
Table 7-6: Degradation kinetic constants and initial degradation rates.	94
Table 7-7: Kinetic rate constant in presence of TA and TBA.	97
Table 7-8: Identified TPs and their structure.	100
Table A-8-1: MS MS fragments and proposed structures.	118

List of Chromatograms

Chromatogram 7-1: CYN elutes at the dead volume when the mobile phase is ACN (0.05% TFA) 5% / H ₂ O (0.05% TFA).....	75
Chromatogram 7-2:CYN retention time in H ₂ O 95% + MeOH 5% and H ₂ O 90% + MeOH 10%.	76
Chromatogram 7-3: CYN's elution in the presence of 0.01% FA (a), 0.05 TFA (b) and without acid (c).	77
Chromatogram 7-4: Calibration curve's chromatograms.	79
Chromatogram 7-5: CYN degradation overlaid chromatograms.....	89
Chromatogram 7-6:TPs chromatograms after 15 minutes of sonication (a) (5 mL CYN 1 mg L ⁻¹ , 250 mL surrounding water, 100% nominal sonication power).....	107
Chromatogram 7-7: TPs chromatograms after 15 minutes of sonication (b) (5 mL CYN 1 mg L ⁻¹ , 250 mL surrounding water, 100% nominal sonication power).....	108
Chromatogram 7-8: TPs chromatograms after 15 minutes of sonication (c) (5 mL CYN 1 mg L ⁻¹ , 250 mL surrounding water, 100% nominal sonication power).....	109
Chromatogram 7-9: TPs chromatograms after 15 minutes of sonication (d) (5 mL CYN 1 mg L ⁻¹ , 250 mL surrounding water, 100% nominal sonication power).....	110
Chromatogram 7-10: MS MS spectrum of TP 321 and proposed fragments structures	111

1 Cyanotoxins

1.1 Introduction

Cyanobacteria, or blue-green algae, belong to an ancient group of prokaryotic organisms that still exists on Earth. Most of them are aerobic photoautotrophs, meaning that they only need water, carbon dioxide, inorganic substances and light to survive[1]. Via this mechanism, they are responsible for the formation of the Earth's atmosphere about two and a half billion years ago. While they are synthesizing chlorophyll a, water acts like electron donor, initializing oxygen formation [2]. They can grow and survive in various environments, such as fresh, brackish, and marine waters, rock surfaces, sand and soils. They may develop in different regions of aquatic environments leading to the formation of blooms, scums, biofilms or mats. These formations prerequisite favorable conditions of temperature, light penetration and water pH.

The formation of blooms adversely impacts the availability, aesthetic quality and safety of water resources for human use, but the major problem is the secondary metabolites that those bacteria produce. Those metabolites can be harmless substances, known as taste and odor (T&O) compounds or harmful compounds, also known as cyanotoxins, which are compounds of great toxicity for humans and animals.

1.2 Cyanobacterial blooms

1.2.1 Occurrence

A bloom is formed when an increase of cyanobacterial biomass occurs in a lake over a relatively short time and is characterized by the dominance (>80%) of one or more cyanobacterial species [3]. On some occasions, a visible dense layer of cells is formed on the surface of the water [4].

There are a lot of bloom-forming bacterial species such as *Aphanizomenon*, *Cylindrospermopsis*, *Dolichospermum*, *Microcystis*, *Nodularia*, *Planktothrix* and *Trichodesmium*. In Greek lakes the dominant species are *Microcystis* sp., *Aphanizomenon* sp., *Anabaena* sp. and *Anabaenopsis* sp.[5].

1.2.2 Traits involved in blooms development

There are three primary environmental factors affecting the cyanobacterial blooms formation. The first one is temperature; many types of cyanobacteria have optimal growth rates at warmer water with temperatures above 25° C. The rise of temperature because of climate change may increase the frequency and magnitude of cyanobacterial blooms. This can be attributed to the fact that, firstly, at higher temperature the cyanobacteria are favored over other phytoplankton species and secondly, the rise of temperature enhances the vertical stratification and lengthens the period that this stratification lasts [4], [6], [7].

The second environmental factor influencing cyanobacterial blooms is the trophic status of the aquatic system. It is broadly supported that cyanobacterial blooms mainly occur in eutrophic reservoirs, usually in ponds and lakes with total phosphorus concentrations greater than 50 µg L⁻¹ [8], [9].

Another environmental factor affecting cyanobacterial blooms is light exposure. Most species of cyanobacteria need a minimum of light to photosynthesize, whereas there are several species which can be considered as hetero- or chemo-trophic. It depends on the species, the quality, intensity and duration of light needed. There are several types of species extremely adaptable to light exposure. Those bacteria may exist in a cave with no light and are capable of growing as soon as they are exposed to light [10].

1.2.3 Problems caused by blooms

Bloom formations can cause major problems for water quality. They increase turbidity and may induce hypoxia and anoxia, causing the death of fish and benthic organisms. Moreover, cyanobacterial blooms can produce a variety of secondary metabolites, such as taste and odor (T&O) compounds and cyanotoxins. Among them taste and odor (T&O) compounds, like geosmin and 2-Methylisoborneol (MIB), have a very low odor threshold, causing odor problems, so those reservoirs cannot be used for drinking water. Cyanotoxins are harmful

compounds affecting the liver and nervous system of birds, mammals and humans when ingested [11], [12].

1.3 Cyanotoxins

Cyanobacterial toxins or cyanotoxins are secondary metabolites produced from cyanobacteria. These compounds have a wide range of structures and exhibit different chemical and toxicological properties. Cyanotoxins are either intracellular or they are found on the cellular membrane of cyanobacteria. Most (>80%) of the toxins are intracellular in healthy growing cells, and their release happens during the shift from growth to stationary phase and cell death.

Cyanotoxins, based on their structure, can be separated in three categories:

1. cyclic peptides
2. alkaloids
3. lipopolysaccharides (LPS).

Cyclic peptides are microcystins (MCs) and nodularin (NOD), while in the wide category of alkaloids belong anatoxins, aplysiatoxins, cylindrospermopsins, Lyngbyatoxin-a and saxitoxins [13].

Toxins produced by cyanobacteria can also be classified based on the target organ, as hepatotoxins (MCs and NODs), neurotoxins (anatoxins and saxitoxins), cytotoxins (cylindrospermopsin) and dermatotoxins.

The following table (Table 1-1) summarizes the known categories of cyanotoxins, the genera that produces them and their mode of action.

Table 1-1: Known Categories of Cyanotoxins, their structure, mode of action and the genera known to produce them [13].

Cyanotoxin	Chemical Structure	Cyanobacteria producer	Mode of action
MCs	Cyclic heptapeptides	<i>Microcystis</i> , <i>Anabaena</i> , <i>Nostoc</i> , <i>Planktothrix</i> , <i>Phormidium</i> , <i>Oscillatoria</i> , <i>Radiocystis</i> , <i>Gloeotrichia</i> , <i>Anabaenopsis</i> , <i>Rivularia</i> , <i>Tolythrix</i> , <i>Hapalosiphon</i> , <i>Plectonema</i>	Hepatotoxic, tumor promoting, inhibition of eukaryotic protein phosphatase PP1, PP2A, and phosphoprotein phosphatases PPP4, PPP5
NODs	Cyclic pentapeptides	<i>Nodularia spumigena</i> , <i>Nostoc (symbiotic)</i>	As for microcystins, plus, weak carcinogenicity
CYNs	Tricyclic guanidine alkaloids	<i>Cylindrospermopsis</i> , <i>Umezakia</i> , <i>Anabaena</i> , <i>Oscillatoria</i> , <i>Raphidiopsis</i>	Multiple organ toxicity, neurotoxic, genotoxic, protein synthesis inhibitor

Anatoxin-a	Bicyclic alkaloids	<i>Anabaena</i> , <i>Phormidium</i> , <i>Aphanizomenon</i>	Neurotoxic, binds competitively at acetylcholine receptors
Anatoxin-a (S)	Phosphorylated cyclic N-hydroxyguanine	<i>Anabaena</i>	Neurotoxic, inhibits acetylcholine esterase
Saxitoxins	Alkaloids	<i>Aphanizomenon</i> , <i>Anabaena</i> , <i>Lyngbya</i> , <i>Cylindrospermopsis</i> , <i>Planktothrix</i>	Neurotoxic, blocks voltage-gated sodium channels
Lyngbyatoxins, Aplysiatoxins	Indole alkaloids	<i>Lyngbya</i> , <i>Oscillatoria</i> , <i>Schizothrix</i>	Tumor-promoting, binds to eukaryotic protein kinase C
BMAA, DAB	Diamino acids	Many genera	Neurotoxic, developmental toxin, erroneous insertion into proteins
LPS	Lipopolysaccharides	All genera	Inflammatory, promotion of cytokine secretion

1.3.1 Microcystins and Nodularins

MCs are cyclic heptapeptides with a basic cyclic structure, which consists of an amino acid, known as ADDA (3-amino-9-methoxy-2,6,8-trimethyl-10-phenyldeca-4,6-dienoic acid) and six other amino acids, while NODs are cyclic peptides with the ADDA and four other amino acids [14]. Structural variations have been reported for these acids but only 6 NODs are known, whereas there are more than 240 different MC variants identified up to now. Most of these variants are highly toxic such as MC-LR with LD₅₀ of 50 µg kg⁻¹ body weight, in mice [15] while others are less toxic compounds [16]. Those toxins have been characterized as hepatotoxins. The mechanism by which they exert their hepatotoxicity is the inhibition of protein phosphatases 1 and 2A.

1.3.2 Saxitoxins

Saxitoxins are highly polar, nonvolatile, tricyclic perhydropurine alkaloids derived from imidazoline guanidinium. There are at least 57 structural analogues [17]. They are characterized as neurotoxins and they are tasteless and odorless.

1.4 Cylindrospermopsin

Cylindrospermopsin (CYN) was first isolated and purified from *Cylindrospermopsis raciborskii* in 1992, characterized and named after that [18] but there are other cyanobacterial species *Anabaena bergii*, *Anabaena lapponica*, *Anabaena planctonica*, *Aphanizomenon gracile*, *Aphanizomenon ovalisporum*, *Aphanizomenon flos-aquae*, *Lyngbya wollei*, *Raphidiopsis curvata*, *Raphidiopsis mediterranea* and *Umezakia natans* known to produce CYN [19], [20].

CYN was first assumed to cause serious human illness after the poisoning of the town Palm Island in Northern Queensland, Australia. The incident, also known as ‘Palm Island mystery disease’, involved a group of Australians consisting of 138 children between the ages of 2 to 16, and 10 young adults. Those people presented symptoms of malaise, vomiting, anorexia and tender livers. After some days the symptoms progressed to bloody diarrhea and hematuria. An epidemiological report revealed that all patients drunk water from the town’s sole water supply, Solomon Dam, which had been treated with copper sulphate because of a

heavy algal bloom [21]. Another incident with CYN happened again in northern Queensland, Australia in 1992, when cows and calves died after drinking water from a source where a cyanobacterial bloom had been formed [22].

1.4.1 Chemistry

CYN is an alkaloid compound consisting of a guanidine coupled with a hydroxymethyluracil moiety. Its chemical formula is $C_{15}H_{21}N_5O_7S$ and has a molecular weight of 415.43 Da. Apart from CYN, two other naturally occurring variants are known: 7-epicylindrospermopsin (7-epi-CYN) with a different HO orientation and 7-deoxycylindrospermopsin (7-deoxy-CYN) without HO group. Stereochemical assignment is important to understand differences in toxicity, chemical and physical properties. 7-epi-CYN is the enantiomer of CYN. Both compounds have six stereocenters and their difference is the stereo-configuration of the C-7 hydroxyl group. CYN has an R configuration, while 7-epi-CYN has an S configuration [23].

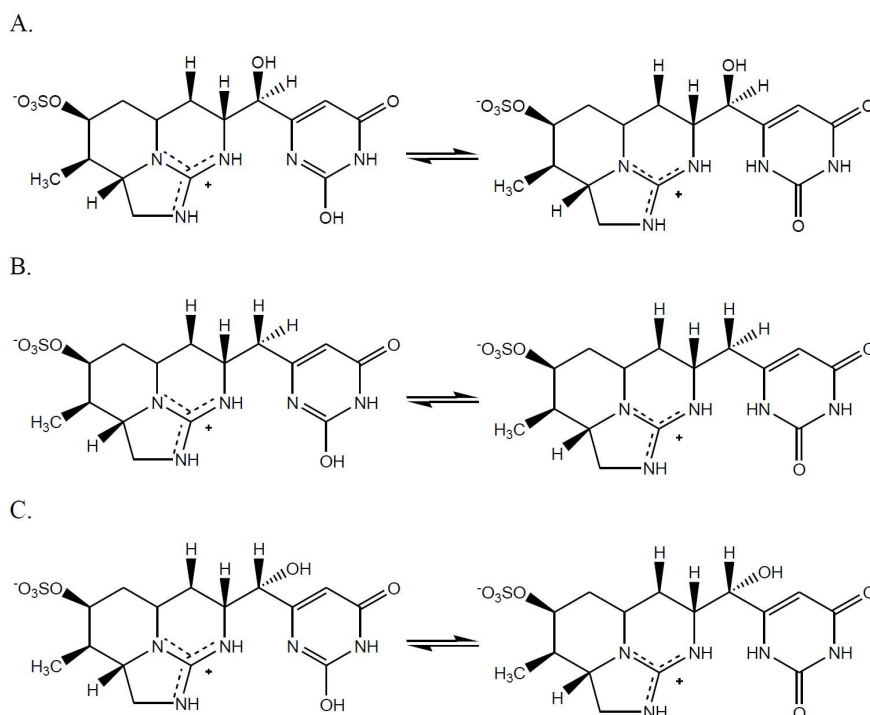


Figure 1-1: Chemical structures of CYN (A), 7-deoxy-CYN (B) and 7-epi-CYN.

CYNs is a zwitterionic molecule, so it is a highly water-soluble molecule. At pH values lower than 7 there is only one form with a negatively sulphate group, while at pH around 9

(dominant pH in lakes) the dominant form has two negative charges, one on the sulphate group and one on the uracil ring (Figure 1-2). The uracil moiety of 7-deoxy-CYN cannot tautomerize to form this negatively charged enolate ion because it has no HO group at the C-7 position [24].

CYN is in general a molecule of great stability; it is stable in a wide range of light, heat and pH conditions, so it can be easily stored in the refrigerator [25]. This great stability makes CYN a potential problem during bloom formation and arises the need for water treatment.

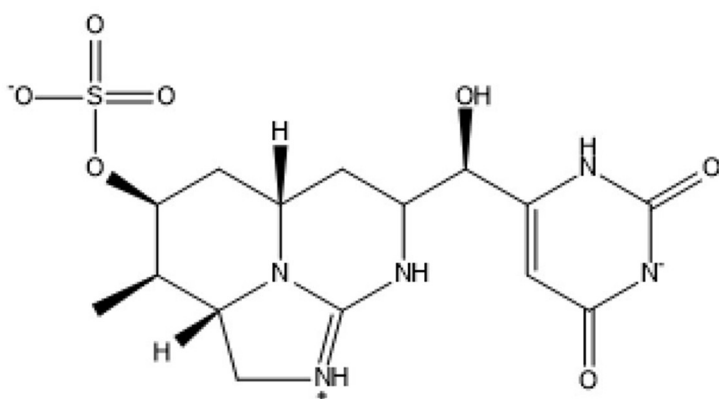


Figure 1-2: CYN's dominant form at pH 9.

Table 1-2: CYN's physicochemical properties.

Molecular formula	C ₁₅ H ₂₁ N ₅ O ₇ S	Physiological Charge	0
Molecular Weight	415,43 g mol ⁻¹	Hydrogen Acceptor Count	11
Color	White powder	Hydrogen Donor Count	5
Water Solubility	6.62 g L ⁻¹	Polar Surface Area	177.7 Å ²
logP	-1.1	Rotatable Bond Count	4
logD	-0.77	Refractivity	94.27 m ³ ·mol ⁻¹
logS	-1.8	Polarizability	37.7 Å ³
pKa (Strongest Acidic)	-1.6		
pKa (Strongest Basic)	10.26		

1.4.2 Toxicity

CYN was first described as an hepatotoxin cyanotoxin, but now is also characterized as cytotoxic and genotoxic because it affects the DNA [26]. CYN poisoning was reported to be in three distinct stages:

1. inhibition of protein synthesis,
2. proliferation of membranes and lipid accumulation within cells
3. and finally cell death [27].

CYN and 7-epi-CYN have similar toxicities as shown in mouse bioassay [28], while the 7-deoxy-CYN is generally nontoxic, exhibiting about ten times lower toxicity than CYN [29]. The LD₅₀ value of CYN and 7-epi-CYN is 200 µg kg⁻¹ mouse for 5 days [23].

It is not clear if the activity of CYN is linked to a specific functional group within the molecule, the existing data propose that the uracil group is partially responsible for its potent toxic activity [23]. Preliminary findings on several synthetic analogues suggest that the –OH group at C-7 may be significant for the cellular transport of CYN and/or be involved in its toxic activity inside the cell [30].

1.4.3 Global levels of CYN in water

CYN cases have been reported all over the globe. It was first reported in Australia in 1979. After that CYN has been detected in Asia, Europe and in North and South America, indicating that the CYN producing cyanobacteria can grow under different environmental conditions. This global distribution of CYN is possibly associated to the climate change [31]

1.4.3.1 Australia and New Zealand

CYN was first reported in Australia and after that 47 reservoirs in Queensland have been regularly monitored; CYN was reported in 14 out of these 47 reservoirs with median concentration 3.4 µg L⁻¹ [32]. In 1999 during a cyanobacterial bloom in a water storage facility at Hervey Bay, Queensland CYN's concentration ranged from 10 to 92 µg L⁻¹ [25]. In a more recent research in New South Wales, Australia 38.2 µg L⁻¹ CYN and 42.2 µg L⁻¹ 7-deoxy-CYN were detected in February 2007 [33]. In New Zealand CYN was first detected in

1999 using LC-MS/MS but there was no quantitation due to lack of pure standard solutions [34].

1.4.3.2 Europe

CYN was first reported in Europe in 1999 in two German lakes [35]. Those two lakes were studied the following years and total CYN reached maximum concentrations of 0.34 and 1.80 $\mu\text{g L}^{-1}$ in Melangsee and Langer See, respectively [36]. In France in 2002 the concentrations of CYN measured by LC-MS/MS ranged between 1.55 and 1.95 $\mu\text{g L}^{-1}$ [37]. In Italy two lakes were examined in 2004 and the extracellular CYN concentrations in surface water ranged from 0.3 (Trasimeno Lake) to 126 ng mL^{-1} (Albano Lake) [38]. Samples from the volcanic lake Albano were analysed using LC-MS/MS showing CYN extracellular values ranging from 2.6 to 126 $\mu\text{g L}^{-1}$ and intracellular values up to 42.3 $\mu\text{g L}^{-1}$. In water columns values ranged from 0.41 to 18.4 $\mu\text{g L}^{-1}$ [19]. In Finland the presence of CYN was confirmed by HPLC-PDA, LC-MS/MS and LC-TOF/MS at a concentration of 242 $\mu\text{g CYN per g}$ freeze-dried cyanobacterial material [39]. In Poland CYN was detected in 13 lakes using HPLC-MS/MS, and its concentrations varied from trace levels to 3.0 $\mu\text{g L}^{-1}$ [40]. In Czech Republic CYN was detected in water blooms collected from the shallow fishery pond Svet in concentrations ranging 55.5 to 241.9 $\mu\text{g g}^{-1}$ dw [41]. In Spain, during a summer bloom in 2004 CYN concentration was up to 9.4 $\mu\text{g L}^{-1}$ [42]. In Portugal CYN was detected for the first time in 2012 at Vela lake. Using HPLC-PDA and LC-MS/MS for confirmation the concentrations measured ranged from a minimum of 1.4 $\mu\text{g L}^{-1}$ to a maximum of 12 $\mu\text{g L}^{-1}$ [43]. First report of CYN in Greek lakes happened in 2010. Lakes Volvi, Kastoria, Pamvotis, and Karla contained CYN in concentrations ranging from 0.34 $\mu\text{g L}^{-1}$ to 2.84 $\mu\text{g L}^{-1}$ [44].

1.4.3.3 Asia

In Thailand samples were collected from a fishpond in Bangkok in May 1997. The concentration of CYN in the strain sample was estimated to be 1.02 mg g^{-1} dry cells [45]. In Japan CYN was first purified from samples collected from Lake Mikata in 1987. The toxin was identified but not quantified [46]. In 1995 samples were collected from a fishpond in Wuhan, China. Both CYN and 7-deoxy-CYN were detected using HPLC-MS/MS in concentrations 1.3 mg g^{-1} dw and 0.56 $\mu\text{g g}^{-1}$ dw respectively [47]. In a more recent (2011-

2013) research in Dongguan City of China CYN was detected with concentrations up to 8.25 $\mu\text{g L}^{-1}$ [48].

1.4.3.4 America

In Mexico the presence of CYN was reported in Lago Catemaco at low concentrations (21.34 ng L^{-1}) [49]. In Florida in 2002 CYN was determined in concentration from 0.05 to 0.2 $\mu\text{g L}^{-1}$ from August to December [50]. CYN has been detected in different areas of the continent like Uruguay, Indiana, Louisiana and Michigan indicating the possible CYN production but there are no clear data [51], [52].

1.4.4 International legislation and guidelines

The main route for human exposure to cyanotoxins is through oral consumption i.e. drinking water or contaminated food, but exposure through dermal contact or inhalation of particles containing CTs is also possible [14]. Exposure may also happen through recreational activities. Therefore, guideline values for the presence of cyanobacteria and CTs in waters used for recreational activities have been set by the World Health Organization (WHO) [53]. An expected concentration of 2-10 $\mu\text{g L}^{-1}$ MCs occurs by a guideline value of 2000 cyanobacterial cells/ml. These values correspond to low probability of adverse health effects, alerting the authorities to initiate further surveillance of the site.

The concentration of CTs in drinking water is of great importance, therefore a lot of countries have developed guidelines for the presence of CTs in drinking water [54]. The World Health Organization (WHO) has published a guideline for MCs in drinking water (1 $\mu\text{g L}^{-1}$ for total MC-LR -free plus cell-bound) [55]. Countries like China, Brazil, New Zealand, France and Spain have adopted WHO's guideline, while Australia has set a guideline for total MCs of 1.3 $\mu\text{g L}^{-1}$ for total MC-LR toxicity equivalents [56].

There is no specific guideline for CYN in drinking water in the EU. The guideline of 1 $\mu\text{g L}^{-1}$ in drinking water has been set in New Zealand [57], while the limits of 15 $\mu\text{g L}^{-1}$ and 0.3 $\mu\text{g L}^{-1}$ have been proposed for Brazil and France, respectively [58]. In Ohio and in Oregon the guideline value is 1 $\mu\text{g L}^{-1}$ for drinking water [59].

In addition, there are enough toxicity and exposure data to calculate tolerable daily intake (TDI) for CYN. The TDI index refers to the dose of a potentially harmful substance that can

be consumed daily over a lifetime without adverse health effects. Ideally, those data refer to humans, but when only animal data are available an uncertain value is used. This value is equal to 10 or 100 [14]. For example, in the case of MCs, WHO derived that the TDI for humans should be $0.04 \mu\text{g kg}^{-1}$ body weight [60]. TDI value for several CTs have been set from the Oregon Public Health Division (OPHD). This value for CYN is equal to $0.03 \mu\text{g kg}^{-1}$ body weight [61].

2 Removal of CYN using oxidative degradation

2.1 Introduction

Conventional water treatment may not effectively remove CYN. For example, removal of CYN using membrane filtration is ineffective in presence of natural organic matter (NOM) [62], while flocculation's efficiency in removing CYN depends on the dose of the flocculant and the quality of water [63]. Several oxidizing agents have also been examined for the removal of CYN. Common oxidants like free chlorine, chlorine dioxide and permanganate have shown varying degrees of CYN degradation and different reactivity towards the compound's functional groups [26]. Uracil ring is more susceptible to oxidation than sulfate or guanidine. Chlorination with free chlorine can degrade CYN up to 50% but its efficiency depends on the pH, temperature and the presence of NOM [64], [20]. Degradation of CYN under treatment with permanganate is even lower, only 10% [64]. These data reveal the need to develop alternative treatment processes for the removal of CYN from water. Advanced Oxidation has been proposed in the past as an effective alternative for the treatment of organic pollution in water [65].

2.2 Advanced oxidation processes (AOPs)

The technologies that take advantage of the formation of Reactive Oxygen Species (ROS) for oxidation consist the group of Advanced Oxidation Processes (AOPs). The most important among the produced ROS, common in all AOPs, are the hydroxyl radicals (HO•). These processes are successfully used for the degradation of compounds which cannot be treated with conventional methods [66].

2.2.1 Radiation

Radiation of water is usually performed using two radioactive sources:

- the electron beam irradiation carried out under an electron accelerator
- gamma irradiation mostly performed using a Cobalt-60 or Caesium-137 source [67].

Under these, the following species are formed in dilute aqueous solutions:

- hydroxyl radical (HO•)
- hydrogen atom (H•)
- hydrated electron (e_{aq}^-)
- H₂
- H₂O₂
- H_{aq}⁺
- HO_{aq}⁻.

In the absence of air, the primary products of water radiolysis are HO•, hydrated electron (e_{aq}^-) and H• [68]. Among them hydrated electron (e_{aq}^-) and H• are converted into peroxy radicals when air is present [69]. Reactions with only the HO• are achieved in N₂O saturated solutions where hydrated electron (e_{aq}^-) and H• are converted to HO•. Radical-radical recombination may also occur so hydroxyl radicals can react with hydrated electron (e_{aq}^-), H• and HO• to produce negative ions HO⁻, H₂O, and H₂O₂.

2.2.2 Photolysis and Photocatalysis

The vacuum ultraviolet photolysis of deaerated water involves the reaction of HO• and H₂O₂ but the degradation of target compounds is reported relatively small [70], whereas the combination of the UV with O₃ (UV/O₃) enhances the degradation of pollutants due to the direct and indirect formation of HO• [71]. Another alternative is the degradation of organic matter by combining the UV light with hydrogen peroxide (UV/ H₂O₂), a combination that may also occur naturally. Finally, the H₂O₂ may be combined with UV/O₃ and the UV/H₂O₂/O₃ process leads to the highest percentage of mineralization compared to UV/O₃ or UV/ H₂O₂ alone [72].

The degradation of compounds under UV light in the presence of various catalysts is of great importance and interest. The most widely used semiconductor catalyst is titanium dioxide (TiO₂). The photo-induced process on the semiconductor surface can be seen in the following figure (Figure 2-1).

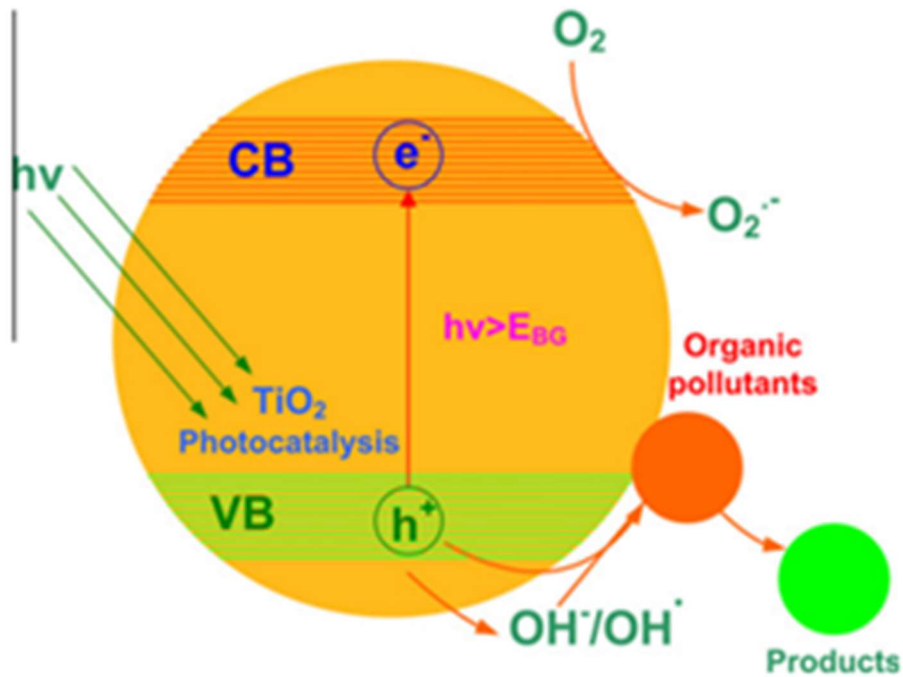
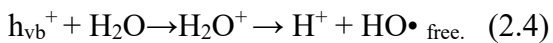
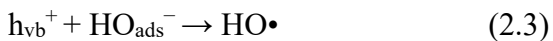
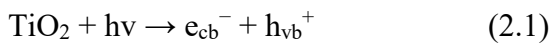


Figure 2-1: Photoinduced process on semiconductors surfaces [73].

When irradiation energy ($h\nu$) matches or exceeds the band-gap energy of the semiconductor ($E_g = 3.2$ eV in the case of anatase TiO_2), electrons (e_{cb}^-) are promoted from the valence band into the conduction band, leaving holes (h_{vb}^+) behind. The generated holes, which do not recombine directly, reach the surface of TiO_2 and react with surface adsorbed hydroxyl groups or water to form adsorbed $\text{HO}\cdot$. The $\text{HO}\cdot$ produced at the surface of semiconductor are released to bulk solution to form free $\text{HO}\cdot$ ($\text{HO}\cdot$ free) [74].

The reactions are the following:

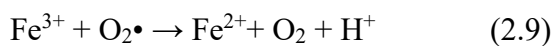
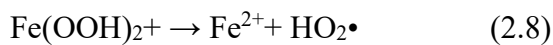
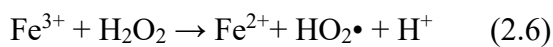
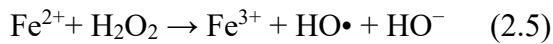


When the system is aerated, $\text{O}_2\cdot^-$ and H_2O_2 are also generated from the reduction site [75].

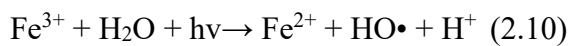
2.2.3 Fenton reactions

Fenton processes are based on the reaction of peroxides or dissolved oxygen with iron species leading to the formation of oxidizing species. Several cyclic reactions happen, initializing the formation of hydroxyl radicals by the decomposition of H_2O_2 in the presence of ferrous or ferric ions [76]. The Fenton reaction is propagated by the regeneration of Fe^{2+} , which happens by the reduction of Fe^{3+} with H_2O_2 .

The reactions involved are the following:



The Fenton reactions assisted by UV or visible irradiation are named photo-Fenton process and generally lead to increased degradation of compounds, due to photocatalytic reduction of Fe^{3+} to Fe^{2+} and the production of additional hydroxyl radicals during this reaction [77].

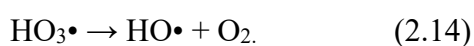
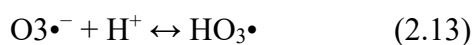
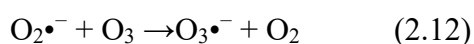
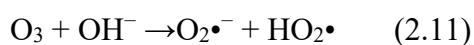


2.2.4 Ozonation

The treatment using ozone happens by two different mechanisms:

- direct electrophilic attack by molecular ozone
- indirect attack through the formation of hydroxyl radicals [78].

The pH of the solution is a dominant factor because it alters the pathway. At acidic pH the direct attack is predominant, whereas at basic conditions the indirect pathway prevails [79].



2.2.5 Sonolysis

Sonochemistry is based on the use of ultrasonic waves having frequencies above the human audible limit (>20 kHz) to produce an oxidative environment. The process includes the formation, growth, and implosive collapse of bubbles in a liquid medium, leading to the formation of ROS. Further information and detailed analysis on the mechanism of sonolysis is given in the next chapter.

2.3 Previous studies on CYN degradation using AOPs

There are several studies degrading CYN using AOPs. Most of them are summarized in table 2-1.

Table 2-1: AOPs previously employed for CYN's degradation.

AOP	Initial concentration	CYN's initial concentration	Degradation	Important details	reference
Ozonation	O ₃ : 0-62.5 μM	20 μM	Up to 60% degradation	Solution's pH 7	[80]
TiO ₂ - assisted ozonation	O ₃ : 0-2.5 mg L ⁻¹ TiO ₂ : 0-500 mg L ⁻¹	2.5 mg L ⁻¹	98.9% maximum degradation	The maximum degradation was achieved at the following conditions O ₃ : 2 mg L ⁻¹ TiO ₂ : 500 mg L ⁻¹ pH 7	[81]

TiO ₂ photocatalysis	TiO ₂ : 100 mg L ⁻¹	4 mg L ⁻¹	Complete degradation after 10 minutes at 350 nm	The complete degradation was achieved when the solution was O ₂ saturated	[82]
TiO ₂ photocatalysis	TiO ₂ : 200 mg L ⁻¹	10 mg L ⁻¹	Complete degradation after 10 minutes at 365 nm	Several catalysts examined. The complete degradation was achieved with Degussa P25	[83]
TiO ₂ photocatalysis	TiO ₂ : 50–500 mg L ⁻¹	1 μM	Complete degradation after 15 minutes when 250 mg L ⁻¹ TiO ₂ were used	A polymorphic titanium dioxide photocatalyst (PM-TiO ₂) which is mainly composed of anatase and brookite phases with a small amount of rutile phase	[84]
G irradiation	⁶⁰ Co steady-state radiolysis under N ₂ O	0.24 mM	65 % removal		[85]

TiO ₂ photocatalysis	TiO ₂ : 100 mg L ⁻¹	100 µg L ⁻¹	Complete degradation after 5 minutes for P-25 and 60% for UV-100	TiO ₂ (P-25) and TiO ₂ (UV-100)	[86]
electrolysis	boron-doped diamond (BDD)	1.83 µg L ⁻¹	The toxin concentration was below detection limit (<0.05 µg L ⁻¹) after 30 minutes	Anode: Silicon Based Boron doped diamond (Si/BDD) Cathode: stainless steel (SS)	[87]
UV-254 nm/H ₂ O ₂	H ₂ O ₂ : 0.5 mM	5 µM	Complete degradation with UV radiation of 600 mJ cm ⁻¹		[88]

2.4 Transformation Products of CYN using AOPs

CYN is susceptible to hydroxyl radical attack at the hydroxymethyl uracil, tricyclic alkaloid and sulphate groups [88]. A list of identified transformation products under radiolysis [85], TiO₂ photocatalysis [83] and ozonation [80] is shown in table 2-2.

Table 2-2: Previously identified CYN's transformation products.

	<i>m/z</i>	Chemical Formula	reference
CYN	416.1235	C ₁₅ H ₂₁ N ₅ O ₇ S	
P ₄₄₇	448.1133	C ₁₅ H ₂₁ N ₅ O ₉ S	[80]
P ₄₆₃	464.1082	C ₁₅ H ₂₁ N ₅ O ₁₀ S	[80]
P ₃₉₁	392.1235	C ₁₃ H ₂₁ N ₅ O ₇ S	[80]
P ₃₇₄	375	C ₁₃ H ₁₈ N ₄ O ₇ S	[83]
P ₃₄₈	349.1176	C ₁₂ H ₂₀ N ₄ O ₆ S	[80]
P ₃₄₉	350.1017	C ₁₂ H ₁₉ N ₃ O ₇ S	[85]
P ₃₁₉	320.0911	C ₁₁ H ₁₇ N ₃ O ₆ S	[85]
P ₂₉₁	292.0962	C ₁₀ H ₁₇ N ₃ O ₅ S	[80]
P ₂₈₉	290.0805	C ₁₀ H ₁₅ N ₃ O ₅ S	[80]
P ₃₆₅	366.0966	C ₁₂ H ₁₉ N ₃ O ₈ S	[80]
P ₃₉₀	391.0918	C ₁₃ H ₁₈ N ₄ O ₈ S	[80]
P ₃₂₁	322.1067	C ₁₁ H ₁₉ N ₃ O ₆ S	[80]
P ₃₃₇	338	C ₁₁ H ₁₉ N ₃ O ₇ S	[83]
P ₄₀₆	407.0867	C ₁₃ H ₁₈ N ₄ O ₉ S	[80]
P ₃₃₅	336.0860	C ₁₁ H ₁₇ N ₃ O ₆ S	[80]
P ₃₀₇	308.0911	C ₁₀ H ₁₇ N ₃ O ₆ S	[80]
P ₃₃₃	334.0704	C ₁₁ H ₁₅ N ₃ O ₇ S	[80]
P ₃₀₅	306.0754	C ₁₀ H ₁₅ N ₃ O ₆ S	[80]
P ₄₃₁	432.054	C ₁₅ H ₂₁ N ₅ O ₈ S	[85]

P ₁₉₄	195	C ₁₀ H ₁₆ N ₃ O ⁺	[83]
P ₂₂₆	227	C ₁₁ H ₂₀ N ₃ O ₂ ⁺	[83]
P ₂₈₆	286	C ₁₃ H ₂₄ N ₃ O ₄ ⁺	[83]
P ₃₁₅	316	C ₁₃ H ₂₃ N ₄ O ₅ ⁺	[83]
P ₃₄₆	347	C ₁₂ H ₁₈ N ₄ O ₆ S	[83]
P ₃₇₃	374	C ₁₄ H ₂₄ N ₄ O ₆ S	[83]
P ₄₃₃	434	C ₁₅ H ₂₃ N ₅ O ₉ S	[83]
P ₄₄₉	450	C ₁₅ H ₂₃ N ₅ O ₉ S	[83]

3 Sonolysis

3.1 Introduction

“Ultrasound” is defined as sound above the upper audible limit of human hearing. This limit varies between people and it is approximately 20 kHz. “Sonochemistry” is the field of high energy chemistry that embraces ultrasound in various applications.

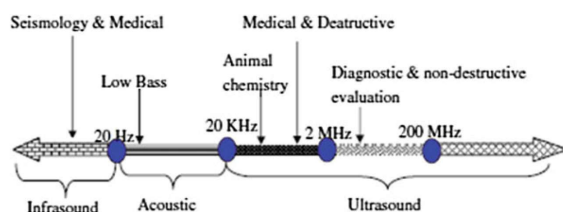


Figure 3-1: Sound frequencies Spectrum [89].

The frequency spectrum ranges from 20 kHz to 10 MHz and it is divided in three main regions:

- Power ultrasound 20 – 100 kHz
- High frequency 100 – 1000 kHz
- Diagnostic ultrasound 1000 – 50000 kHz [89].

Among them, diagnostic range acoustic waves, which possess lower wavelengths and lower power are used in medicine for fetal and soft tissue imaging (echography) [90]. Power ultrasound is mainly used in chemical applications as there is enough energy to cause bubbles cavitation [91].

Four types of sonochemical reactions are known:

- the acceleration of conventional reactions (initiates reactions surpassing energy barriers/changes reaction pathway/accelerates rates)
- redox processes in aqueous solutions via production of reactive species
- the degradation of polymers

- the decomposition of organic solvents [92].

3.2 Principle of the method

When high-intensity ultrasound waves interact with dissolved gases in liquid medium, acoustic cavitation takes place. Acoustic cavitation is the formation, growth and implosive collapse of small gas bubbles in liquids exposed to ultrasound. Ultrasound waves consist of compression and expansion cycles. During the expansion, waves having sufficient intensity to exceed the molecular forces of liquid, generate bubbles. They expand and collapse when they reach a critical size [93].

Two theories have been formulated to explain the chemical effect of cavitation: the hot spot theory and the electrical theory. Among them the last one was rejected in the late 50s [92].

Hot spot theory postulates that bubbles collapsing in a liquid medium create a localized “hot spot” which reaches temperatures of $\sim 5000\text{K}$ and pressures of $\sim 500 - 1000$ atm. These conditions induce the rupture of water molecules (homolytic bond cleavage) and thermal dissociation of oxygen, generating various reactive radical species ($\text{HO}\cdot$, $\text{H}\cdot$, $\text{O}\cdot$, and $\text{HO}_2\cdot$), with the subsequent formation of hydrogen peroxide (H_2O_2) and H_2 , due to recombination of $\text{HO}\cdot$ and $\text{H}\cdot$, respectively.

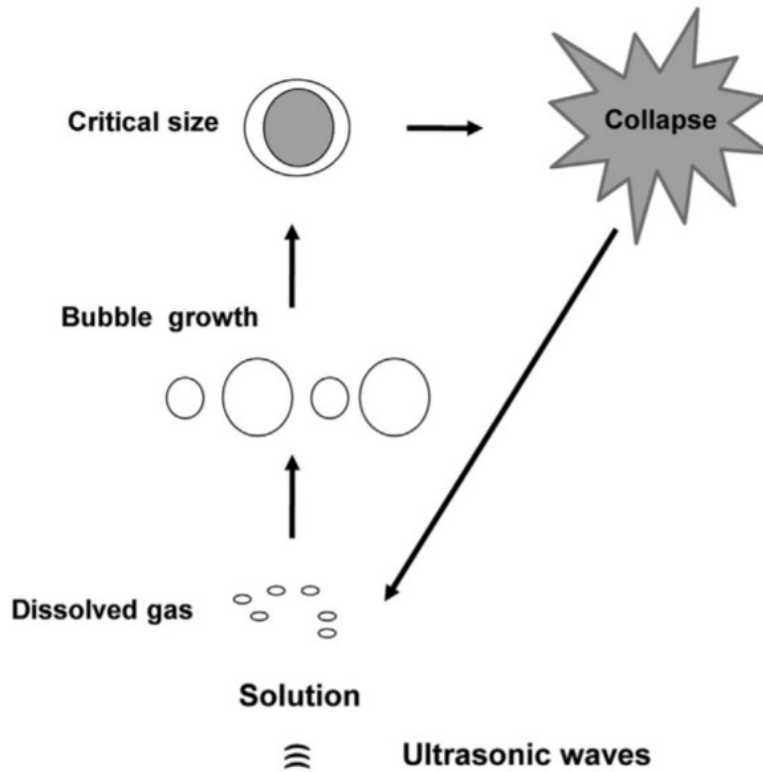
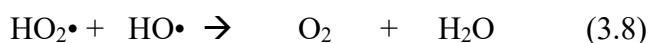
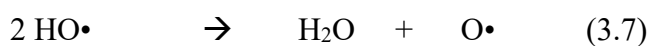
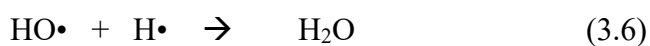
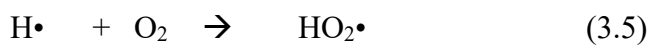
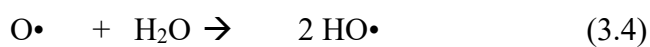
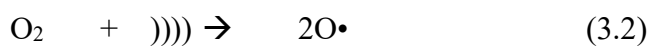


Figure 3-2: Schematic presentation of cavitation [94].

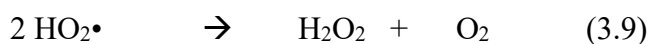
The hot spot theory reactions are the following

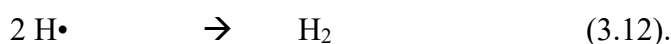
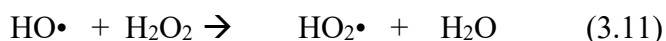


If there is oxygen available in the solution, the following reactions also take place leading to the production of superoxide radicals.



The recombination of superoxide radicals produces hydrogen peroxide as shown in the reaction 3.9.





3.3 Reaction zones

The sonochemical activity is divided in three reaction zones as shown from several EPR studies. The three zones have the following characteristics:

Zone 1: Gaseous region. It contains both permanent gas and the vaporized mixture.

Zone 2: The gas – liquid interface between the inner bubble and the bulk solution.

Zone 3: The bulk solution [95].

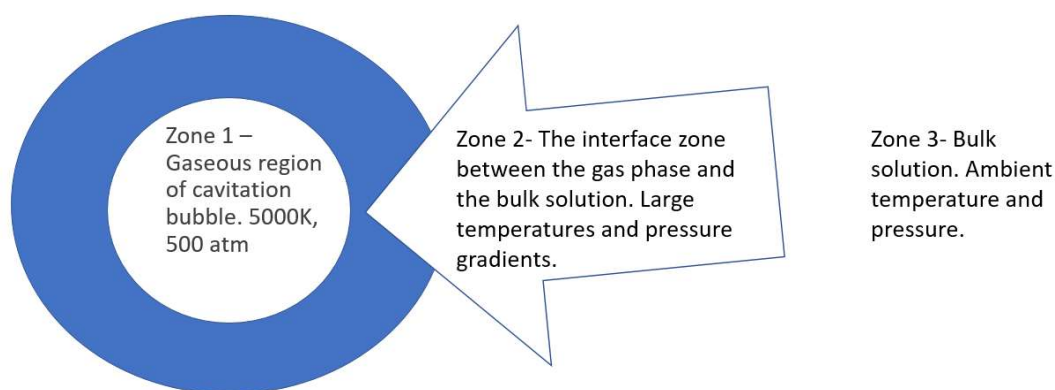


Figure 3-3: Bubble zones.

Inside the gaseous region, volatile compounds are exposed to extreme temperatures and pressures so the molecules break down due to pyrolysis [96]. In this region $\text{HO}\cdot$ and $\text{H}\cdot$ radicals are produced when the water molecules break down. It is estimated that 10% of these radicals escape to the bulk solution [97]. Non-volatile compounds react primary in the interface between the gaseous phase and the bulk solution (zone 2) or in the bulk solution [98]. The reactions on the bulk solution are similar with those of radiation chemistry. The radicals are produced inside the cavitation and escape to the bulk [99]. Based on these data, researchers can explore the role of $\text{HO}\cdot$ and the reactivity of each zone during the degradation of different compounds. For example, Song et al., employed polar and non-polar dosimeters during the ultrasonically induced degradation of MC-LR. Their observations helped them

conclude that MC-LR is degraded at the interfacial region between the cavitation and the bulk solution [100].

3.4 Parameters affecting production of reactive species

3.4.1 Bubble Dynamics

Two cavitation events, stable and transient, are responsible for the chemical and physical effects of ultrasound [101]. Stable cavities exist for many acoustic cycles and sometimes they do not collapse at all. During those cycles, they oscillate around a mean radius. The rate of growth and contraction, at the rarefaction and the compression phase respectively, are equal, specifying that rectified diffusion or unequal mass transfer are not occurring. The bubbles oscillate with a resonance frequency and when the frequency of the ultrasound is equal to the frequency of the bubble resonant cavitation occurs. Operating at these conditions increases the rate and yield of some reactions [102]. Some ultrasonic transducers are manufactured with a set frequency so operating at resonant conditions is possible by changing other operating parameters in order to alter the bubble frequency [103]. A transient cavity exists for a few acoustic cycles. Its size becomes several times larger than the initial size of the bubble and during collapse it creates extreme pressures and temperatures in the cavity [101]. It is believed that transient cavities occur in liquids when higher sound intensities ($>10 \text{ W cm}^{-1}$) are applied [92]. In addition, transient cavitation bubbles contain mainly vapor of the liquid, while stable cavitation bubbles are filled with a permanent gas and only some vapor.

3.4.2 Sonication Power

The rate of a reaction increases as the power applied to the system increases and after reaching a maximum, a decrease follows [104]. The optimum power for a reactions depends on the frequency, therefore the applied power and frequency should correlate [105].

3.4.3 Ultrasonic Frequency

The frequency of ultrasound can alter the critical size of cavitation bubbles. This happens for two reasons; a negative pressure with insufficient duration is produced and the compression

cycle begins faster than the time needed for the bubble to collapse [106]. In addition, when higher frequencies are applied, bubble lifetimes are shorter and the HO• can escape the bubble before a possible recombination happens [107]. Theoretical simulations summarize that there is a frequency range where the cavitation process is enhanced. This range depends on the solution type [108]. In general, higher frequencies increase the number of free radicals whereas, lower frequencies lead to more violent cavitation and as a consequence to higher temperatures and pressures [109], [110].

3.4.4 Dissolved Gasses

Dissolved gasses act as cavitation bubbles nuclear. If the gases are removed from the reaction system, cavitation barely occurs. Different gas properties affect the cavitation event variously. Gas parameters affecting the cavitation are the specific heat ratio, the atomicity of the gas, the solubility and the thermal conductivity. In general, a greater cavitation effect occurs when a gas with a high specific ratio is present in the reaction. Thus, monoatomic gases, which have greater ratio of specific heats than the diatomic, convert more energy upon cavitation. It is believed that cavitation occurs adiabatically [111]. However, some heat is transferred to the bulk. This amount of heat depends on the thermal conductivity of the gas, and it is increased when a gas with a higher thermal conductivity is used. Solubility of the gas also affects the cavitation because the bubbles, which are formed by extremely soluble gases, may re-dissolve reducing the overall cavitation effect. A research on carbon disulfide dissociation revealed that the reaction had the highest reaction rate when He was used. The order of the reaction rates for the different gases examined was He > H₂ > air > Ar > O₂ > CO₂. The main factor affecting this system was gas solubility as He, which is the least soluble among those gases, gave more nucleation sites [106].

3.4.5 Ambient Temperature

When ambient temperature is increased, the sonochemical effect is decreased because of a series of events. Firstly, as the temperature rises, the equilibrium vapor pressure of the system is increased, so the bubbles are more easily formed. However, these bubbles contain more vapor leading to a reduction of the ultrasonic energy as discussed previously. Regularly greater sonochemical effects are observed at lower ambient temperatures when most of the

bubble content is gas. For certain reactions optimum ambient temperatures exist. In those reactions, if a further increase of the temperature happens the cushioning effect of the vapor in the bubbles dominate the system leading to a decrease in the rate of the reaction [112]. The ambient temperature may also affect reaction kinetics. This was first observed in a degradation reaction where thymine was degraded. Thymine is a relatively nonvolatile compound, so it is believed that the degradation reaction happens in the gas – liquid zone rather than inside the cavity. When temperature was increased thymine diffused faster from the bulk to the reaction zone, however at the same time the intensity of the cavitation was decreased, reducing the amount of free radicals produced in the bubble [113].

3.4.6 Ambient Pressure

The ambient reaction pressure can affect the cavitation process. An increase in ambient pressure decreases the vapor pressure of the mixture inducing an increase to the intensity of the implosion [110]. However, this has an upper pressure limitation; a pressure equal to 200 psi or more increases the cavitation threshold in the system to a level where the cavitation bubbles can no longer be produced [114], [115].

3.4.7 Solvent

Viscosity, vapor pressure and surface tension are associated with pressure build up, diffusion and bubble growth during a cavitation event [116]. When a solvent with high vapor pressure, low surface tension and low viscosity is preferred cavities formation occurs faster whereas, using solvents with the opposite characteristics leads to more intense cavitation [110], [117].

3.5 Types of Reactors

The main reaction systems in sonochemistry are ultrasonic baths and ultrasonic probes. In any case, ultrasound waves are generated by the transducer, the part of the system that turns electrical power into waves. This part is assisted to a tip (on the probe system) or to a vibrating plate (for the bath). The ultrasound reaches the reaction system through two possible routes. Either by direct sonication where the waves source is in direct contact with the liquid medium, or by indirect sonication, where a vessel with the solution is dipped in a

liquid which is in direct contact with the transducer. In addition, reactors need a cooling system, since the process produces heat and there is a need to maintain the temperature of the solution stable [118].

The configuration of the reactor affects the disinfection process and influences the reaction yields. Several parameters, such as geometry, energy flow and diameter of the transducer, may alter the amount of acoustic waves reaching the reaction liquid [119]. In a probe type reactor (Figure 3-4 C) the acoustic amplitude, which is the pressure amplitude of an ultrasonic wave, near the probe can be as high as 10 atm, while the typical acoustic amplitude in a bath type sonochemical reactor (Figure 3-4 A & B) is much smaller than that [120].

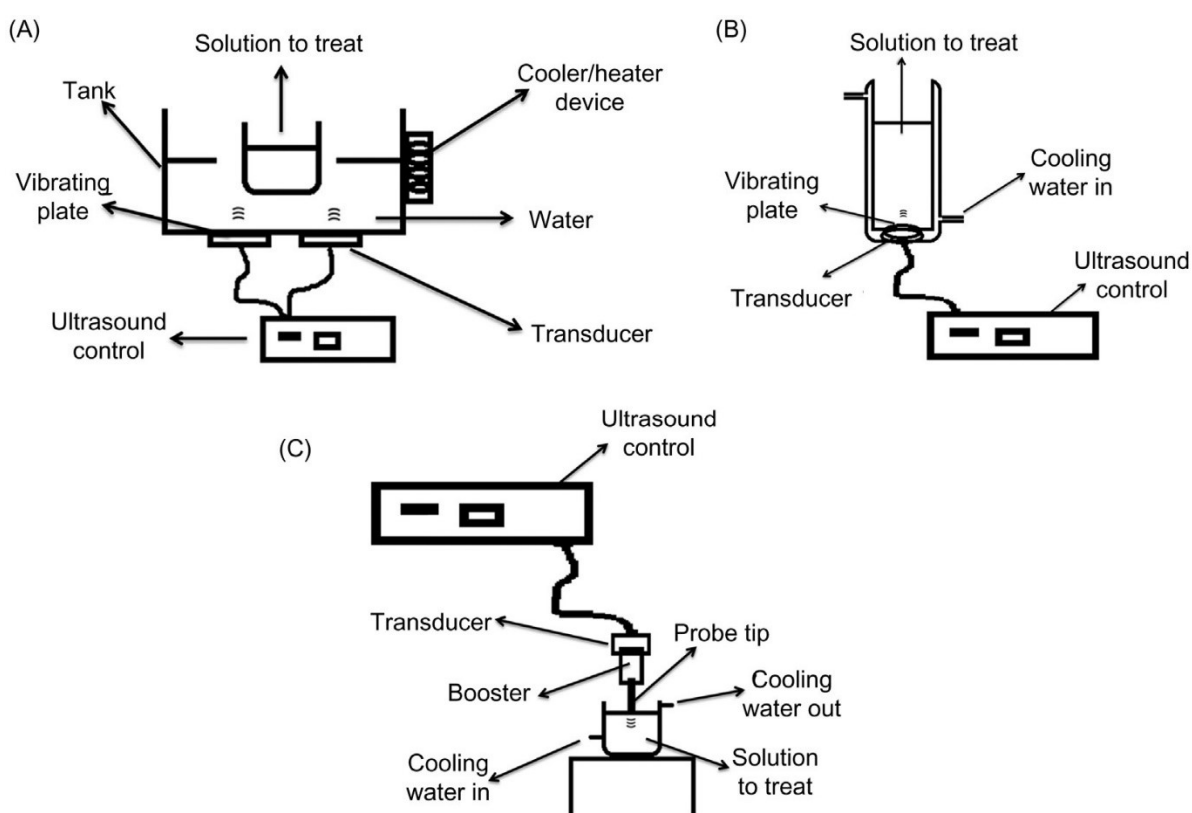


Figure 3-4: Type of reactors [94]. Type of reactors [94] A) bath system for indirect sonication B) bath system for direct sonication C) probe system.

3.6 Advantages and applications of sonolysis

Sonolysis presents several advantages. In most cases, sonication produces reactive radical species, without the need to add oxidants or catalyst. Moreover, sonication process does not generate additional waste. When the experimental conditions are optimized, the application of ultrasound is in agreement with the twelve principles of green chemistry [121]. Because of

the ability to produce radical species that degrade substances in water, sonolysis is considered as an alternative AOP. It is used for water treatment with the potential to eliminate chemical and microbiological pollutants [94].

Due to the characteristics of the sonochemical process, sonolysis has been applied as a water treatment method for various organic compounds. It is an effective method for the degradation of pesticides such as organochlorine pesticides [122] and atrazine [123]. In addition it has been used for the degradation of a wide variety of pharmaceuticals like the non-steroidal anti-inflammatory drugs, piroxicam [124] and ibuprofen [125] and several antibiotics belonging to fluoroquinolones (ciprofloxacin and norfloxacin), penicillins (oxacillin and cloxacillin) and cephalosporins (cephalexin and cephadroxy) [126]. When ultrasound is assisted with another AOP, like catalysis or ozonolysis, the degradation of pharmaceuticals in water is enhanced [127]. In addition, ultrasonically induced degradation has been applied in compounds known as emerging contaminants, like estrogen hormones [128].

Moreover, ultrasound has been used for the control of cyanobacterial blooms in surface water. Ultrasound affects the algal cells in different ways and leads to their destruction by the disruption of their gas vesicles, the destruction of the cell membrane and the prevention of photosynthesis [129]. Ultrasound has been applied in lakes and reservoirs all over the world [130], [131]. An important factor is to apply the ultrasound in an early stage of cyanobacterial life cycle to avoid the release of CTs in the water [132]. The use of ultrasound for the degradation of these CTs is limited to MC-LR and MC-RR [100], [133]. Finally, only two T&O compounds have been degraded by ultrasound, geosmin and 2-methylisoborneol [134].

3.7 Dosimetry of the ROS-producing system

Chemical dosimeters are used to quantitatively measure a chemical change at the end of a series of reactions involving radicals [135]. Dosimeters are used mainly in radiation chemistry, but they can also be used in sonolytical systems, due to the production of radicals. The aim is to relate the efficiency of sonochemical reaction to the energy of ultrasonic irradiation used to produce them. There are many experimental parameters affecting the number of radicals produced in an ultrasound system, like frequency, temperature, amount of dissolved gasses and existence of scavenging compounds [136]. The sonochemical efficiency is given by chemical dosimeters. These dosimeters are usually sensitive to HO• and other

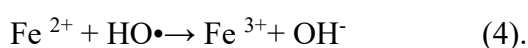
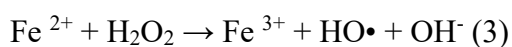
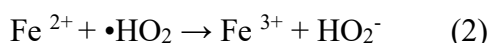
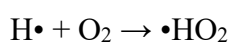
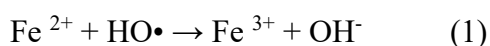
related oxidants. When it comes to sonochemical reactions, the dosimeters that are mainly used are coumarin, terephthalate, Fricke solution, salicylic acid and potassium iodine.

3.7.1 Coumarin

Coumarin (COU) is an organic molecule known to form several hydroxycoumarins when it reacts with hydroxyl radicals in aqueous solutions. Among them 7-hydroxycoumarin (7-OH-COU) is a highly fluorescent compound, with a fluorescence maximum at 456 nm. All the others hydroxycoumarins are poorly- or non- fluorescent compounds. The advantage of using coumarin as a dosimeter is that it reacts only with HO• to form hydroxycoumarins [137]. During experiments with coumarin you can follow the trend of both the degradation of coumarin and the production of 7-hydroxycoumarin over time. However, there is no clear correlation between the amount of transformed coumarin and the amount of 7-hydroxycoumarin produced. In an experimental system at 500 kHz and 50 W, the 7-hydroxycoumarin produced was about 1% of the coumarin disappeared [138]. In some cases, there is an inner filter effect that decreases the rate of 7-hydroxycoumarin formation [139], [140]. Another factor affecting the formation of 7-hydroxycoumarin is the presence of dissolved gasses. O₂ plays an important role and its absence reduces the reaction yield [141].

3.7.2 Fricke solution

Fricke solution consists of FeSO₄, H₂SO₄ and NaCl and its dosimetry is based on the formation of free radicals, hydrogen peroxide and hydroperoxyl radicals. Based on the reactions of Fricke solution with HO• produced in radiation chemistry, we can assume that in sonochemistry the reactions are the following:



The number of HO• can be estimated by measuring spectrophotometrically the Fe³⁺ ions at 305 nm. Based on the reactions above the number of Fe³⁺ produced is equal to 4 times the number of HO• produced [142]. In US systems free radicals are formed by a small amount of acoustic energy. This amount is estimated as 0.08% of the acoustic energy but depend also in other parameters, i.e. frequency.

3.7.3 Terephthalic Acid

Terephthalic acid (benzene-1,4-dicarboxylic acid) is a compound used for the specific trapping of HO•. When it reacts with HO•, several hydroxy-terephthalic acids are formed. Among them 2-hydroxy-terephthalic acid is a fluorescent compound. In general, in sonochemical systems the HO• add rapidly to the *ortho*- and to a much lesser extent to the *ipso*-positions [143] so, 2- hydroxy-terephthalic acid is mainly produced (84%) but from radiation chemical studies, it is known that when O₂ is present, the yield of 2-hydroxy-terephthalic acid is only 35% of the HO• yield [144].

pH is an important factor when terephthalic acid is used as a dosimeter because in pH greater than 6 the compound is anionic and has a great water solubility, whereas in water solutions with pH lower than 3 is poorly soluble. This factor also affects whether the compound will reside on the bulk solution, the gaseous phase, or the interface during the cavity formation.

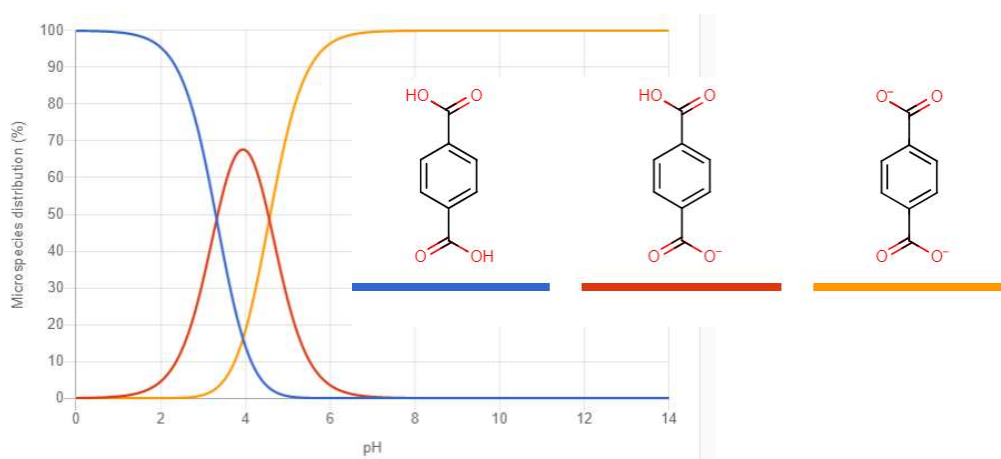


Figure 3-5: Terephthalic Acid distribution.

4 Analytical methods for the determination of CYN and its TPs

4.1 High performance Liquid Chromatography (HPLC)

4.1.1 Principle of the method

High Performance Liquid Chromatography (HPLC) is a suitable method for the separation, identification and/or determination of substances. This separation is based on the distribution of the analyte between a stationary and a mobile phase. The stationary phase is the packing material of the column and the mobile phase the eluent [145]. Different compounds of a sample are eluted at different times based on their structure, the structure of the stationary phase and the composition of the mobile phase. In that way the separation is achieved.

4.1.2 Liquid Chromatography types

The classification is based on the separation mechanism or on the type of stationary phase.

1. Partition, or liquid-liquid chromatography. The stationary phase is a liquid absorbed or bonded to a solid phase and the equilibrium is based on the partitioning between the two immiscible liquids.
2. Adsorption, or liquid-solid chromatography. In this chromatography type the stationary phase is a solid where the analyte is adsorbed on.
3. Ion exchange chromatography. Ion exchange happens between the ion-exchange resin used as a stationary phase and the mobile phase.
4. Size-exclusion chromatography. A liquid in interstices of a polymeric solid is used as stationary phase. In this type of chromatography partitioning or sieving takes place.

- Affinity chromatography. The stationary phase is a group specific liquid bonded to a solid surface and the separation happens due to the partitioning between the liquid stationary phase and the mobile phase.

4.1.3 System components

A basic High-Performance Liquid Chromatography system is shown in figure 41 and consists of the following equipment:

- solvent reservoir
- solvent delivery system
- sample injector
- column
- detector
- computer

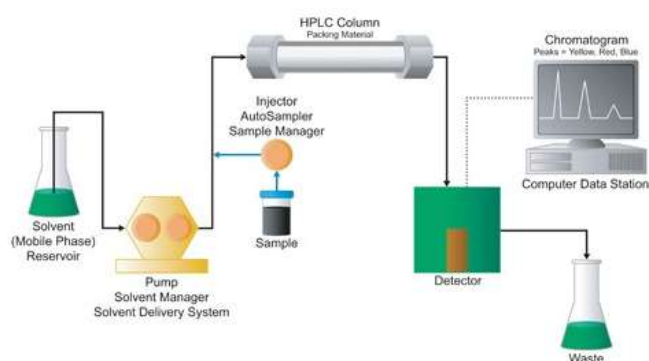


Figure 4-1: HPLC basic equipment [146].

4.1.3.1 Mobile phase

The solvents are placed in glass reservoirs. In different instrument models, bubbles and dust are removed from the solutions either on-line by a degasser or by filtration using 47 mm membranes before placing them in the reservoirs. Depending on the composition of the mobile phase, there are two elution types. When the mobile phase is made-up from a single solvent or a mixture of solvents which composition remains constant during the separation, the elution is called isocratic. In other case, gradient elution takes place. In gradient elution the solvents used usually vary in polarity and their ratio is changed during the separation process [147].

4.1.3.2 Chromatographic Column

Most of the analytical columns used in HPLC are made up of stainless steel. Their length varies from 20 mm to 500 mm and their internal diameter for 1 mm to 100 mm. The column contains the chromatographic packing material, which is the stationary phase. When the stationary phase is combined with the right mobile phase, effective separation is achieved [146]. When the stationary phase is non-polar and the mobile phase is polar the chromatography is called reversed-phase chromatography (RP - chromatography). A commonly used non-polar stationary phase is 18-carbon-long hydrocarbon attached to the surface of silica. This stationary phase is combined with a very polar mobile phase, usually water. In RP – chromatography the hydrophobic analytes are the more retained while the polar analytes are eluted first [148]. On the other hand, in normal phase chromatography the stationary phase is polar and the non-polar analytes are eluted first.

4.1.3.3 Detector

Detectors should be able to recognize when a substance is eluted thus, they have to monitor changes in mobile's phase composition and then to convert these changes into electrical signal [149]. Sometimes the chromatographs are coupled with spectroscopic instruments such as mass spectrometers. Those instruments will be presented in a different section. The desirable specifications should be:

1. Adequate sensitivity.
2. Good stability and reproducibility.
3. A linear response to solutes that extends over several orders of magnitude.
4. Low internal volume.
5. A short response time independent of flow rate.
6. High reliability and ease of use. The detector should be foolproof in the hands of inexperienced operators, if possible.
7. Similarity in response toward all solutes or alternatively a highly predictable and selective response toward one or more classes of solutes.
8. The detector should be nondestructive.

Two types of liquid chromatography detectors are known. Those who respond to a mobile phase property, such as refractive index, named bulk-property detectors and the solute-property detectors who respond to solute properties such as UV-absorbance.

4.1.3.3.1 UV-Visible Detector (UV-vis)

UV-vis detectors are most frequently used for components showing an absorption spectrum in this region. A deuterium discharge lamp (D₂ lamp) is usually employed as light source. The wavelength of a D₂ lamp light ranges from 190 to 380 nm (UV area). In addition, a tungsten lamp (W lamp) is used with light wavelength from 380 to 900 nm. The main parts of a UV-vis detector are:

- Sources i.e. deuterium lamp
- wavelength selectors, filter or monochromator
- sample containers
- radiation transducers

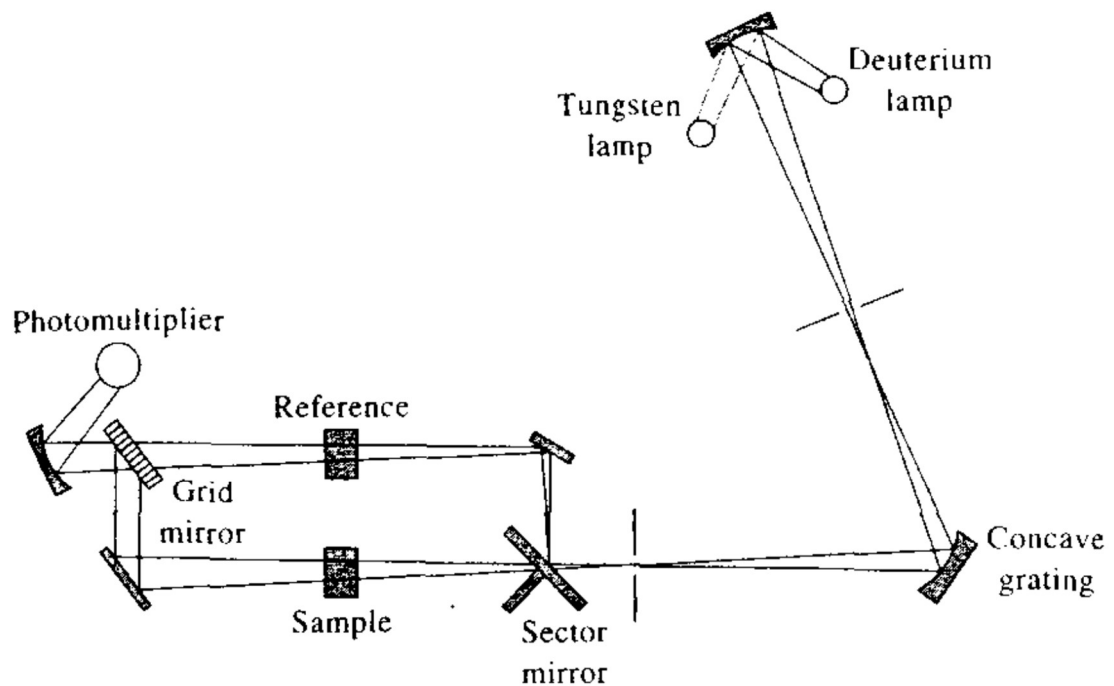


Figure 4-2: UV-vis reactor layout [145].

4.1.3.3.2 Photodiode array detector (PDA)

A photodiode array (PDA) is a linear array of discrete photodiodes on an integrated circuit (IC) chip. For spectroscopy it is placed at the image plane of a spectrometer to allow a range of wavelengths to be detected simultaneously. The components of a PDA detector are shown in the following figure (Figure 4-3).

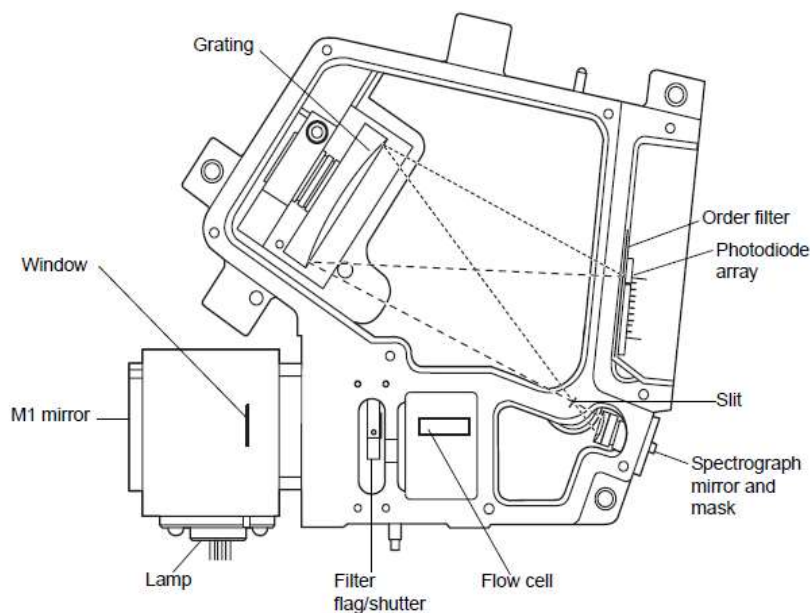


Figure 4-3: Layout of a PDA detector [150].

The detector measures the amount of light striking the photodiode array to determine the absorbance of the sample in the flow. The array consists of a row of photodiodes each of them acts as a capacitor holding a fixed amount of charge. Light striking a photodiode discharges the diode. The magnitude of the discharge depends on the amount of this light.

4.2 Mass Spectrometry

4.2.1 General information on mass spectrometric techniques

Mass spectrometry is an analytical technique used to identify unknown substances and to elucidate their structure by the conversion of the sample into gaseous ions, with or without fragmentation, which are then characterized by their mass to charge ratios (m/z) and relative abundances.

Initially, gas-phase ions are formed using some type of ionization source. Each of these ions undergoes fragmentation and then is separated according to their mass-to-charge ratio. The ions' detection is in proportion to their abundance.

4.2.2 Instrumentation

4.2.2.1 Ion Source

The ion sources are responsible for the production of gaseous ions of the compounds. There are two main categories. The gas phase sources were the sample goes to the gaseous phase before the ionization and the desorption sources were gaseous ions occur directly from the solid or liquid sample.

Also, the sources are classified as hard and soft, based on the amount of energy used. Hard ionization sources impart enough energy to analyte molecules to leave them in a highly excited energy state. Relaxation then involves rupture of bonds, producing fragment ions that have mass-to-charge ratios less than that of the molecular ion. Soft ionization sources cause little fragmentation [145].

One of the most important ionization techniques is Electrospray Ionization (ESI). Electrospray ionization takes place under atmospheric pressures and temperatures, and is commonly used after liquid chromatography separations. A solution of the sample is pumped through a stainless-steel capillary needle at a rate of a few microliters per minute. The needle is maintained at several kilovolts with respect to a cylindrical electrode that surrounds the needle. Evaporation of the solvent and attachment of charge to the analyte molecules take place when the charged spray of droplets passes through a capillary. As the droplets become smaller because of evaporation of the solvent, their charge density becomes greater until the Rayleigh limit, where the surface tension can no longer support the charge. A coulombic explosion occurs and the droplet is torn apart into smaller droplets. These small droplets can repeat the process until all the solvent is removed from the analyte, leaving a multiply charged analyte molecule. A drawback of ESI is that because of the soft ionisation, structural elucidation is a difficult task.

4.2.2.2 Mass Analyzer

Resolves the ions into their characteristic mass components according to their mass-to-charge ratio. Ideally, the mass analyzer should be capable of distinguishing masses with minimum differences. An important factor is the resolution (R). $R = \frac{m}{\Delta m}$ where Δm is the mass difference between two peaks that are just resolved and m is the nominal mass of the first peak.

The most used mass analyzers are:

- Magnetic sector Analyzer
- Single Quadrupole (Q)
- Ion Trap
- Time of Flight (TOF)

Fourier Transform Cyclotron Resonance (FT-ICR). The heart of a quadrupole instrument is the four-parallel cylindrical (originally hyperbolic) rods that serve as electrodes. In addition, variable radio-frequency alternative current voltages, which are 180° out of phase, are applied to each pair of rods. To obtain a mass spectrum with this device ions are accelerated into the space between the rods by a potential difference of 5 to 10 V.

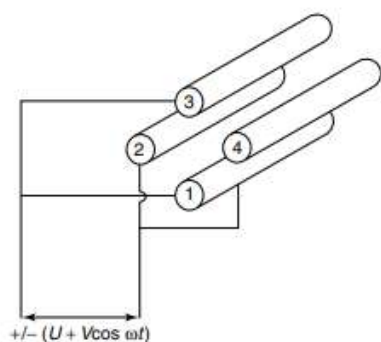


Figure 4-4: Layout of a Quadrupole (Q) [147].

Meanwhile, the alternative and direct current voltages on the rods are increased simultaneously while maintaining their ratio constant. At any given moment, all of the ions, except those with a certain m/z value, strike the rods and are converted to neutral molecules. Thus, only ions having a limited range of m/z values reach the transducer.

4.2.3 Tandem Mass Spectrometry (MS/MS)

Tandem mass spectrometry (MS/MS) allows the mass spectrum of preselected and fragmented ions to be obtained. An ionization source, usually soft, produces ions and some fragments. These are then the input to the first mass analyzer, which selects the precursor ion and sends it to the interaction cell, where it can decompose spontaneously, react with a collision gas, or interact with an intense laser beam to produce fragments, called product ions. These ions are then mass analyzed by the second mass analyzer and detected by the ion detector.

The most used MS/MS instrument is the Triple Quadrupole. It consists three quadrupoles in series. The second set of rods is not used as a mass separation device but as a collision cell, where fragmentation of ions transmitted by the first set of quadrupole rods is carried out, and as a device for focussing any product ions into the third set of quadrupole rods. Both sets of rods may be controlled to allow the transmission of ions of a single m/z ratio or a range of m/z values to give the desired analytical information [151].

4.3 Analytical Determination of CYN

An HPLC method for CYN's detection was first developed in 1994 [46]. A C18 column and an isocratic mobile phase consisted of 95% water / 5% methanol were used. Later, a method with a C18 column and a 20 min gradient from 0% to 50% aqueous methanol with 5% trifluoroacetic acid showed good results [152]. The extraction of CYN from real samples proved problematic when cells were present. Thus, several extraction methods like SPE with C18 or polygraphite cartridges were developed [153], [154]. Lower concentrations were determined by HPLC-MS/MS by monitoring the transition of $[M+H]^+$ ion (416 m/z) to 194 m/z fragment [155]. A method for the direct injection of filtered lake samples is available. The LC-MS/MS equipped with triple quadrupole detects CYN with an LOD of 300 ng L⁻¹ [156]. Recently, CYN was determined simultaneously with 12 MCs, ANA and NOD [157]. Finally, hydrophilic interaction liquid chromatography coupled with mass spectrometry (HILIC-MS) is a more recent technique that can be used to detect polar compounds and thus can also be used for the determination of CYN [158].

5 Scope of this study

The objectives of this study were a) to set-up an ultrasonication apparatus for the degradation of organic compounds in small reaction volumes, b) to optimize the operational parameters and to study their effect in the production of oxidative species using chemical dosimetry, c) to effectively degrade CYN using ultrasound and to study the kinetics of the process under various conditions, c) to develop an analytical method using HPLC-PDA in order to monitor the degradation of CYN, e) to identify the transformation products of CYN during ultrasound degradation using LC-MS/MS.

First of all, a sonolytic device was set-up and optimized in order to degrade expensive, scarce or very toxic compounds. For this optimization 2,4-DCP was degraded as a model compound under various operational parameters. After that, two chemical dosimetry methods were used under various operation conditions. Initially, Fricke dosimetry was employed to study the total oxidative potential of the device followed by COU dosimetry, which selectively reacts with HO• that are the main ROS in ultrasound systems.

Additionally, a chromatographic method for the monitoring of CYN degradation in water was developed using HPLC-PDA. Different chromatographic columns and mobile phases were examined to establish a fast and reliable way to detect CYN.

CYN's degradation was performed under different conditions (sonication power, pH, concentration, presence of inorganic ions or organic matter). The kinetics of the process were studied and the kinetic constants and the initial reaction rates were calculated for each condition.

In addition, the zone of reaction where CYN is degraded in the mixture of sonolytically-produced bubbles and the bulk solution, was studied using different scavengers.

Finally, LC-MS/MS was used to identify the transformation products of CYN degradation and to propose their structure.

6 Experimental procedure

6.1 Materials and methods

6.1.1 Reagents

Cylindrospermopsin (CYN, #CAS: 143545-90-8) was purchased from Abraxis (Warminster, USA). Methanol (MeOH) of HPLC grade (99.9 %) was obtained from Fischer Scientific (Leics, UK) and acetonitrile (ACN) of gradient grade for HPLC (≥ 99.9 %) was obtained from Sigma-Aldrich (St. Louis, MO, USA). High purity water (18.2 M Ω -cm at 25°C) was produced on-site using a Temak TSDW 10 system (Temak S.A.). Sodium hydroxide (NaOH) 2 M and perchloric (VII) acid (HClO₄) were used for sample pH adjustment. NaOH was prepared from NaOH pellets (purity 98%) purchased from Sigma-Aldrich (Steinheim, Germany). Perchloric (VII) acid (HClO₄) was obtained from Riedel-de Haën (Seelze, Germany). Coumarin, 7-hydroxycoumarin, humic acids and terephthalic acid were purchased by Sigma-Aldrich (Steinheim, Germany). Methanoic acid (HCOOH) (>98%) and Trifluoroacetic acid (TFA) were purchased by Riedel-de Haën (Seelze, Germany). Ferrous sulfate (FeSO₄), sulfuric acid (H₂SO₄) and sodium chloride (NaCl) were purchased by Sigma-Aldrich (Steinheim, Germany).

6.1.2 Apparatus and Devices

The solutions were prepared, and the experiments were conducted using the following equipment:

- Customized glass reactor (test tube 25 cm long)
- Ring Stand and clamps
- Adjustable volume pipettes
 - 10 – 100 μ L, Eppendorf

- 100 – 1000 μ L, Eppendorf
- Volumetric flasks of 1, 5, 10, 25, 100 and 250 mL, A class
- Volumetric cylinders of 10, 25 and 500 mL
- Beakers
- 2 mL vials for autosampler with caps
- Glass electrode pH-meter
- Ultrasonic bath Bandelin sonorex super RK 106
- Ultrapure water Temak TSDW 10 system
- Glassware washer Miele Professional G7883

6.1.3 Instrumentation

An ultrasound generator K 80 equipped with Transducer E/805/T and Ultrasound Bath 5/1575 was employed for CYN's degradation, operating at 850 kHz frequency with nominal power 100W. During dosimetry a UV/VIS/NIR spectrometer (Lambda 19, Perkin Elmer) and a spectrofluorometer (FP-777, Jasco) were used. CYN's degradation was monitored in a HPLC system equipped with a photodiode array detector (HPLC-DAD, Waters Cooperation). The analytical columns examined were:

- Zorbax Eclipse XDB-C18, 4.6 x 150 mm, 3.5 μ m – Micron, Agilent Technologies, USA
- Kromasil 100-5C18, 150 x 2.1 mm, Nouryon, Sweden
- Hibar Pre-packed Column RT 250 – 4, LiChrospher 100, RP – 18, 5 μ m, MERCK, Germany

Identification of reaction intermediates of CYN was carried out using a Thermo Finnigan LC-MS/MS system (San Jose, USA) consisting of a Thermo Surveyor LC pump, a Thermo Surveyor AS autosampler and a TSQ Quantum Discovery MAX triple quadrupole mass spectrometer equipped with an electrospray ionization (ESI) interface operating in the positive ionization mode. Chromatographic separation was performed using a Kromasil 100-5 C18, 150 x 2.1 mm, reversed phase LC column.

6.2 Standard solutions preparation

Stock solution of CYN was prepared by dissolving 0.5 mg of solid CYN in 1 mL of ultrapure water. This solution was used for the preparation of standard working solutions after several dilutions. With these solutions the method was validated. After that, the CYN working solutions were prepared and degraded in the US system.

6.3 Analytical Method Development

CYN is a hydrophilic, highly soluble molecule, thus HPLC employed with a C-18 column is suitable for its determination. Based on its spectrum the selected wavelength was 262 nm.

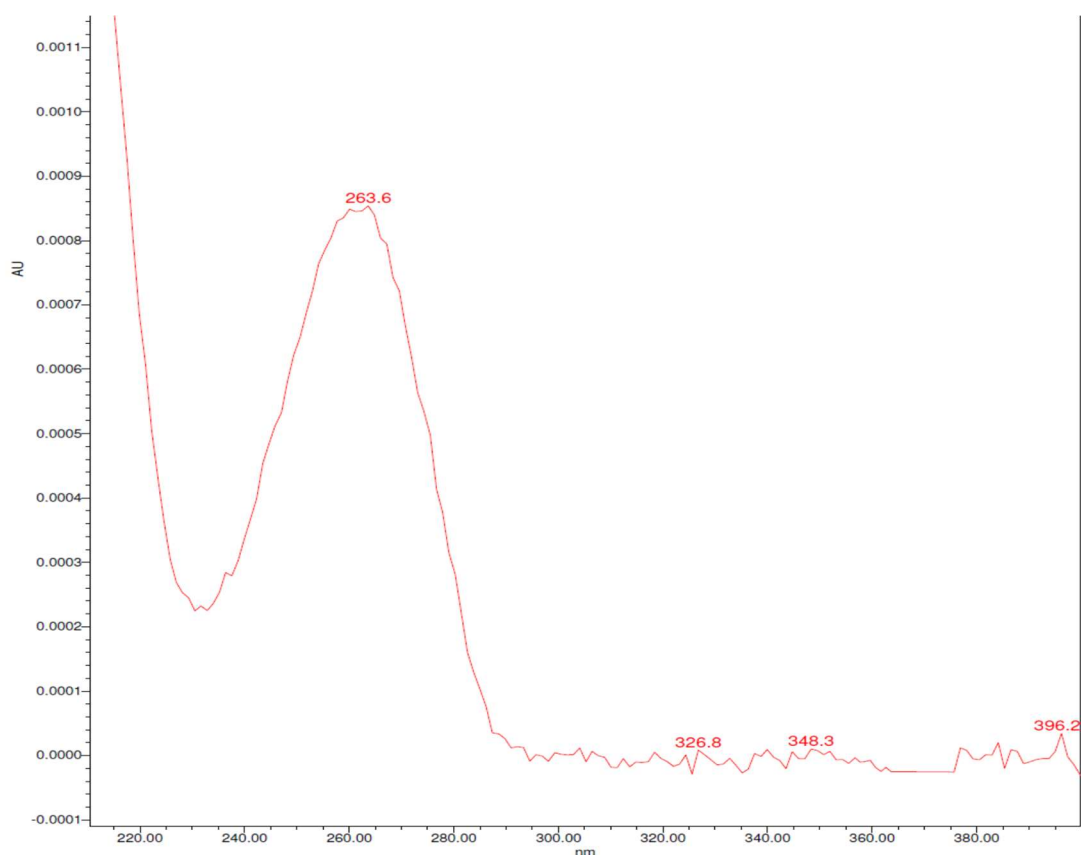


Figure 6-1: CYN's spectrum.

The chromatographic columns examined were:

- Zorbax Eclipse XDB-C18, 4.6 x 150mm, 3.5 μ m – Micron, Agilent Technologies, USA

- Kromasil 100-5C18, 150 x 2.1 μm , Nouryon, Sweden
- Hibar Pre-packed Column RT 250 – 4, LiChrospher 100, RP – 18, 5 μm , MERCK, Germany

At the selected column, a 2-day validation were performed for the final analytical method. The examined parameters are the following.

6.3.1 Calibration curve

Calibration is an essential part of most measurement procedures. It is a set of operations which establish, under specified conditions, the relation between indication and corresponding measured quantity value. Standard solutions of 50, 100, 250, 500 and 1000 $\mu\text{g L}^{-1}$ were analyzed 3 times each and the results fitted to a calibration curve used for the determination of CYN concentration in all samples.

6.3.2 Repeatability

Repeatability is defined as the proximity of agreement between independent test results, obtained with the same method, on the same test material, in the same laboratory, by the same operator, and using the same equipment within short intervals of time. The repeatability of the method (intra-assay precision) was evaluated by assaying 7 replicate injections of CYN at the same concentration (250 $\mu\text{g L}^{-1}$), during the same day, under the same experimental conditions.

6.3.3 Limit of Detection & Limit of Quantitation

The limit of Detection (LOD) is the lowest concentration of analyte that can be detected and reliably distinguished from zero (or the noise level of the system), and it is taken typically as three times the noise level for techniques with continuous recording. Also, it is commonly estimated from the mean and standard deviation of the replicate blank readings by using the expression: $\text{LOD} = Y_{\text{blank}} + 3S_{\text{blank}}$.

6.4 Sonolytical device description

6.4.1 Full extent and small-scale device

The ultrasound bath 5/1575 has a maximum volume of 500 mL and cooling water flows outside the walls throughout the experiment.

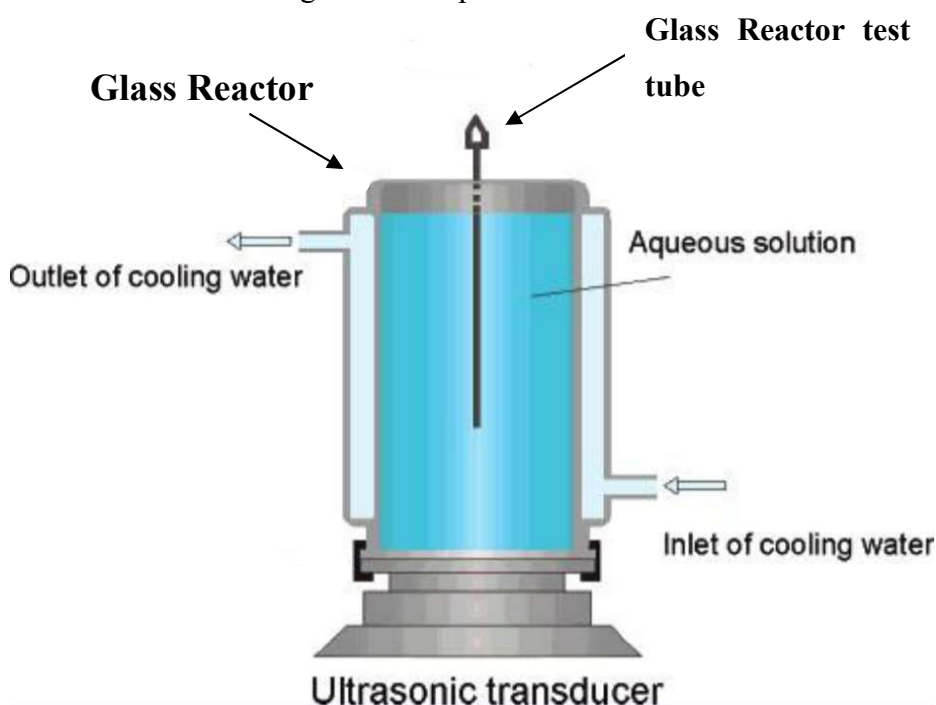


Figure 6-2: Apparatus used for experimental procedure.

A small tube was immersed in the bath which was filled with water as the transducer E/805/T cannot operate without liquid. With this addition it is possible to degrade expensive compounds in solutions of small volume (5 or 10 mL). It is also possible to use extreme pH as the transducer will not be directly to the acidic solution.

6.5 Optimization of Ultrasonic Reactor

6.5.1 Initial operation check

The optimal position for this tube (vertical and horizontal position) and its material (plastic or glass) were examined using 2,4-Dichlorophenol (2,4-DCP), which is frequently used as a model compound for the study of oxidative treatment processes. The experiments were

conducted using 10 mL of 2,4-DCP of 1 mM initial concentration. For the determination of the optimal position, 3 different spots in the vertical arrangement and 3 in the horizontal were examined. Additionally, reactors with different material (glass or plastic) were evaluated .

2,4-DCP was monitored in the HPLC-PDA system using a method previously developed in the lab.

6.5.2 Dosimetry

Two dosimeters, the Fricke solution dosimeter and the COU dosimeter were employed to understand the operation of this sonolytical reactor. At first, Fricke solution was used since it provides an indication of the total oxidative potential of the system and then COU which reacts selectively with the HO•.

6.5.2.1 Fricke solution

Fricke solution is made of FeSO₄ 0.001 M, H₂SO₄ 0.4 M and NaCl 0.001 M. The concentration of produced ferric ions (Fe³⁺) was measured spectrophotometrically at 305 nm using a 1 cm cell at specific experimental times. As the transducer could not be exposed at acidic pH all the Fricke solution experiments were conducted in the glass tube. Different parameters were examined: sonication power, surrounding liquid volume and the distance from the transducer.

6.5.2.2 Coumarin

Coumarin working solution was prepared by diluting solid coumarin in ultrapure water. Working solution concentration was 1 mM. Both the degradation of coumarin (COU) and the production of 7-hydroxycoumarin (7-OH-COU) were monitored at several experimental times. The decreased concentration of COU was measured spectrophotometrically at 275 nm after diluting the sample 10 times. The (7-OH-COU) produced was monitored fluorespectrophotometrically. The excitation λ is 332 nm and the luminescence intensity was measured at 456 nm. In both cases a 1 cm quartz cell was used. The experiments were conducted in the glass tube. Several experimental parameters were examined: sonication power, solution's volume, outside liquid volume and the distance from the transducer.

The spectrofluorometer gives only analogue data so a MATLAB code was developed to transform the analogue spectrum into digital data.

6.6 Experiments of CYN degradation

6.6.1 Kinetics of CYN degradation

CYN's degradation experiments were conducted with samples of 1 mg L⁻¹ initial CYN concentration. 5 mL of the sample were placed on the glass tube and the bath was filled with 250 mL ultrapure water. Sonication power, initial CYN's concentration, pH, bottled water matrix and presence of humic acids were examined. Samples were taken at several times and the degradation was monitored in the HPLC-PDA system.

For the determination of sonolytic degradation of CYN the first order kinetic model was evaluated. The time-based pseudo-first order rate constants (k_{obs}) were determined according to Eq.

$$\ln[C/C_0] = -k_{obs}t$$

where C is the concentration of CYN and C₀ is the initial concentration of CYN. For the calculation of the initial reaction rate, only the experimental data of first 30 min were obtained, in order to avoid the gradual contribution of transformation products.

6.6.2 Localization

To further understand the role of HO• and the different reaction zones produced during the ultrasonically induced degradation of CYN, HO• scavengers, terephthalate (TA) and tert-butyl alcohol (TBA), were added prior to irradiation. The TA is anionic in working pH, so it is expected to scavenge the radicals at the bulk solution, while the TBA scavenges the radicals inside and on the surface of the bubble. Two different concentrations of each were examined, namely 50 and 5000 times higher than CYN's concentration.

6.7 Determination of CYN

6.7.1 Chromatographic conditions for degradation monitoring

The analytical column used is Hibar Pre-packed Column RT 250 – 4, LiChrospher 100, RP – 18, 5 μm , MERCK, Germany. The column temperature was adjusted at $25 \pm 1^\circ \text{C}$ and the injection volume at 40 μL . Isocratic elution was performed and the mobile's phase composition was MeOH (+ 0.01 % HCOOH) : H₂O (+ 0.01 % HCOOH), 10 % : 90 %. The flow was 0.8 mL min⁻¹ and the CYN's retention time was 4.5 min. The method was validated for these conditions.

6.7.2 Mass spectrometry parameters for determination of transformation products

Detection was performed in full scan mode (100–520 m/z). High-purity nitrogen was used as sheath and auxiliary gas and argon was the collision gas. For full MS scan spectrum, the selected precursor ions were isolated with an isolation width of 1 Da and product ions were formed with collision energy of 30 eV. Chromatographic separation was performed using a Kromasil 100-5 C18 (5 μm , 150 mm x 2.1 mm) reversed-phase LC column. Mobile phase solutions were A: 97.8% H₂O, 2% acetonitrile, 0.2% acetic acid and B: 99.8% acetonitrile and 0.2% acetic acid. Gradient elution was programmed as 2% B for 10 min, followed by a linear increase to 95% B in 50 min and then held constant for an additional 10 min. Flow rate was set at 0.2 mL min⁻¹ and injection volume was 100 μL .

7 Results and Discussion

7.1 Method development for the chromatographic determination of CYN

7.1.1 Column Selection

The chromatographic parameters that were examined are described in Table 7-1. The chromatographic columns Zorbax XDB Eclipse 4.6x150 mm, 3.5 μ m, Kromasil 100 SC-18 150x2.1 mm, 5 μ m and Hibar Pre-packed Column RT 250 – 4, LiChrospher 100 were tested.

Table 7-1: Columns examined for CYN determination.

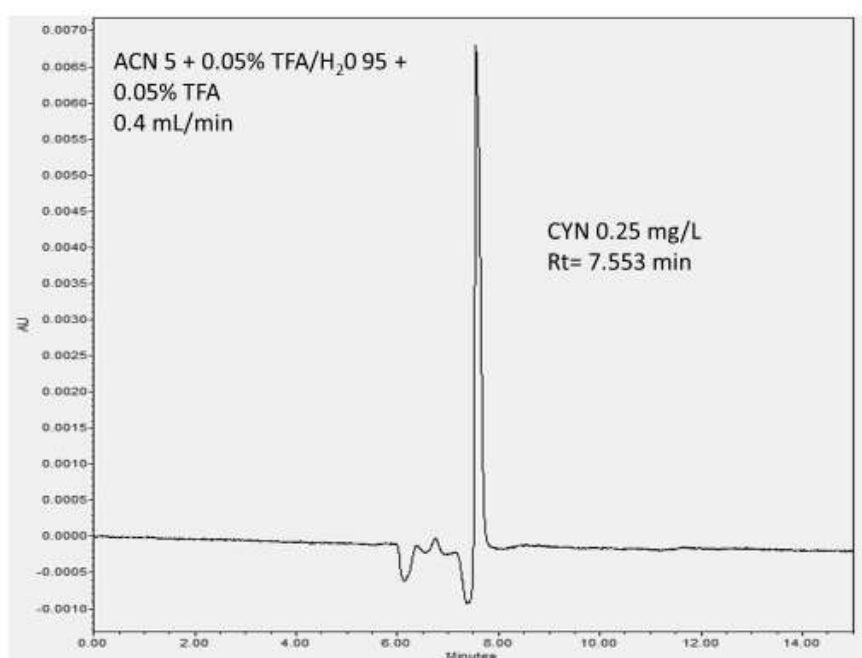
Column	Mobile phase	Flow	Injection Volume	Dead Volume	Retention time (CYN)
Zorbax XDB Eclipse 4.6x150 mm 3.5 μ m	H ₂ O (0.05% TFA) 95% - ACN (0.05% TFA) 5%	0.8 ml/min	50 μ L	1.5 min	Dead volume
	H ₂ O (0.05% TFA) 98% - ACN (0.05% TFA) 2%	1 ml/min	50 μ L	1.5 min	Dead Volume

Kromasil 100 SC-18 150x2.1 mm 5 µm	H ₂ O (0.05% TFA) 98% - ACN (0.05% TFA) 2%	0.35 ml/min	40 µL	1.8 min	2.7 min
	H ₂ O (0.05% TFA) 97% + ACN (0.05% TFA) 3%	0.4 ml/min	40 µL	1.8 min	2.6 min
Hibar Pre- packed Column RT 250 – 4, LiChrospher 100	H ₂ O (0.05% TFA) 95% - ACN (0.05% TFA) 5%	0.4 ml/min	20 µL	7.8 min	Dead Volume
	H ₂ O 95% - MeOH 5%	0.8 ml/min	40 µL	3.3 min	10.1 min
	H ₂ O 90% - MeOH 10%	0.8 ml/min	40 µL	3.4 min	5.1 min
	H ₂ O (0.05% TFA) 90% + MeOH (0.05% FA) 10%	0.8 ml/min	40 µL	3.3 min	4.8 min
	H ₂ O (0.01% FA) 90% + MeOH	0.8 ml/min	40 µL	3.2 min	4.4 min

	(0.01% FA) 10%				
--	-------------------	--	--	--	--

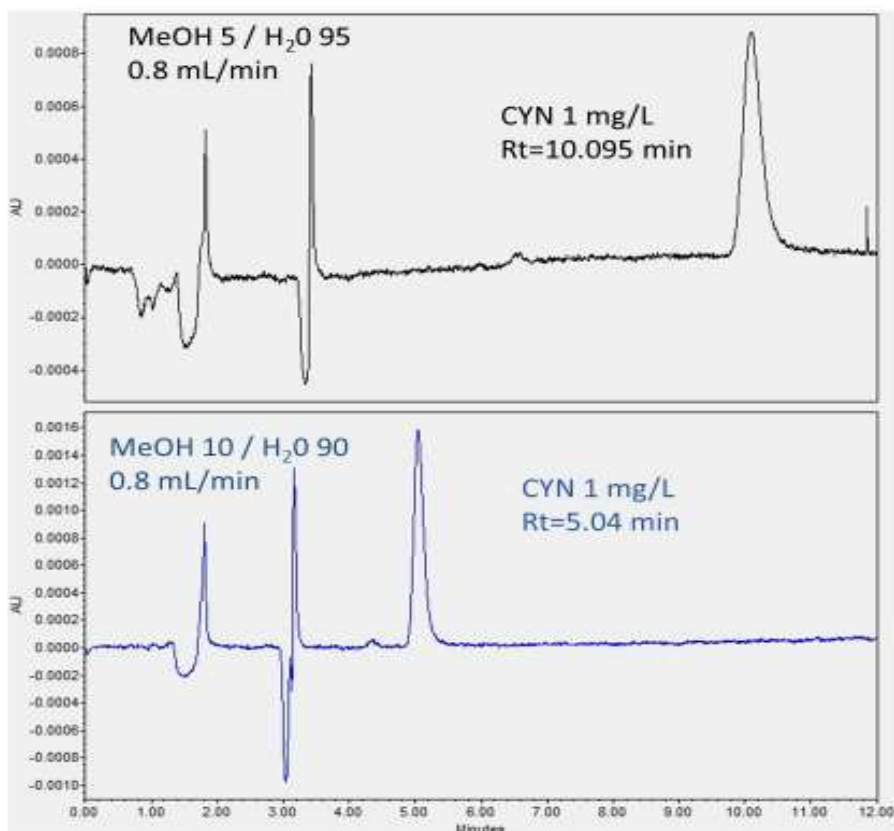
When Zorbax XDB Eclipse 4.6x150 mm 3.5 μm is used, CYN is eluted in the dead volume.

When Hibar Pre-packed Column RT 250 – 4, LiChrospher 100 was examined with a mobile phase that consisted of ACN (0.05% TFA) 5% / H₂O (0.05% TFA) CYN was eluted in the dead volume as shown in the following chromatogram (Chromatogram 7-1).



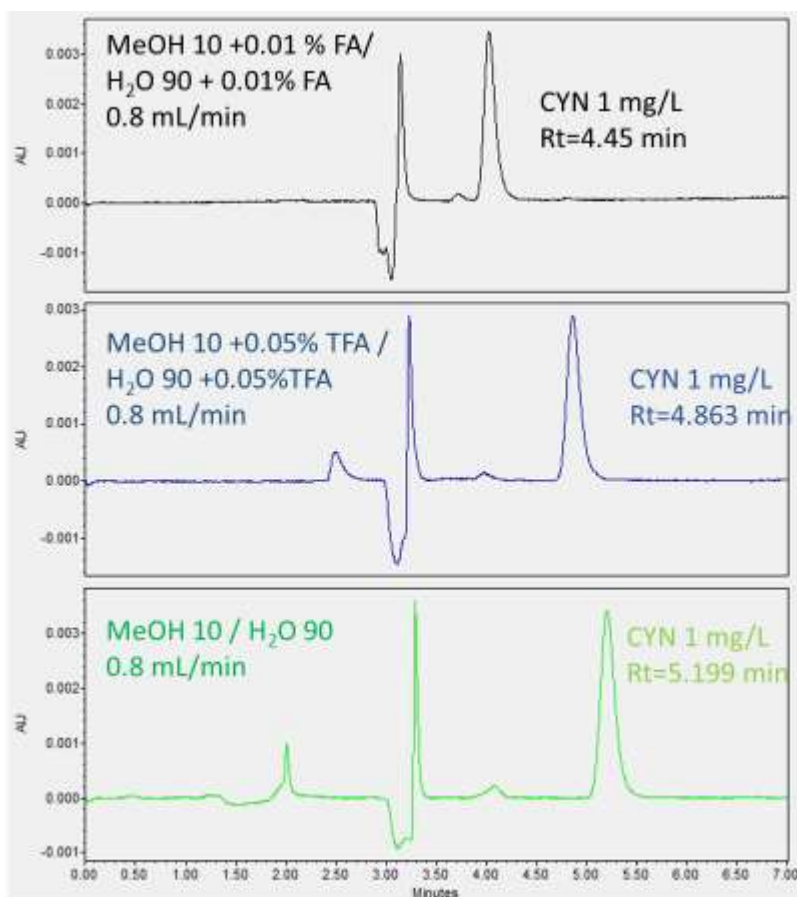
Chromatogram 7-1: CYN elutes at the dead volume when the mobile phase is ACN (0.05% TFA) 5% / H₂O (0.05% TFA).

CYN eluted a bit later than the dead volume when methanol (MeOH) was used instead of acetonitrile (ACN) maintaining the same chromatographic conditions (Chromatogram 7-2). When water was increased (95%) in the eluent system, CYN eluted after 10.1 min whereas when the water percentage was 90% CYN eluted faster (after 5.1 min). A fast method is preferable for the purpose of this study, so the mobile phase composition was 90% H₂O and 10% MeOH with flow rate 0.8 mL min⁻¹ for the rest of the experiments.



Chromatogram 7-2:CYN retention time in H₂O 95% + MeOH 5% and H₂O 90% + MeOH 10%.

Formic acid (FA) 0.01% and trifluoroacetic acid (TFA) 0.05%, which are compatible with LC-MS, were added to the mobile phase in order to keep the pH of the eluent acidic. Among them FA was selected because it led to a sharper chromatographic peak and a stronger signal as shown in Chromatogram 7-3.



Chromatogram 7-3: CYN's elution in the presence of 0.01% FA (a), 0.05 TFA (b) and without acid (c).

Based on these data, the selected chromatographic method has a Hibar Pre-packed Column RT 250 – 4, LiChrospher 100 chromatographic column with a mobile phase that consisted of H₂O (0.01% FA) 90% and MeOH 10% (0.01% FA). When the flow rate is 0.8 mL min⁻¹ CYN is eluted after 4.5 min. A method validation was performed using the above mentioned parameters.

7.1.2 Calibration Curve

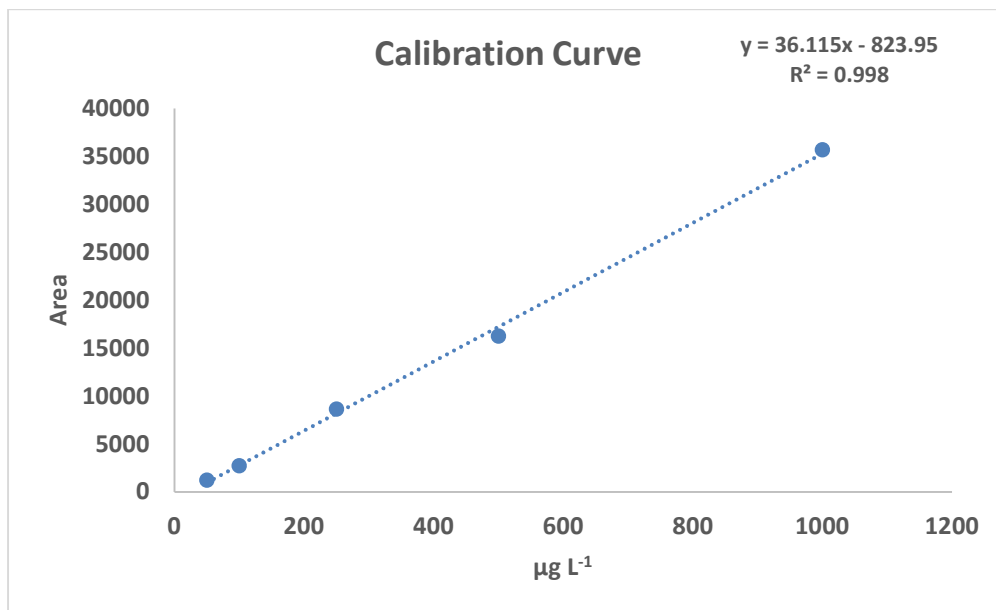
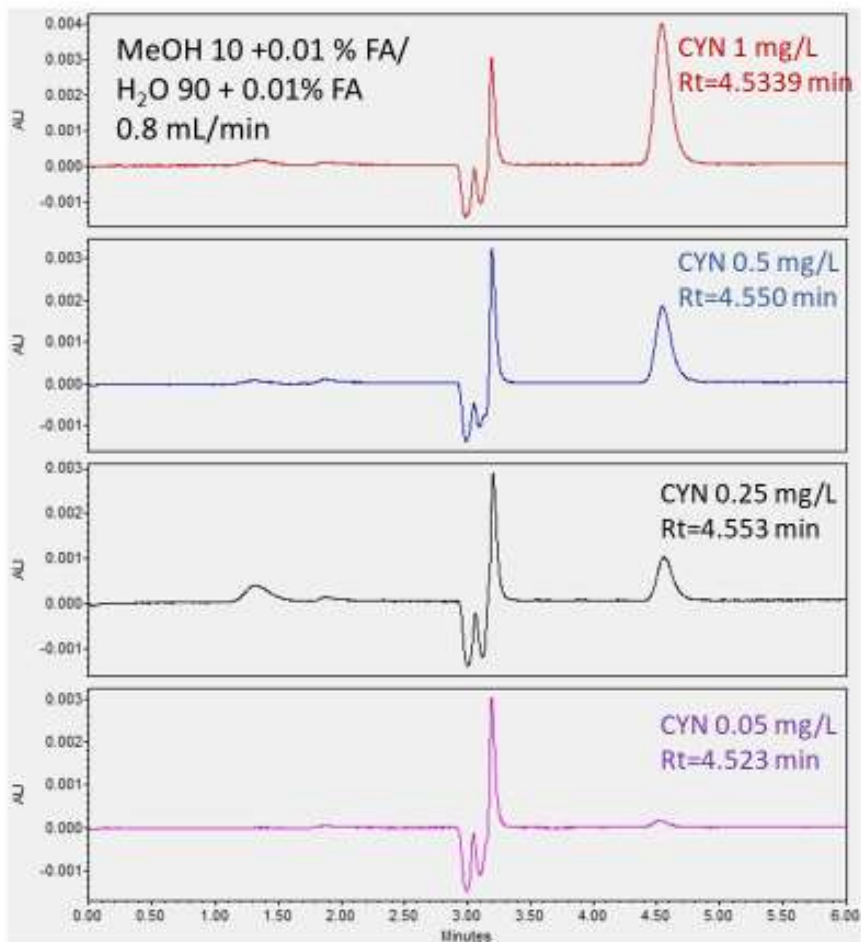


Figure 7-1: Calibration curve with concentrations range from 50 to 1000 µg L⁻¹.

CYN's response is linear at range from 50 to 1000 µg L⁻¹. The coefficient of determination (R^2) was higher than 0.995. The chromatograms of CYN's different concentration standards are shown below (Chromatogram 7-4).



Chromatogram 7-4: Calibration curve's chromatograms.

7.1.3 Repeatability

A 250 $\mu\text{g L}^{-1}$ CYN standard solution was injected 7 times and the results are shown in table 72. The % RSD for the retention time and the peak area were both under 1%, which is considered rather satisfactory for an LC method.

Table 7-2: Method Repeatability

Injection Number	R _t (min)	Peak Area
1	4.52	8664
2	4.55	8625
3	4.55	8823
4	4.52	8863
5	4.54	8716
6	4.53	8680
7	4.50	8684
Average	4.53	8722
Standard Deviation	0.018	81
% RSD	0.394	0.93

7.1.4 LOD-LOQ

The LOD was calculated based on the equation: $LOD = t_{(n-1, 0.95)} * SD$ from repeated measurements of standard solutions ($50 \mu\text{g L}^{-1}$) using the formula where $t_{(n-1, 0.95)}$ was the t-test value for n-1 degrees of freedom at 95% confidence level and SD was the standard deviation of measurement. The LOQ was calculated as 3 times the LOD. Thus, the LOD of the method is $3 \mu\text{g L}^{-1}$ and the LOQ $9 \mu\text{g L}^{-1}$.

Table 7-3: LOD & LOQ determination.

LOD-LOQ			
7 injections of CYN 50 µg L ⁻¹			
	RT	Peak Area	C (µg L ⁻¹) [calibration curve]
SD	0.02	55.26	1.53
LOD= $t_{(n-1,0.95)} \times SD =$			3.0
LOQ= $3 \times LOD =$			9.0

7.2 Optimization of Ultrasonic Reactor

7.2.1 Initial operation check

The manufacturer instructions for the ultrasonication reactor state that the preferable operational temperature should not exceed 40⁰C. During the experiments with the glass reactor tube, the solution temperature remained at 30-35⁰C. The temperature of the solution during the initial experiments with the plastic PE tube reached 43⁰C, therefore the glass reactor tube was selected.

The position of the glass reactor tube in the ultrasonication apparatus was also an important factor. The proximity of the tube to the ultrasonication transducer or the walls of the sonicator apparatus, are directly related to the degradation rate of the model compound 2,4 DCP.

Figure 7-2 shows the differences in the degradation profile of model compound 2,4 DCP, when the tube is located at different distances from the transducer. The experiments were conducted with 5 mL 2,4-DCP 1 mM. The surrounding water was 250 mL and the acoustic power 100% of the nominal.

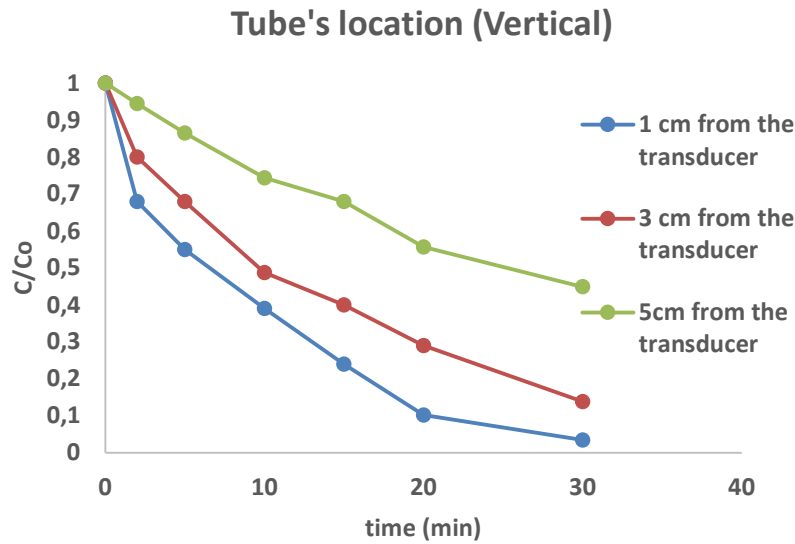


Figure 7-2: Degradation of 2,4-DCP in relation to irradiation time at different distances from the transducer ($C_0=1$ mM, 5 mL volume & 250 mL surrounding water. Acoustic power 100% of the nominal)

Figure 7-3 shows the differences in the degradation profile of model compound 2,4 DCP, when the tube is located at different distances from the walls of the ultrasonicator water tank.

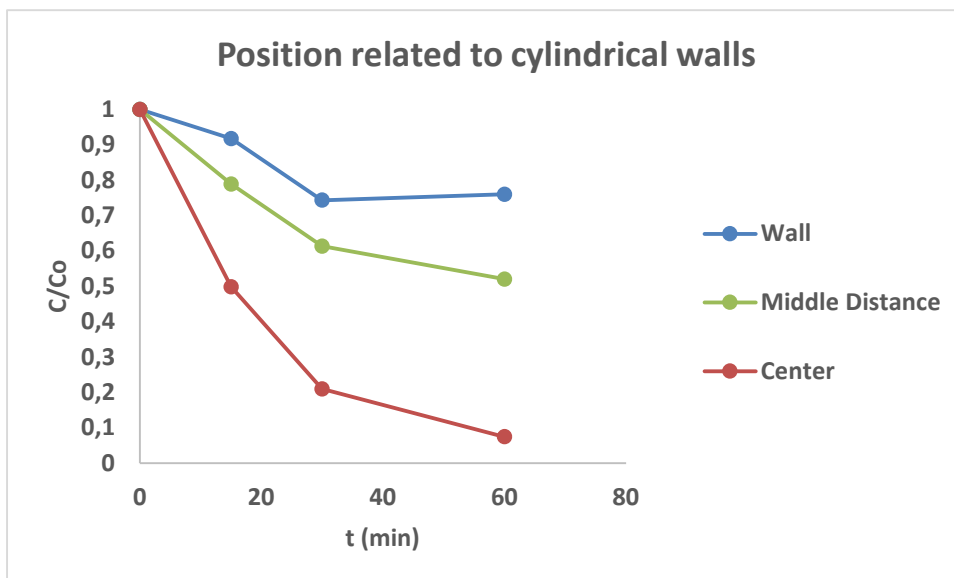


Figure 7-3: Degradation of 2,4-DCP after several irradiation time at different horizontal positions ($C_0=1$ mM, 5 mL volume & 250 mL surrounding water. Acoustic power 100% of the nominal).

As it is obvious, the maximum degradation was achieved at 1 cm distance from the transducer and in the center of the water tank.

For the rest of the experiments the tube was adjusted in a repeatable way at 1 cm distance and in the centre of the water bath, where the maximum degradation of the model compound is achieved, except when noted differently.

7.2.2 Chemical Dosimetry

Fricke dosimeter and COU were employed to understand the kind and function of ROS produced by the sonicator under several experimental conditions (sonication power, water volume, distance from the transducer).

7.2.2.1 Fricke Dosimetry

In Fricke dosimeter the yield can be expressed as a linear combination of the yields of radicals produced by the sonication energy [$G(\text{Fe}^{3+}) = G(\text{HO}\cdot) + 2G(\text{H}_2\text{O}_2) + 3G(\text{HO}_2\cdot)$]. Thus, the concentration of the produced Fe^{3+} gives the total oxidative potential of the method.

7.2.2.1.1 Effect of Sonication Power

These experiments were conducted with 5 mL Fricke solution consisted of 1 mM ferrous ammonium sulphate and 1 mM sodium chloride in 0.4 M sulfuric acid. The volume of water outside the tube was 250 mL and the tube was adjusted at 1 cm from the transducer. The Sonication Power effect was examined.

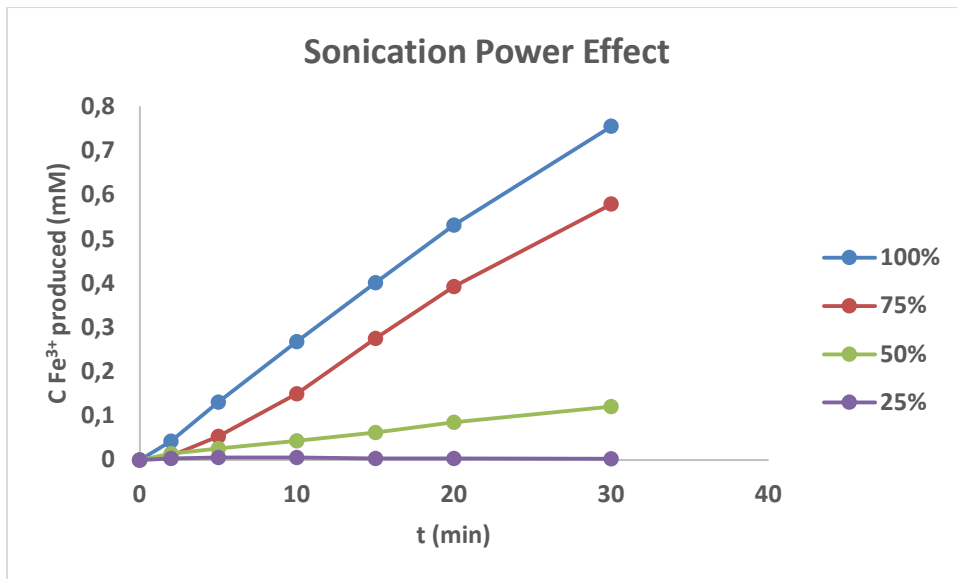


Figure 7-4: Concentration of Fe³⁺ produced under different operation sonication powers (5mL solution volume & 250 mL surrounding water, 1 cm distance from the transducer).

When the sonication power was the only parameter that changed greater production of Fe³⁺ occurred under higher nominal sonication power. There is no linear correlation between the applied sonication power and the production rate as shown in figure 7-5.

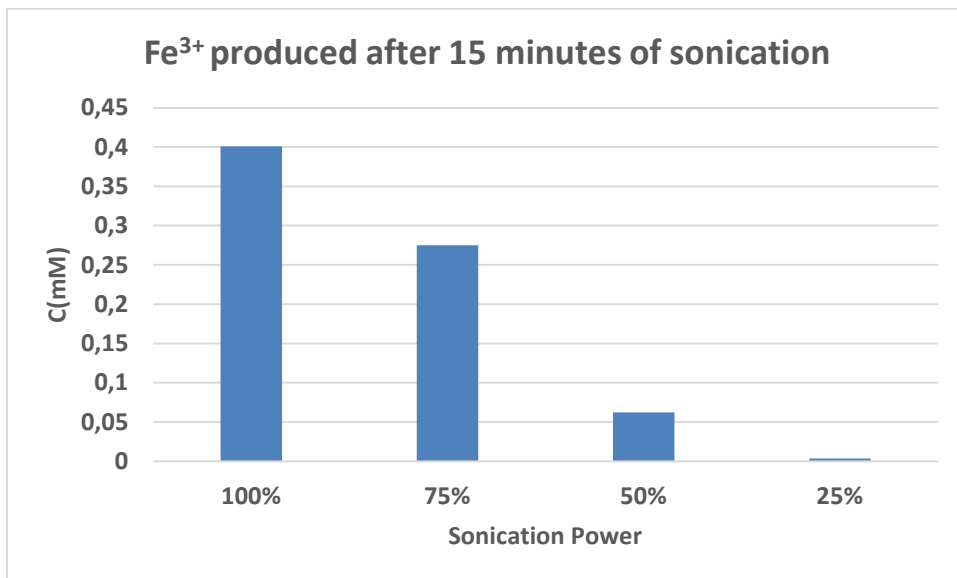


Figure 7-5: Produced Fe³⁺ under different sonication power after 15 minutes of sonication (5 mL solution volume & 250 mL surrounding water, 1 cm distance from the transducer).

A characteristic spectrum of the produced Fe³⁺ is shown in the Appendix (Figure A-1).

7.2.2.1.2 Volume of water outside the tube

The effect of the surrounding water was examined by sonicating Fricke solutions of 1 mM ferrous ammonium sulphate and 1 mM sodium chloride in 0.4 M sulfuric acid. The acoustic power was 100% of the nominal and the transducer adjusted at 1 cm from the transducer.

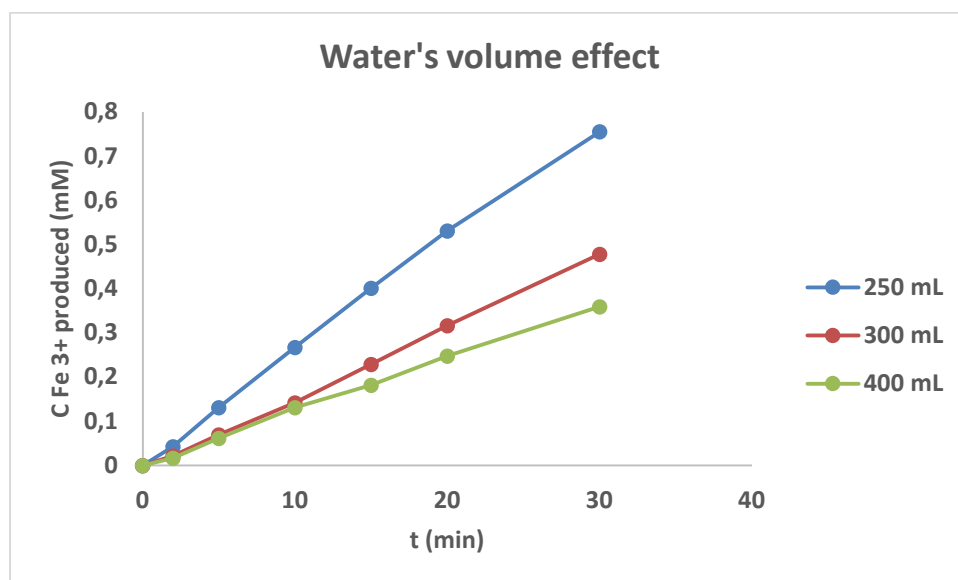


Figure 7-6: Effect of the volume of water on the amount of Fe³⁺ produced (5 mL solution volume, 100% nominal acoustic power, 1 cm distance from the transducer).

The volume of the surrounding water affects the Fe³⁺ production (Figure 7-5). The greater the volume, the less Fe³⁺ produced. The water seems to consume some amount of the acoustic energy produced. Therefore, it is important to use the same external water volume in all the experiments that will be carried out. A 250 mL water volume was selected for the rest of the experiments to ensure that the glass reactor tube is immersed in the water bath, the level of reaction solution inside the glass reactor is also lower than the level of the water bath and the transducer is satisfactorily cooled down.

7.2.2.1.3 Distance of glass reactor from the transducer

The experiments were conducted with 1 mM ferrous ammonium sulphate and 1 mM sodium chloride in 0.4 M sulfuric acid. The sonication power was 100% of the nominal and the surrounding water was 250 mL.

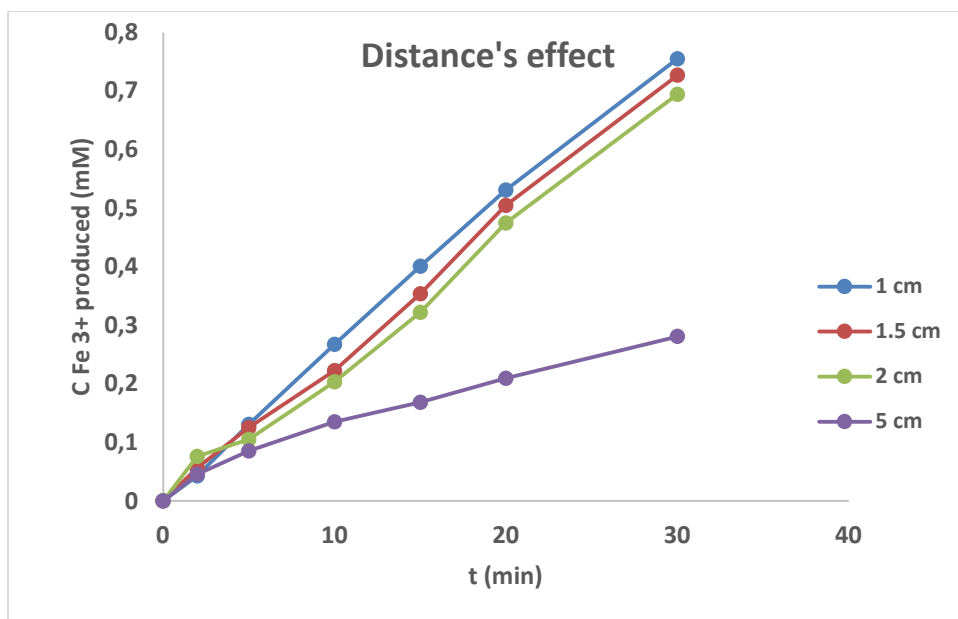


Figure 7-7: Effect of the distance from the transducer (5 mL solution volume & 250 mL surrounding water, 100% nominal acoustic power).

A closer tube's distance affects the production of Fe^{3+} indicating that the ROS production is not equal under all the possible positions of the tube (Figure 7-7). So, it is crucial for the compound degradation experiments to fix the position of the tube.

Based on the above, the preferable position of the glass reactor tube and the operational parameters were: 100% of the nominal sonication power, 250 mL surrounding water and 1 cm distance of glass reactor from the transducer.

7.2.2.2 Coumarin

The experiments with COU further confirm the conclusion based on the Fricke experiments for the sonication power effect, the water's volume and the distance of the glass tube from the transducer. COU reacts selectively with $\text{HO}\cdot$ and the production of 7-OH-COU follows the trend of Fe^{3+} production under distinct experimental conditions.

Table 7-4: Rate of production of Fe³⁺ and 7-OH-COU

Condition	rate of Fe³⁺ production (mM/s)	rate of 7-OH-COU production (μM/s)
Nominal Energy		
100%	0.0004	0.0002
75%	0.0003	0.0001
50%	7.00E-05	2.00E-05
25%	6.00E-08	
Surrounding Water		
250 mL	0.0004	0.0002
300 mL	0.0003	0.0001
400 mL	0.0002	0.00005
Distance from the transducer		
1 cm	0.0004	0.0002
1.5 cm	0.0004	0.0002
2 cm	0.0004	0.0002
5 cm	0.0002	9.00E-06

Moreover, the simultaneous monitoring of the degraded COU and the produced 7-OH-COU (spectra are shown in Appendix Figure A-2 & A-3) have shown that the amount of 7-OH-COU produced is equal to 1% of the degraded COU, when the power intensity is 100W.

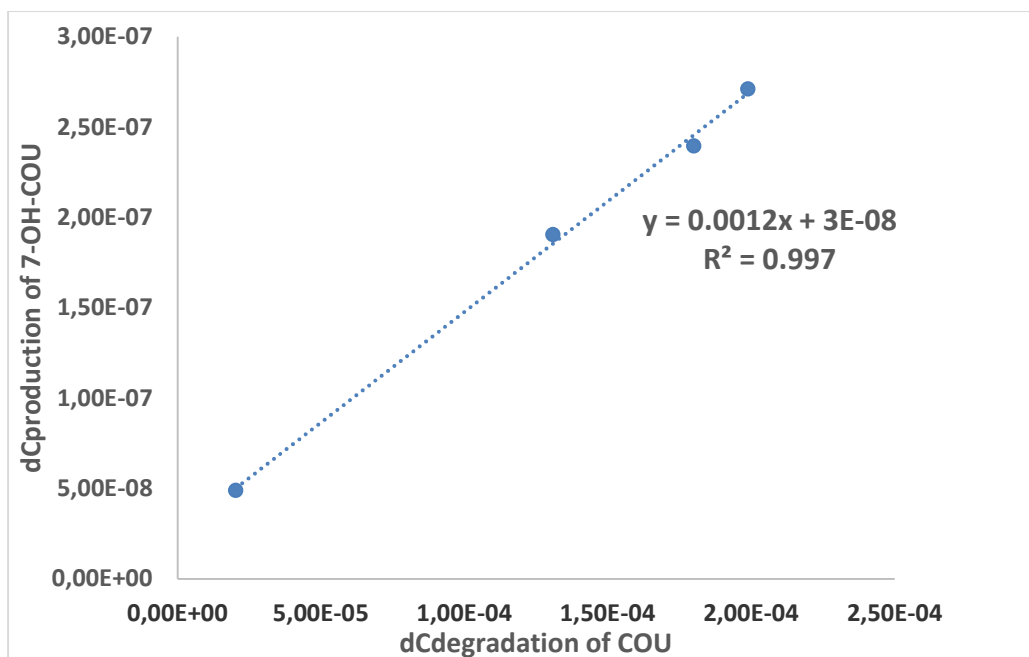


Figure 7-8: Concentration of the produced 7-OH-COU vs concentration of the COU degraded.

In a previous study at 500 kHz with 50 W, the 7-OH-COU produced was about 1% of the coumarin disappeared [138] indicating that other parameters except frequency and power are important for the degradation.

The reaction of COU with HO• is not 1:1 as 7-OH-COU is not the only produced hydroxycoumarin but the only fluorescent. Thus, the COU dosimeters cannot be used for the direct quantification of the HO• produced by the sonicator.

7.3 CYN sonolytic degradation

7.3.1 Effect of ultrasonication power

Firstly, CYN solutions of 1 mg L⁻¹ were degraded under different nominal sonication power to test its degradation.

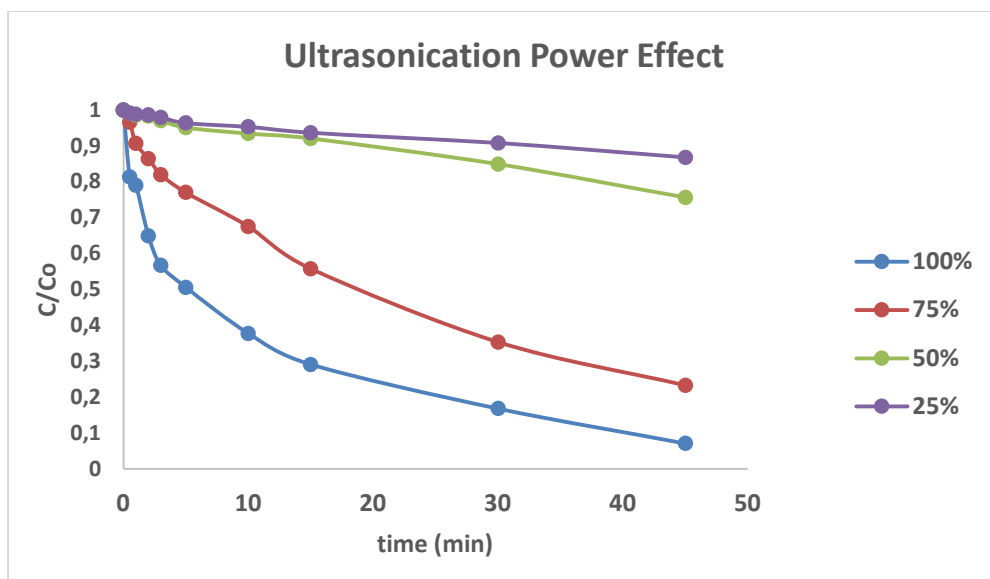
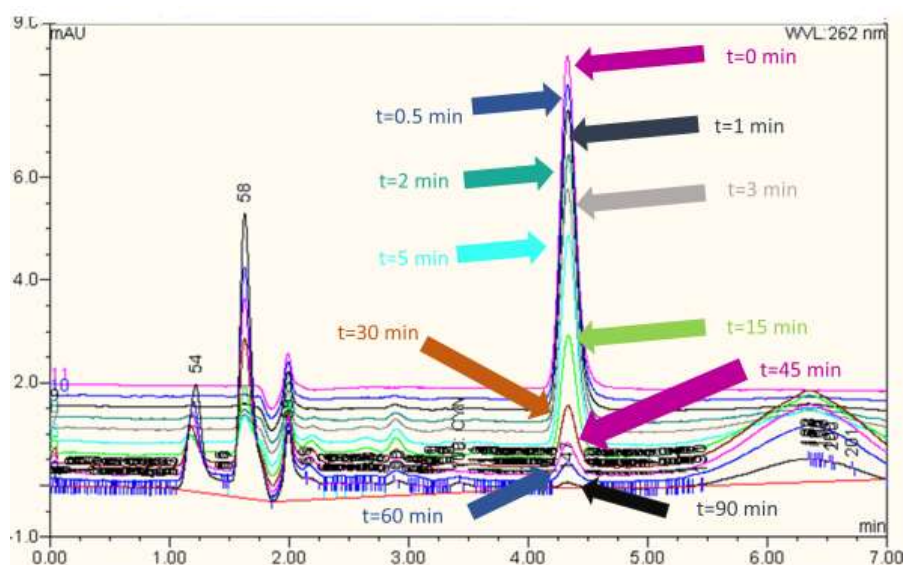


Figure 7-9: Effect of power intensity on CYN's degradation (5 mL CYN 1 mg/L, surrounding water 250 mL, pH=5.8).

Figure 7-9 shows CYN's degradation under 4 nominal sonication powers. When the system operates in higher nominal power intensity the degradation is greater and faster. There is no linear connection between the nominal power intensity and the amount of the degraded CYN because there are also other parameters i.e. frequency affecting the production of radicals. This trend is in agreement with previous results for the degradation of compounds under several acoustic intensities [159]. A chromatogram of a degradation experiment is shown below (Chromatogram 7-5).



Chromatogram 7-5: CYN degradation overlaid chromatograms.

7.3.2 pH effect

CYN can be found in the environment in lakes and water receivers where the pH is slightly higher than the pH of the standard solutions. This is why degradation was also examined in neutral and slightly alkaline solutions with pH values of 7, 8 and 9.

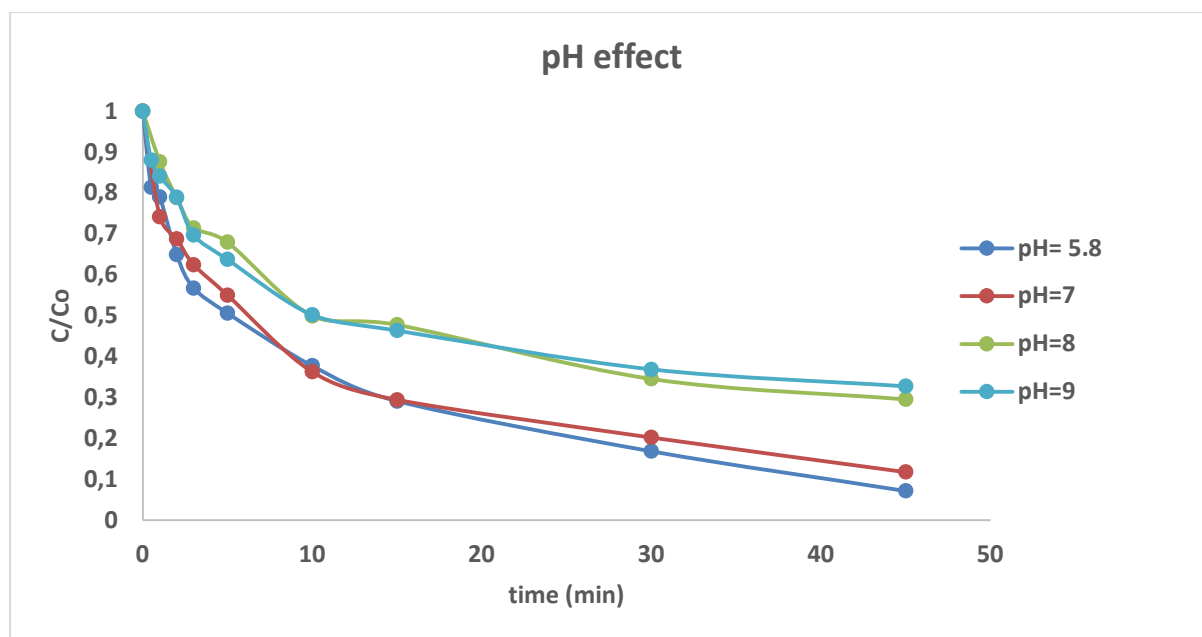


Figure 7-10: pH effect on CYN's degradation (5 mL CYN 1mg L⁻¹, 250 mL surrounding water, 100% nominal sonication power).

Figure 7-10 shows the degradation of CYN under different pH values. Degradation at higher pH values (8 & 9) leads to slightly slower degradation, possibly due to the partial recombination of HO• to form H₂O₂ [160].

The ionic form of organic compounds under different pH values, is an important factor in determining sonochemical degradation kinetics at different pH conditions [161]. As shown in figure 7-11, at pH values lower than 8, there is only one dominant ionic form of CYN. The degradation profile of CYN under pH 5.8, 7, 8 and 9 (Figure 7-10) does not present significant differences, that could be attributed to various ionic forms of CYN present in the solution.

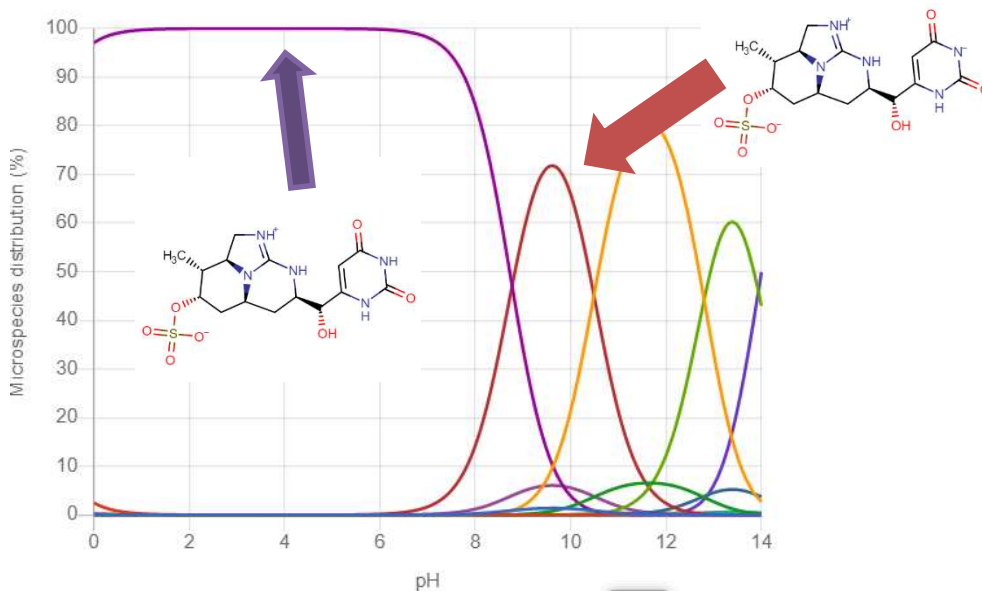


Figure 7-11: CYN's microspecies distribution under different pH values.

7.3.3 Effect of CYN initial concentration

The effect of the initial concentration of CYN was tested by degrading samples of different initial concentration (0.5, 1 and 2 mg L⁻¹)

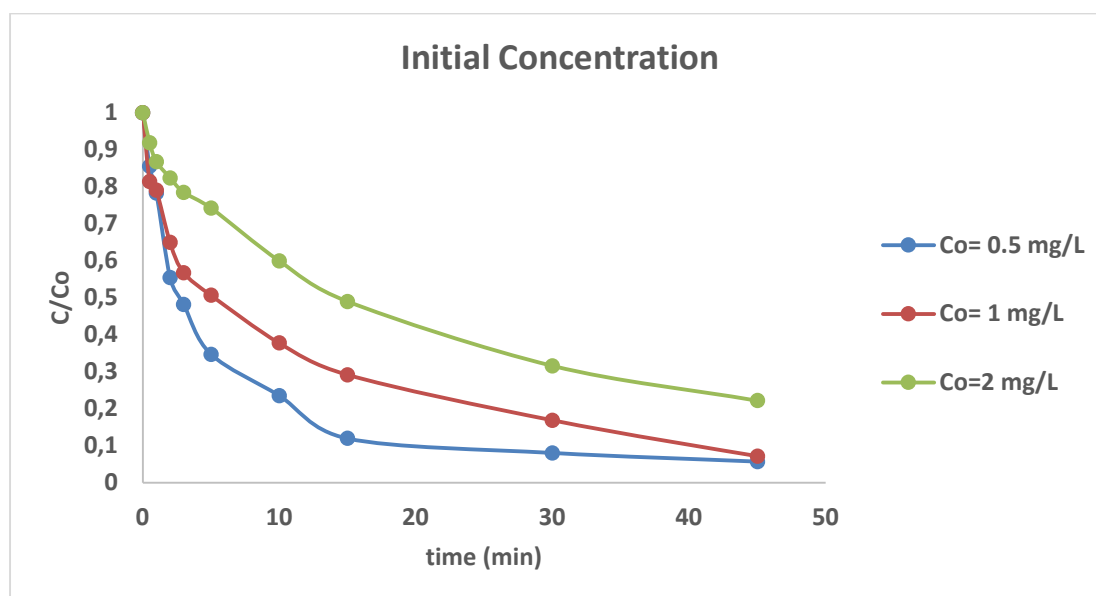


Figure 7-12: Initial concentration Effect during CYN's degradation (5 mL CYN, 250 mL surrounding water, 100% nominal sonication power)..

As shown in figure 7-12, at lower concentrations CYN is degraded at faster rates. Total CYN degradation occurs under 15 min at initial concentration of 0.5 mg L⁻¹.

7.3.4 Application in real water matrices

Ultrasonication of CYN water solutions in real water matrices were carried out, to examine the effect of the present inorganic compounds. Initially experiments were realised using bottled water, which contains various ionic substances that could potentially hinder the process.

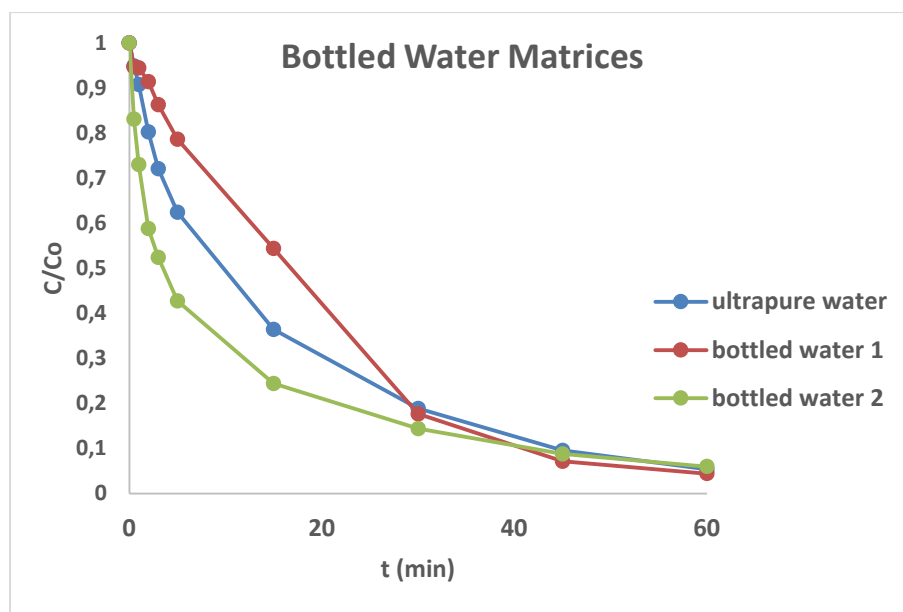


Figure 7-13: CYN's degradation under different water matrices (5 mL CYN 1mg L⁻¹, 250 mL surrounding water, 100% nominal sonication power).

The chemical analysis of the bottled water is shown in the table below (Table 7.4)

Table 7-5: Chemical Analysis of Selected bottled Waters.

	Bottled Water 1	Bottled water 2
HCO ₃ ⁻ (mg L ⁻¹)	237.9	145
Cl ⁻ (mg L ⁻¹)	3.84	<5
NO ₂ ⁻ (mg L ⁻¹)	0.0	<0.05
SO ₄ ²⁻ (mg L ⁻¹)	7.92	<5
NO ₃ ⁻ (mg L ⁻¹)	1.05	1.5
F ⁻ (mg L ⁻¹)	0.07	-

Ca²⁺ (mg L⁻¹)	75.5	47.7
Mg²⁺ (mg L⁻¹)	5.10	0.1
NH⁴⁺ (mg L⁻¹)	0.0	<0.1
Na⁺ (mg L⁻¹)	2.10	1.2
K⁺ (mg L⁻¹)	0.65	0.3
TDS (mg L⁻¹)	254	130
Conductivity (μS cm⁻¹)	356 (20 °C)	238 (25 °C)
Total Hardness (CaCO₃) (mg L⁻¹)	210	119
pH	7.5	8.0

As shown in Figure 7-13, the degradation is affected by the matrix. In bottled water 2 the degradation is enhanced whereas in bottled water 1 it is delayed but in both matrices full degradation is achieved after 60 minutes of sonication.

Previous studies have shown that the presence of sulphate ions does not have any effect on the degradation rate [162] while the bicarbonate ion is a well-known HO• radical scavenger, whose reaction produces the carbonate radical [163]. The carbonate radical can migrate towards the bulk of the solution and therefore induce the degradation of the pollutants present in the bulk solution. This could explain the initial delay of CYN's degradation shown in bottled water 1, followed by the enhancement of the degradation.

7.3.5 Presence of Humic Acids

The effect of the present organic matter was examined. Humic acids of a higher (10 mg L⁻¹) and a lower (1mg L⁻¹) concentration were spiked to CYN solutions.

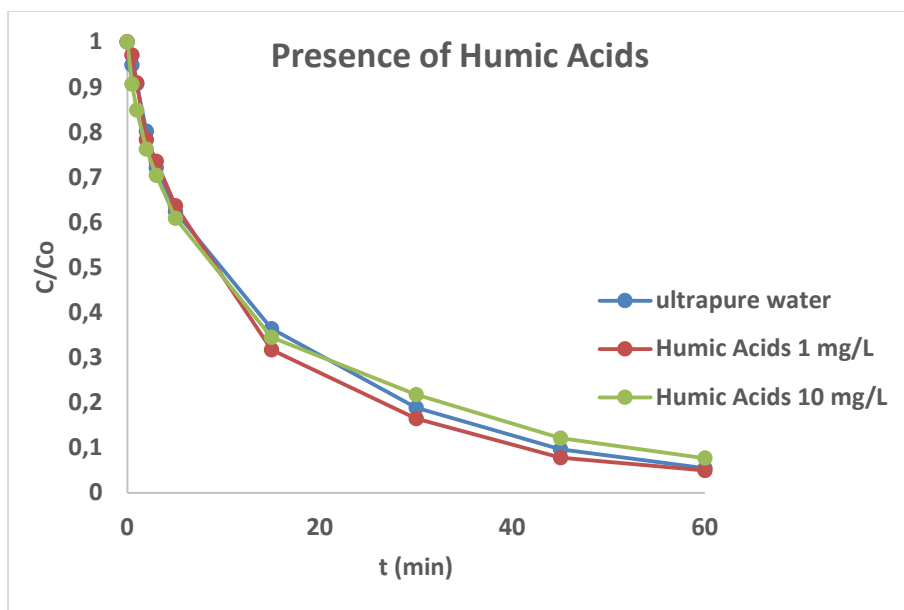


Figure 7-14: Degradation of CYN in presence of Humic Acids (5 mL CYN 1 mg L⁻¹, 250 mL surrounding water, 100% nominal sonication power).

Figure 7-14 shows that there is no significant difference in the rate and the yield of the degradation of CYN in presence of 1 or 10 mg L⁻¹ humic acids. The second order reaction rate of humic acids with hydroxyl radicals is $1.9 \times 10^4 \text{ s}^{-1} (\text{mg of C L}^{-1})^{-1} \approx 1.6 \times 10^3 \text{ M}^{-1}\text{s}^{-1}$ [164] while the reaction rate constant for the reaction of hydroxyl radicals with CYN is $(5.08 \pm 0.16) \times 10^9 \text{ M}^{-1} \text{ s}^{-1}$ [85], so it is assumed that CYN reacts faster with HO• than humic acids, so its degradation is not affected by the presence of humic acids.

Table 7-6: Degradation kinetic constants and initial degradation rates.

	First Order		
	k (s ⁻¹)	R ²	r ₀ (mmol L ⁻¹ s ⁻¹)
100%	0.0009	0.926	0.5698
75%	0.0006	0.989	0.4039
50%	9.00E-05	0.981	0.0609
25%	5.00E-05	0.949	0.0339
pH=5.8	0.0009	0.926	0.5698

pH=7	0.0008	0.895	0.5822
pH=8	0.0006	0.894	0.4367
pH=9	0.0005	0.860	0.3934
Co=0.5 mg/L	0.0014	0.878	0.4844
Co=1 mg/L	0.0009	0.926	0.5698
Co=2 mg/L	0.0006	0.980	0.4004
ultrapure water	0.0009	0.926	0.5698
Humic Acids 1 mg/L	0.001	0.980	0.6887
Humic Acids 10 mg/L	0.0008	0.957	0.5619
ultrapure water	0.0009	0.926	0.5698
Bottled water 1	0.0009	0.978	0.6220
Bottled water 2	0.001	0.904	0.7164

As it shown in the table CYN is degraded faster when it is spiked in real water matrices (initial degradation rate in bottled water 2 matrix 0.7164 mM s^{-1}) at 100% nominal sonication power, while CYN is degraded slowly under 25 % nominal sonication power.

7.4 Localization of CYN reaction in the sonication solution

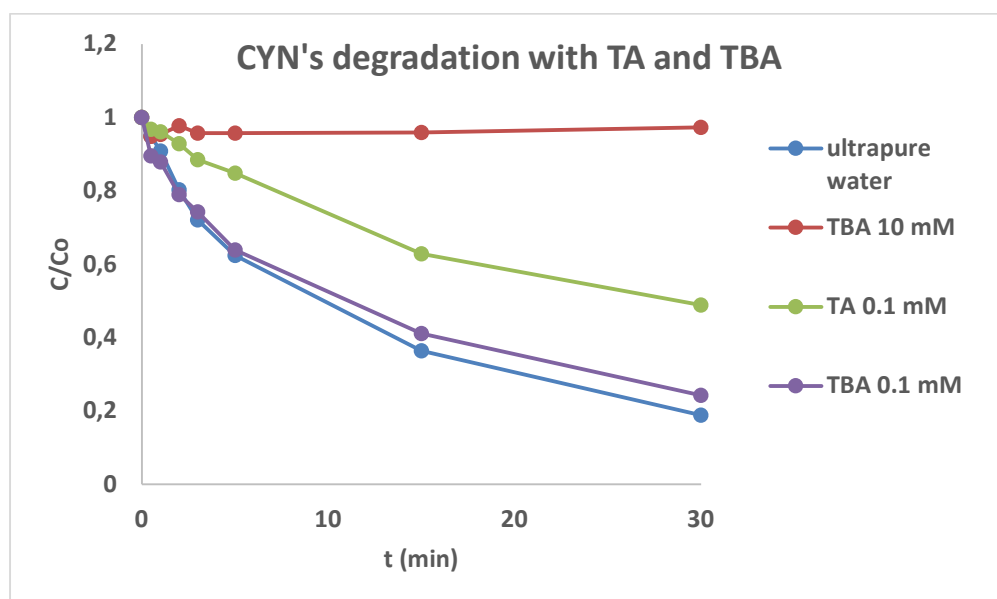


Figure 7-15: Degradation of CYN in presence of TA and TBA (5mL CYN 1mg L⁻¹, 250 mL surrounding water, 100% nominal sonication power).

To evaluate the zone of reaction that CYN is degraded in the sonication solution (bulk, bubble interface, bubble core), TBA and TA were used as scavengers. TBA is a volatile compound and it is present in the bubble and the bubble/solution interface during the cavitation effect and scavenges the radicals produced in this area (Figure 7-16, Zone 1 & 2). TA is anionic in these experimental conditions thus it is mainly found in bulk solution (figure 7-16, zone 3). The reaction rate of TA with hydroxyl radicals is $3.3 \times 10^9 \text{ M}^{-1} \text{ s}^{-1}$ [165]. Therefore, the assessment of degradation kinetics of CYN in the presence of each of these scavengers could give an estimation of the reaction zone where CYN is mainly degraded under these experimental conditions.

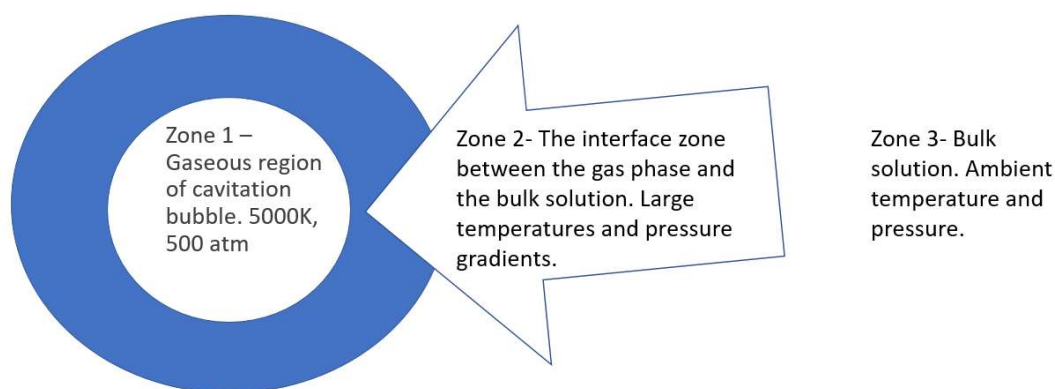


Figure 7-16: Reaction zones.

Initially, the concentration of the scavengers was assessed. At first a high concentration of TBA was applied (10mM). In the past it has been shown that no hydroxyl radicals reach the liquid phase beyond a TBA concentration of $1.5 \times 10^{-3} \text{ mol L}^{-1}$ [166], thus when TBA's solution was 10 mM there was no CYN's degradation because no radicals reach the bulk solution. The same concentration of TA (10 mM) negatively affect the chromatographic quality so monitoring of CYN is impossible. Therefore, a lower concentration of scavengers was selected, in order to effectively scavenge the production of radicals in different zones without interfering with chromatography.

The overall degradation process of CYN in the presence of TA and TBA was consistent with first order kinetics model.

Table 7-7: Kinetic rate constant in presence of TA and TBA.

	First order kinetic model		
	k (s⁻¹)	R²	r₀ (mmol L⁻¹ s⁻¹)
No scavenger	9.00E-04	0.9804	0.64
TBA (0.1 mM)	8.00E-04	0.9746	0.54
TA (0.1 mM)	4.00E-04	0.9809	0.27

TA is expected to partition in the bulk solution. The initial degradation rate for reduction in the CYN concentration without scavenger is $0.64 \text{ mmol L}^{-1} \text{ s}^{-1}$, while in the presence of TA the observed rate is $0.27 \text{ mmol L}^{-1} \text{ s}^{-1}$, representing a decrease of 58% in the presence of a bulk solution HO• scavenger. This means that when a scavenger of HO• in bulk solution is

present (TA) the process rate is decreased 58%, therefore it is only carried out on the interface of the bubble and the inside of the bubble.

TBA is expected to partition into the vapor phase during the growth of the cavitation bubble, and upon bubble collapse, the TBA scavenges the hydroxyl radicals in the vapor and interfacial regions before they can diffuse to the bulk solution. The degradation rate of CYN in the presence of TBA is $0.54 \text{ mmol L}^{-1} \text{ s}^{-1}$. The decrease of the degradation in the presence of TBA, compared to the experiment without any scavenger is 21%.

Assuming that the cavitation dynamics are not significantly changed by the TBA these results indicate that $\text{HO}\cdot$ reactions in the bulk solution occur at 58% (Figure 7-16, Zone 3) and at the bubble interface at 21% (Figure 7-16, Zone 2), representing the major reaction zones for the degradation of CYN during ultrasonic irradiation. The remaining portion of the degradation, 21%, is likely due to the hydrolysis and pyrolysis processes at the interfacial region. The same study have been conducted in the past for MC-LR. This toxin is degraded 39 % in the bulk solution, 35% in the interface and 26 % due to pyrolysis and hydrolysis [100].

7.5 Detection and structure elucidation of transformation products using Mass Spectrometry

Under ultrasonication ROS are produced. Among them the predominant species is $\text{HO}\cdot$, which react through addition, hydrogen abstraction and less often electron abstraction. When α -hydrogen is available, hydrogen abstraction happens and a carbonyl group occurs, while electron abstraction requires electron rich substrate and it is relatively slow compared to $\text{HO}\cdot$ addition.

In order to detect the TPs produced during the oxidative sonolytical degradation of CYN, several analytical steps were carried out. Initially, a chromatographic method was applied in order to separate and identify newly-produced TPs. The samples that were analyzed included the initial CYN solution at concentration of 1 mg L^{-1} , at pH 5.8 and volume 5 mL before any sonolytic treatment. Consequently, samples from various experimental time points (0, 3, 15, 30, 60 min) were retrieved and analyzed for TPs.

The workflow of the analysis is described below:

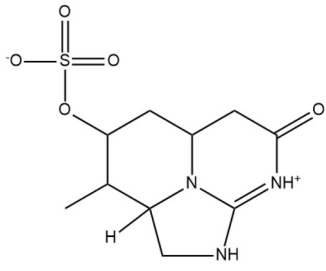
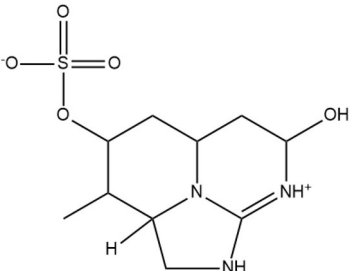
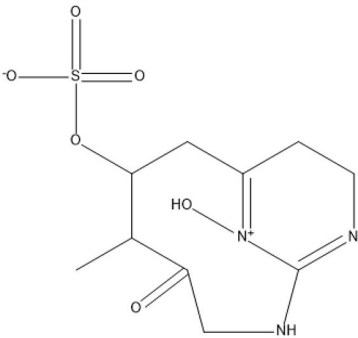
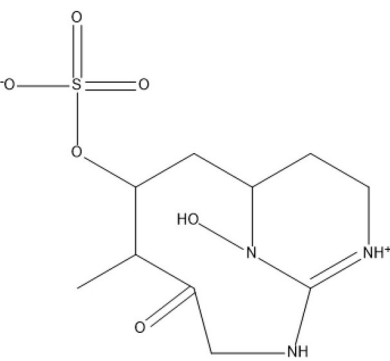
Initially, a list of suspected precursor ions were monitored based on previous studies related to the degradation of CYN using AOPs. The m/z values found in previous studies upon chlorination (m/z 350, 375), upon radiolysis (m/z 320, 350, 375, 414, 432, 448) [85] upon TiO_2 photocatalysis (m/z 195, 227, 280, 287, 316, 338, 347, 374, 434, 450) [83] and upon ozonation (m/z 290, 292, 306, 308, 322, 334, 338, 349, 350, 366, 375, 391, 392, 407, 448, 464) [80] served as a basis for the present study.

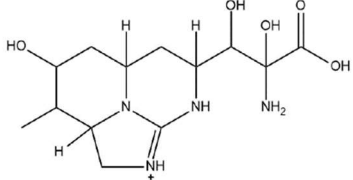
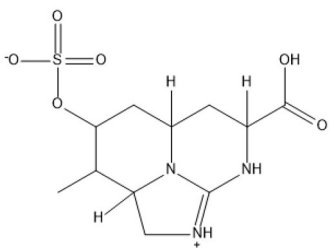
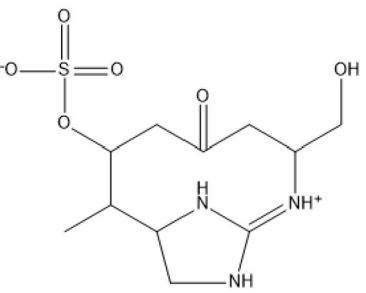
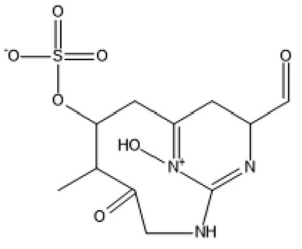
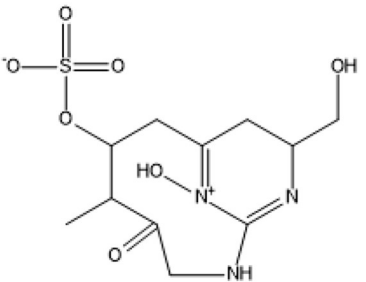
Therefore, based on the list of previously reported m/z of precursor ions (Table 2-2) the samples were analyzed for single ion monitoring and extracted chromatograms were obtained, in order to evaluate the presence of this possible TPs in the solutions. Additionally, the presence of these suspect ions was checked in the initial solution of CYN before any sonolytical treatment occurred, in order to determine whether these peaks correspond to TPs or they pre-existed as contaminant compounds. The peaks in the extracted chromatograms (Chromatograms 7-6, 7-7, 7-8 & 7-9) present the main TPs identified in the solutions at 15 minutes.

The next step included the fragmentation of the identified precursor ions using MS/MS at predefined fragmentation conditions. The produced MS/MS spectra gave an indication of the fragmentation pattern of each identified TP, and therefore resulted in better structure elucidation of the TPs.

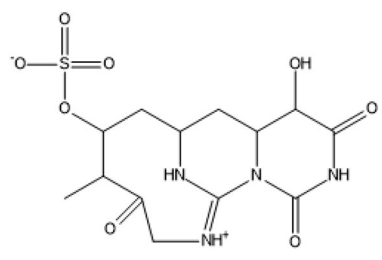
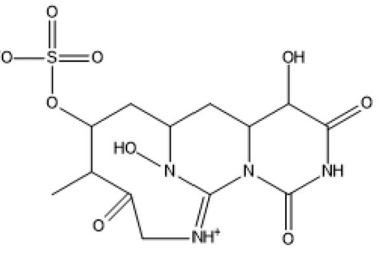
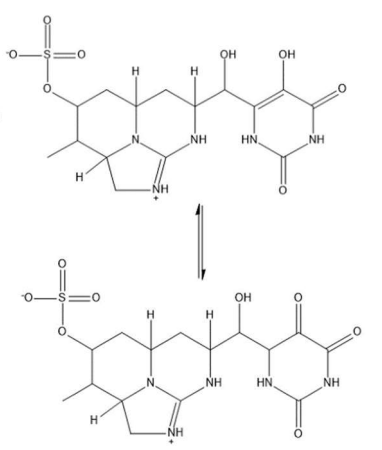
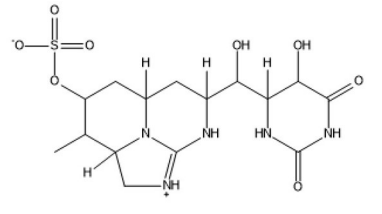
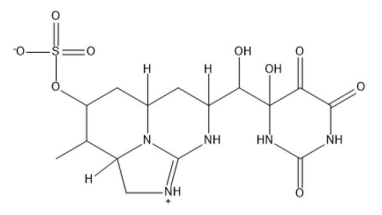
Final step was the full MS scan. For each m/z the molecular ions $[\text{M}+\text{H}]^+$ were recorded. After that the chromatograms of these molecular ions were extracted (extracted ion chromatogram, IEC). Those chromatograms have been by the ions with a specific m/z , For each IEC the produced fragments were detected at the ESI. Finally, the fragmentation of the produced molecular ions happened in the MS/MS (daughter scan, DAU).

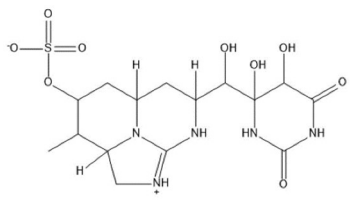
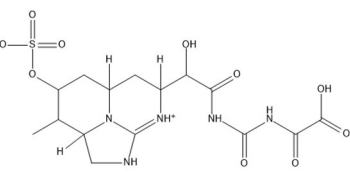
Table 7-8: Identified TPs and their structure.

TP	[M+H] ⁺	t _R	Molecular Formula	Structure
289	290	2.9	C ₁₀ H ₁₅ N ₃ O ₅ S	
291	292	5.3	C ₁₀ H ₁₇ N ₃ O ₅ S	
305	306	2.7	C ₁₀ H ₁₅ N ₃ O ₆ S	
307 a 307 b 307 c	308	2.9 3.6 4.3	C ₁₀ H ₁₇ N ₃ O ₆ S	

315	316	2.7	$C_{13}H_{23}N_4O_5^+$	
319 a 319 b	320	2.6 3.7	$C_{11}H_{17}N_3O_6S$	
321	322	4.1	$C_{11}H_{19}N_3O_6S$	
333 a 333 b 333 c 333 d 333 e	334	2.6 3.1 4.1 5.6 11.5	$C_{11}H_{15}N_3O_7S$	
335	336	2.9	$C_{11}H_{17}N_3O_7S$	

337	338	2.9	$C_{11}H_{19}N_3O_7S$	
348	349	4.0	$C_{12}H_{21}N_3O_7S$	
349 a 349 b 349 c	350	2.6 3.4 5.0	$C_{12}H_{19}N_3O_7S$	
365	366	2.7	$C_{12}H_{19}N_3O_8S$	
374	375	7.9	$C_{14}H_{22}N_4O_6S$	

391	392	5.5	$C_{13}H_{18}N_4O_7S$	
407	408	2.9	$C_{13}H_{18}N_4O_9S$	
Tautomers (431 a & 431 b)	432	2.6 3.0	$C_{15}H_{21}N_5O_8S$	
432 432 b	433	2.6 3.2	$C_{15}H_{23}N_5O_8S$	
447	448	2.6	$C_{15}H_{21}N_5O_9S$	

449 a	450	2.8	$C_{15}H_{23}N_5O_9S$	
449 b		4.1		
463 a	464	2.1	$C_{15}H_{21}N_5O_{10}S$	
463 b		2.8		
463 c		4.2		
463 d		5.9		

CYN is an uracil derivative with a tricyclic guanidine and a sulphate group. Upon its sonolytical degradation, $HO\bullet$ primarily react through substitution on the unsaturated carbon bond on the uracil group, resulting in the formation of products m/z 432 which were detected at t_R 2.6 and 3.0 min. The alcohol on a double bond can give a ketone tautomer explaining the two peaks appearing on the TIC chromatogram for m/z 432 (Chromatogram 7-7) with chemical formula $C_{15}H_{21}N_5O_8S$. From product with m/z 432, product with m/z 450 is formed with further hydroxylation. This m/z shows two different chromatographic peaks at t_R 2.8 and 4.1 min. Their proposed chemical formula $C_{15}H_{23}N_5O_9S$ and they have also been detected during the photocatalytic degradation of CYN [83]. Product with m/z 433 can be a result of $HO\bullet$ addition in uracil's double bond. This TP has is eluted at 2.6 & 3.2 min and its chemical formula is $C_{15}H_{23}N_5O_8S$. Further oxidation on the uracil group of product m/z 432 can lead to the formation of product m/z 375, eluted at 7.9 min, with ring opening at urea group moiety. This product has been detected when CYN was photocatalytically degraded and the proposed formula is $C_{14}H_{22}N_4O_6S$. Through further oxidations cylindrospermopsic acid (m/z 350, multiple peak, Chromatogram 7-7) is produced. Th TP shows three different chromatographic peaks at at 2.6, 3.4 & 5.0 min. Previously, it has been detected in CYN radiolysis and the proposed formula is $C_{12}H_{19}N_3O_7S$ [85]. By further oxidation the acid with m/z 320 may occur with t_R 2.6 and 3.7 min and proposed formula $C_{11}H_{19}N_3O_7S$. Further oxidation of m/z 320 forms m/z 292 through loss of CO (t_R 5.3 min), and continuous oxidation of alcohol group yields the corresponding ketone, m/z 290 (t_R 2.9 min), also detected when CYN was ozonated [80]. Oxidation of the tertiary nitrogen on TP with m/z 350 forms a product with m/z 366 with

proposed chemical formula $C_{12}H_{19}N_3O_8S$ and further loss of CO_2 forms TP with m/z 322. This TP was eluted after 4.1 min and its proposed chemical formula is $C_{11}H_{19}N_3O_6S$.

Also, oxidation to either of the secondary alcohols on m/z 450 product (bridging methane group or on the uracil group) with hydrogen abstraction results in the formation of product with m/z 448 which was eluted at 2.6 minutes and its proposed formula is $C_{15}H_{21}N_5O_9S$ [80]. Oxidation of product with m/z 448 can lead to the formation of TP with m/z 464. This TP has 4 isobaric compound, eluted at t_R 2.1, 2.8, 4.2 and 5.9 min. The proposed chemical formula is $C_{15}H_{21}N_5O_{10}S$. A loss of oxalic acid from TP 447 leads to the formation of product with m/z 392. The proposed chemical formula is $C_{13}H_{18}N_4O_7S$ and it is eluted after 5.5 min. Via loss of $CONH_2$ the TP with m/z 348 is formed with proposed chemical formula $C_{12}H_{21}N_3O_7S$.

Substitution of the sulphate group with $HO\cdot$ on CYN, can result in the formation of intermediate with m/z 338 with t_R 2.9 min. Based on past bibliographic data this TP has been detected in the past during the photocatalytic degradation of CYN [83]. The proposed chemical formula is $C_{11}H_{19}N_3O_7S$. Oxidation on the uracil group of m/z 338 can produce a compound with m/z 316, eluted at 2.7 min and proposed formula $C_{13}H_{23}N_4O_5^+$ [83]. The m/z 338 can be further oxidized to TP with m/z 336 which can be decarboxylated to TP with m/z 307. The proposed chemical formulas are $C_{11}H_{17}N_3O_7S$ and $C_{10}H_{17}N_3O_6S$, respectively. In the same way TPs with m/z 334 and 306 can be formed from TP 336.

In Table 7-7 all intermediate products found are presented with their m/z ratios, formulas, their monoisotopic molecular masses and the proposed structures.

The temporal changes in the production of those TPs is shown in the following figures (Figure 7-17 & 7-18). Those produced in higher concentrations are presented in figure 7-17 and the rest in figure 7-18.

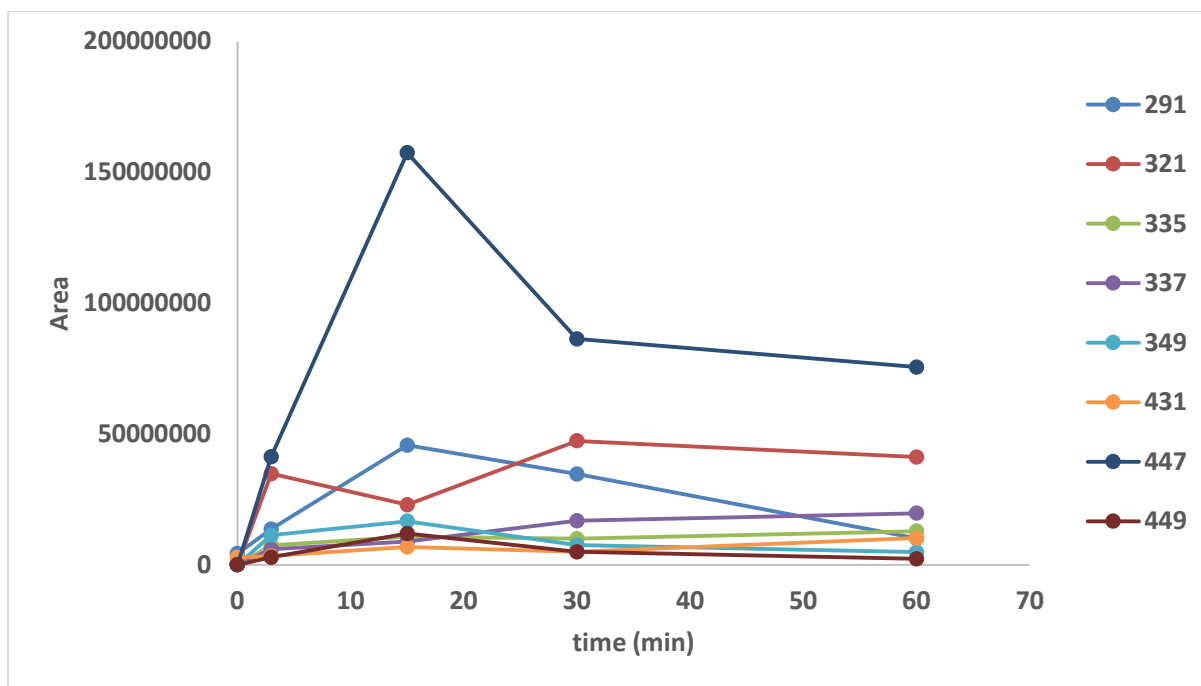


Figure 7-17: TPs formation (higher concentrations).

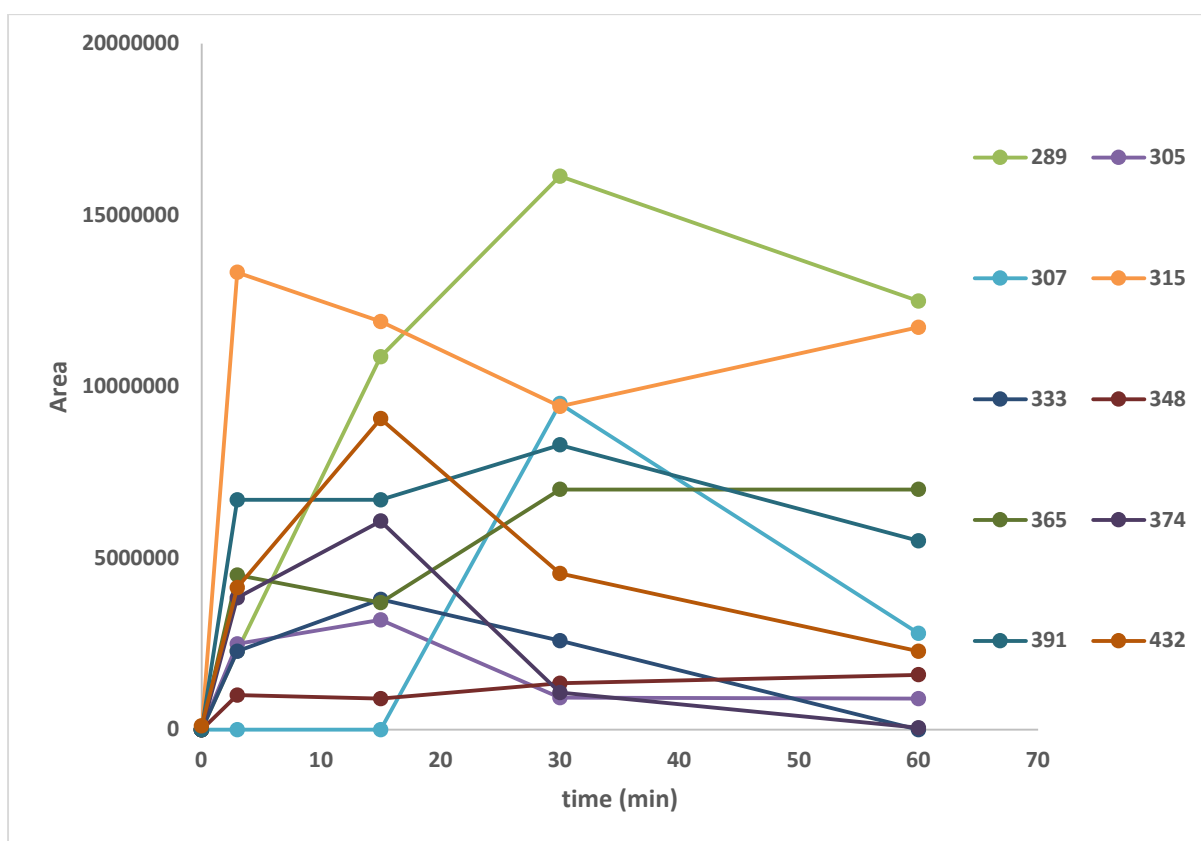
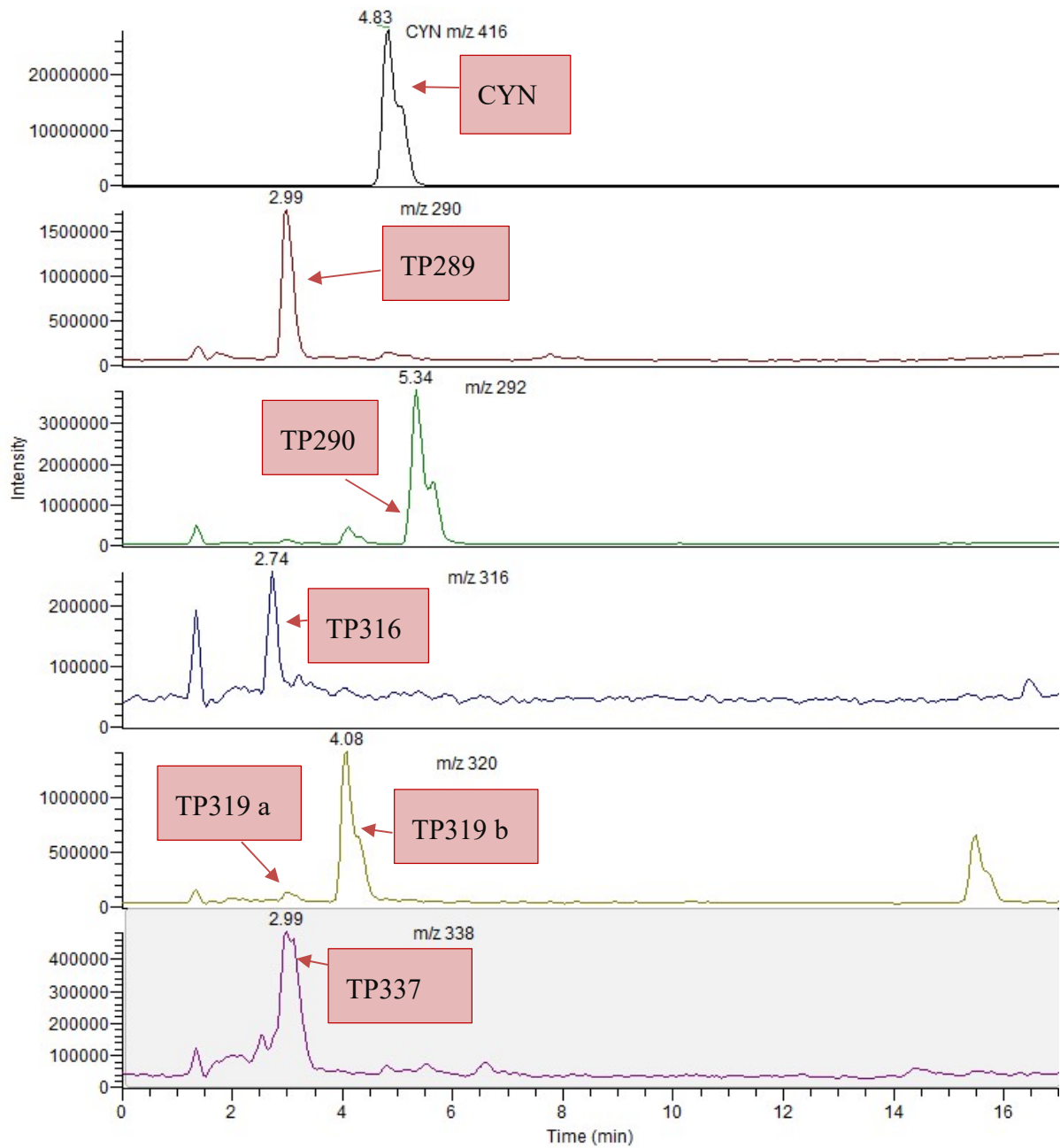
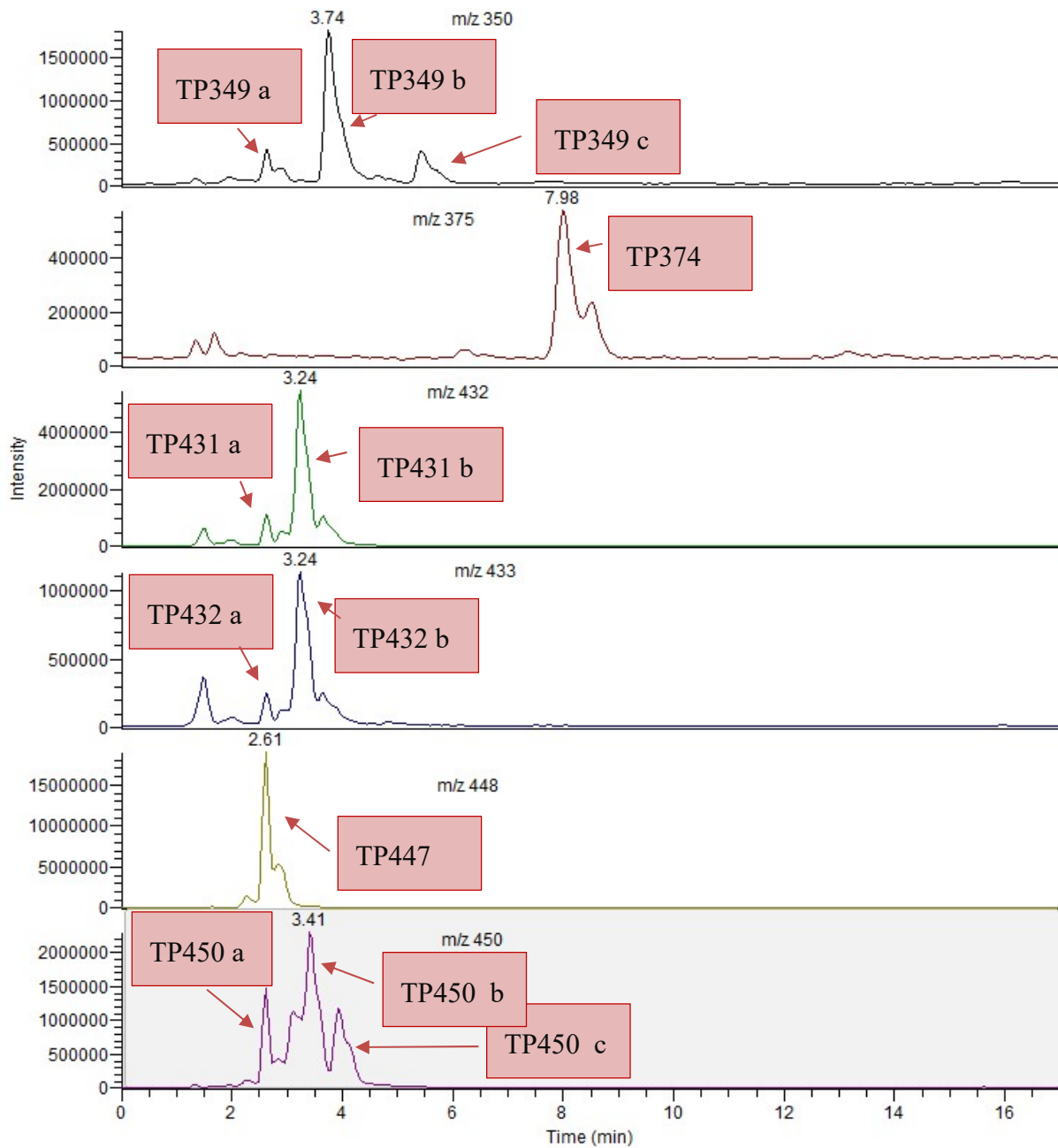


Figure 7-18: TPs formation (lower concentrations).

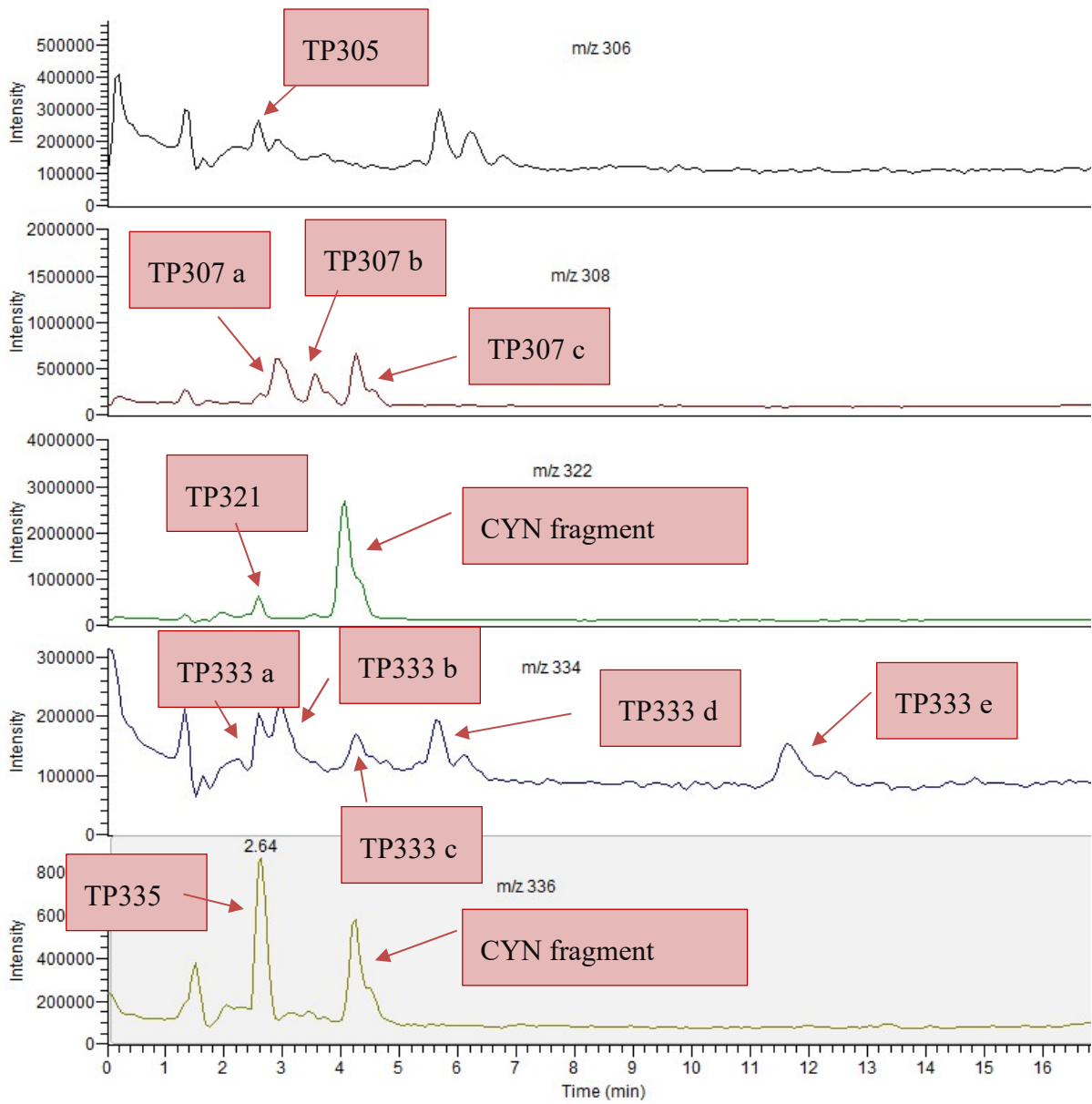
Chromatograms 7-6, 7-7, 7-8, 7-9 & 7-10 present the TPs produced after 15 minutes of sonication.



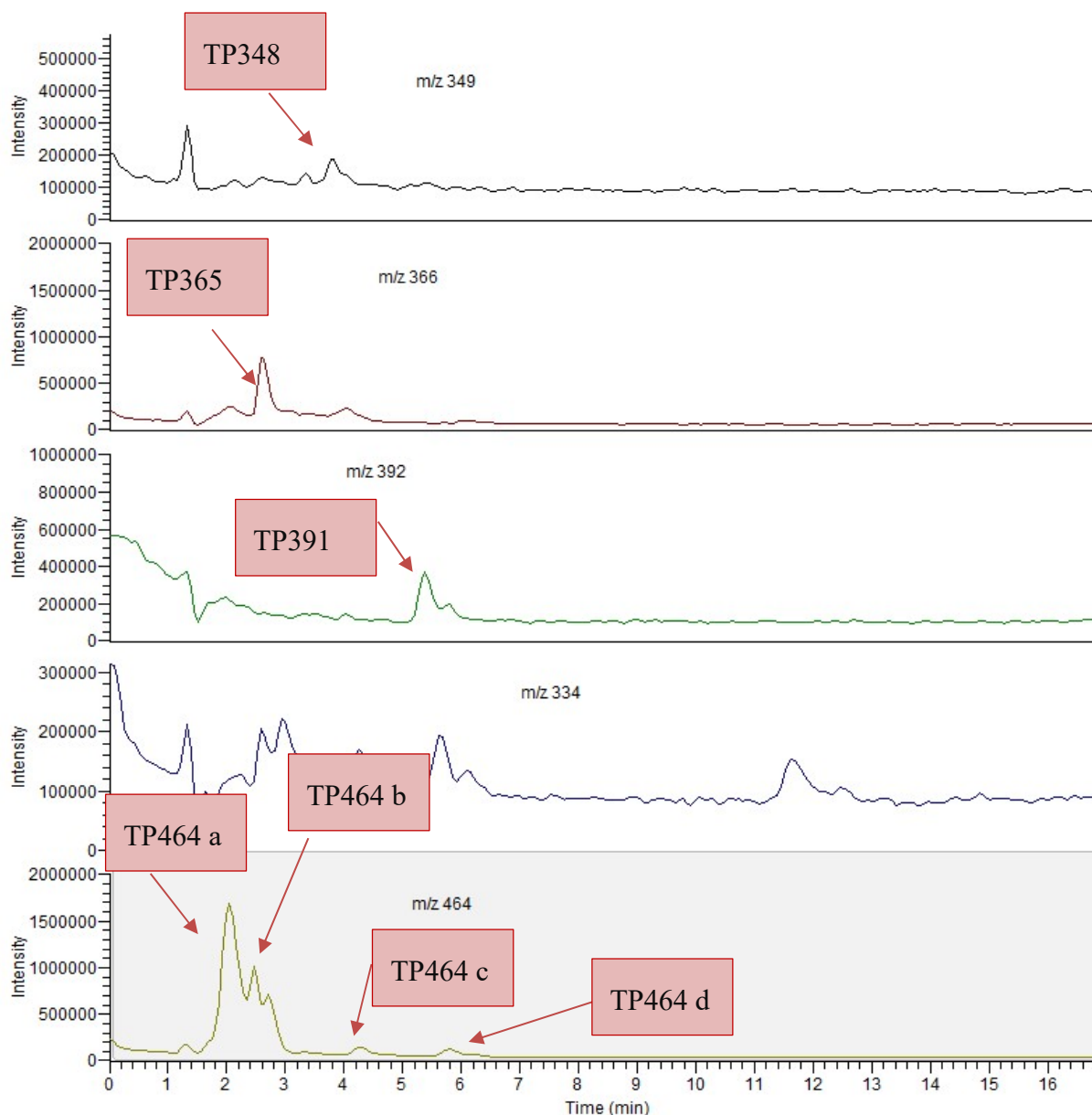
Chromatogram 7-6:TPs chromatograms after 15 minutes of sonication (a) (5 mL CYN 1 mg L⁻¹, 250 mL surrounding water, 100% nominal sonication power).



Chromatogram 7-7: TPs chromatograms after 15 minutes of sonication (b) (5 mL CYN 1 mg L⁻¹, 250 mL surrounding water, 100% nominal sonication power).

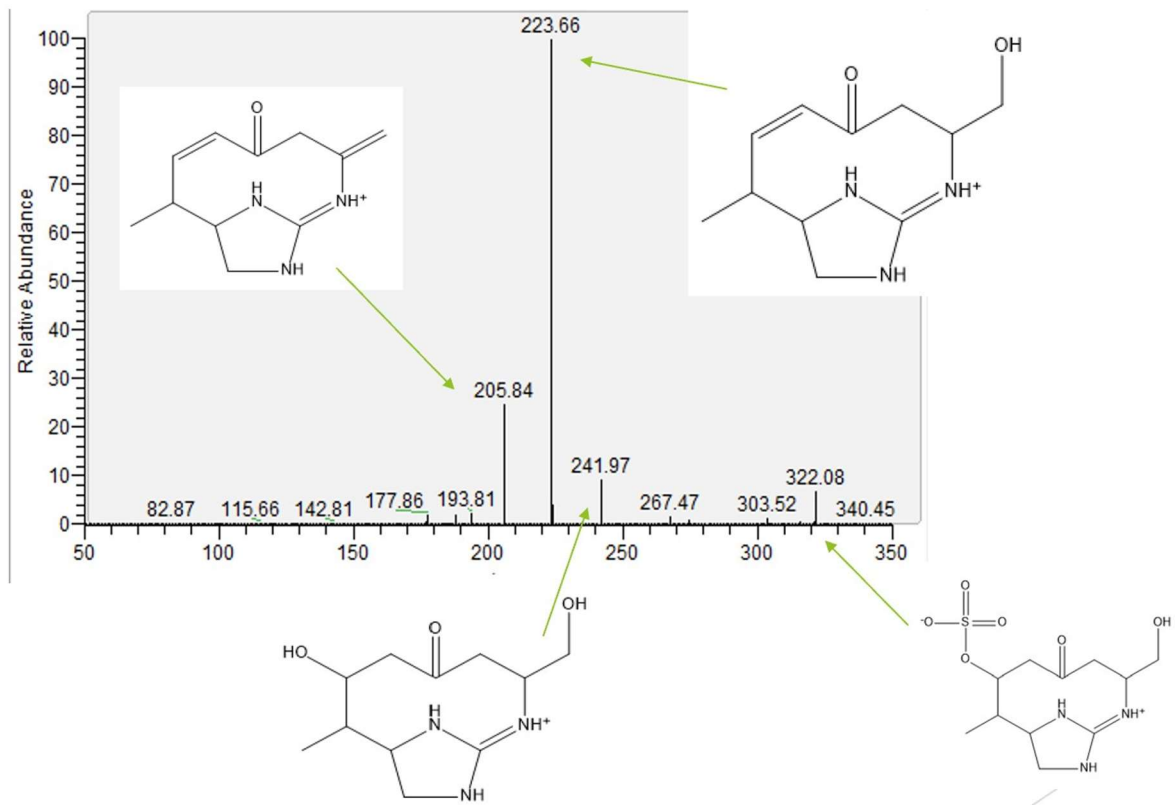


Chromatogram 7-8: TPs chromatograms after 15 minutes of sonication (c) (5 mL CYN 1 mg L⁻¹, 250 mL surrounding water, 100% nominal sonication power).



Chromatogram 7-9: TPs chromatograms after 15 minutes of sonication (d) (5 mL CYN 1 mg L⁻¹, 250 mL surrounding water, 100% nominal sonication power).

An example of the work on the MS MS spectrum and the proposed structures for the fragments are given in Chromatogram 7-10. The proposed structures are in accordance with previously proposed structures. Table A-1 contains all the available MS MS spectrums and the proposed fragment structures.



Chromatogram 7-10: MS MS spectrum of TP 321 and proposed fragments structures .

8 Conclusions

In this study, the sonolytical degradation of CYN was effectively carried out. At first, a sonolytical device operating at 850 kHz was optimized for the degradation of small compound volumes. A glass reactor tube was adjusted and its optimal position (1 cm distance from the transducer and centered) was determined using 2,4-DCP as a model compound. In addition, Fricke and Coumarin (COU) dosimeters were used to determine the Reactive Oxygen Species (ROS) and the hydroxyl radicals (HO•) produced, respectively. The experiments were conducted at several operating conditions and the 7-hydroxycoumarin (7-OH-COU) production follows the trend of Fe³⁺ production, indicating that the main operational parameters responsible for the production of ROS are the sonication power, the volume of the surrounding water and the distance of the glass tube from the transducer and that HO• is the dominant ROS of the process. The amount of 7-OH-COU produced is 1% of the degraded COU therefore it is difficult to quantitatively use the production of 7-OH-COU for the estimation of HO• produced in the system.

A fast and reliable HPLC-PDA method was developed for the monitoring of CYN degradation using a C-18 column and isocratic elution. CYN was eluted at 4.5 min and the Limit of Detection (LOD) of the method was 3 µg L⁻¹.

CYN degradation was performed under various levels of sonication power, pH and initial concentration of CYN. The degradation of CYN in every case follows the first order reaction kinetic model and the initial degradation rate ranged from 0.0339 to 0.7164 mM s⁻¹. The effect of the presence of inorganic ions (as bottled water) and organic matter (as humic acids) was also examined. Bicarbonate ions seem to enhance the degradation kinetics while the presence of humic acid does not seem to affect the degradation efficiency, since CYN reacts faster with HO• than with humic substances.

A volatile (tert-butyl alcohol, TBA) and an ionic (terephthalate, TA) scavenger were used, in order to determine the zone of reaction where CYN is degraded in the reaction mixture. 58 % of CYN was found to be degraded at the bulk solution, 21 % at the interface of the bubble/bulk solution and the rest was attributed to pyrolysis and hydrolysis.

Finally, the transformation products (TPs) of CYN were determined by ESI- LC-MS/MS. The TPs found in different reaction times correspond to molecular masses 289, 291,305, 307, 315, 319, 321, 335, 337, 348, 349, 365, 374, 391, 407, 431, 432,447, 449 and 463.

Abbreviations

ACN	Acetonitrile
AOP	Advanced Oxidation Process
COU	Coumarin
CTs	Cyanotoxins
CYN	Cylindrospermopsin
DAU	Daughter Scan
EIC	Extracted Ion Chromatogram
ESI	Electrospray Ionization
FT-ICR	Fourier Transform Cyclotron Resonance
HILIC	Hydrophilic Interaction Liquid Chromatography
HPLC	High Performance Liquid Chromatography
HPLC-PDA	High Performance Liquid Chromatography- Photodiode array detector
LC-MS/MS	Liquid Chromatography tandem Mass Spectroscopy
LOD	Limit of Detection
LOQ	Limit of Quantitation
LPS	Lipopolysaccharides
MCs	Microcystins
MIB	2-Methylisoborneol
MS	Mass Spectroscopy
NOD	Nodularin
NOM	Natural Organic Matter
OPHD	Oregon Public Health Division
PDA	Photodiode array detector
ROS	Reactive Oxygen Species

T&O	Taste and Odor Compounds
TA	Terephthalic Acid
TBA	Tert-butanol
TDI	Total Daily Intake
TFA	Trifluoroacetic acid
TIC	Total Ion Chromatogram
TPs	Transformation Products
UV	Ultraviolet
UV-vis	Ultraviolet-visible
WHO	World Health Organisation
2,4-DCP	2,4-Dichlorophenol
7-deoxy-CYN	7-deoxy-cylindrospermopsin
7-epi-CYN	7-epi-cylindrospermopsin
7-OH-COU	7-hydroxycoumarin

Appendix

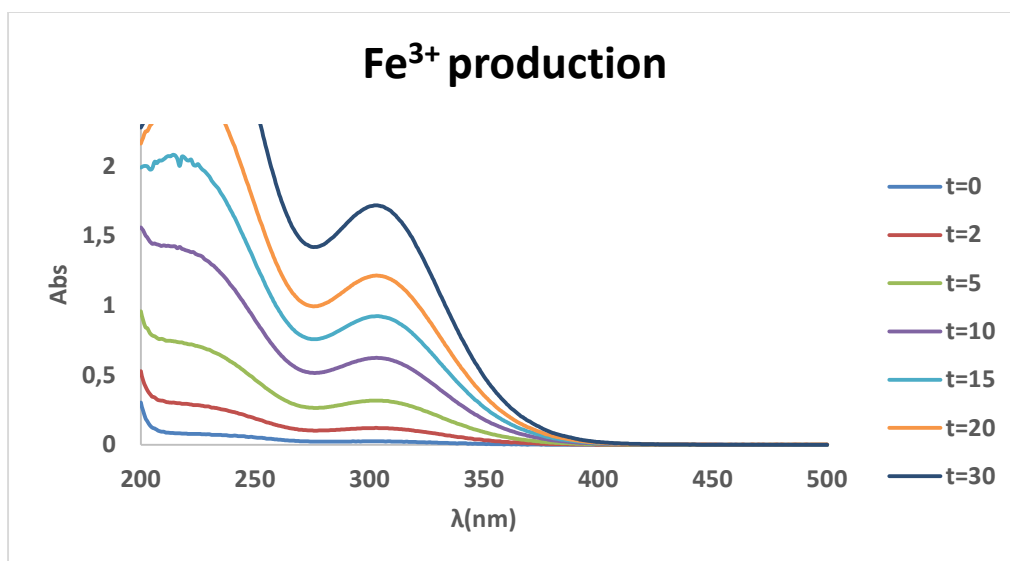


Figure A-8-1: Spectrum of the produced Fe³⁺ after several sonication times (5 mL Fricke solution, 250 mL surrounding water, 100% nominal sonication power).

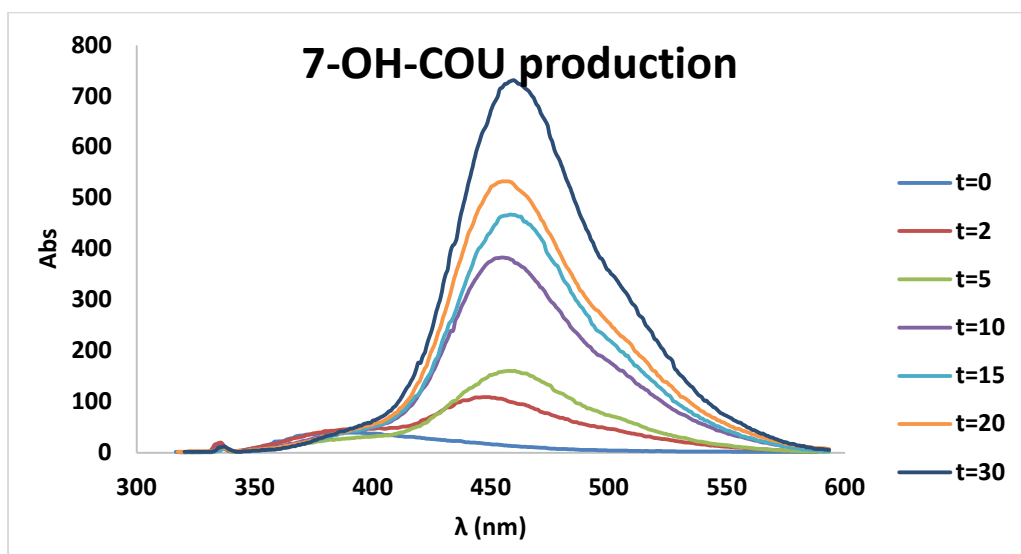


Figure A-2: Spectrum of the produced 7-OH-COU after several sonication times (1 mM COU 5 mL, 250 mL surrounding water, 100% nominal sonication power).

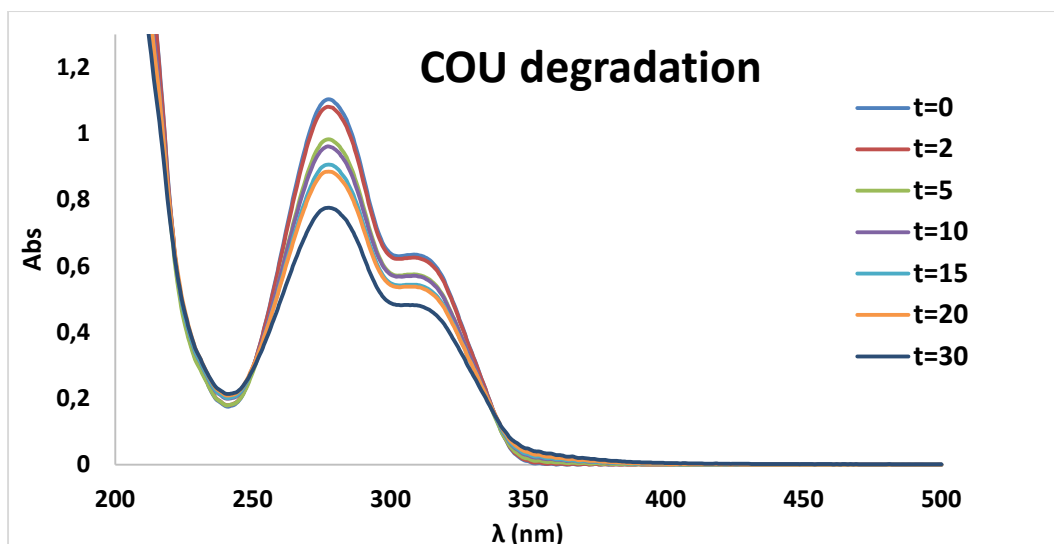
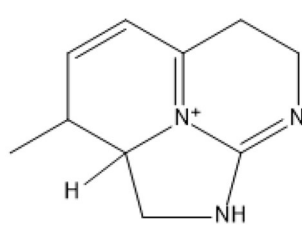
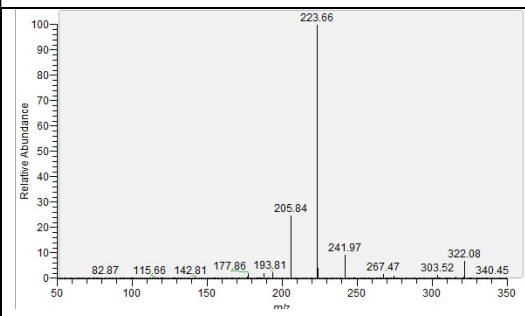
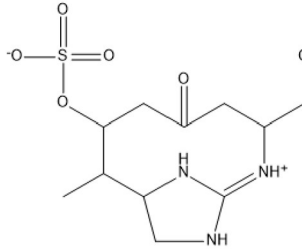
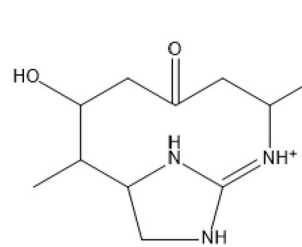
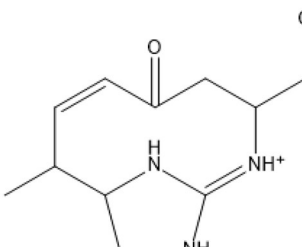
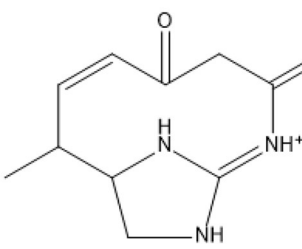
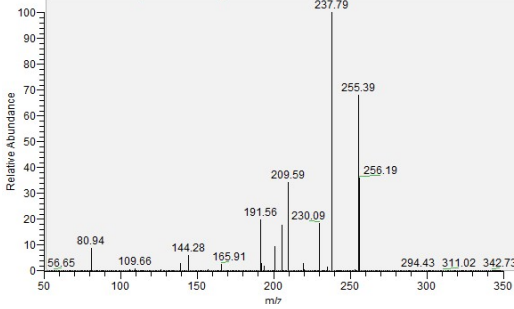
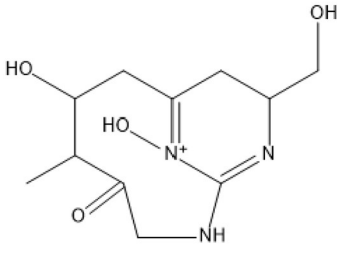
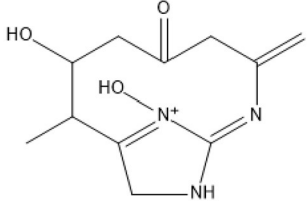
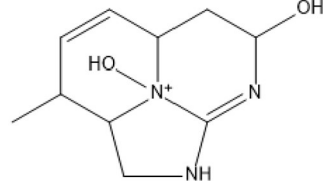
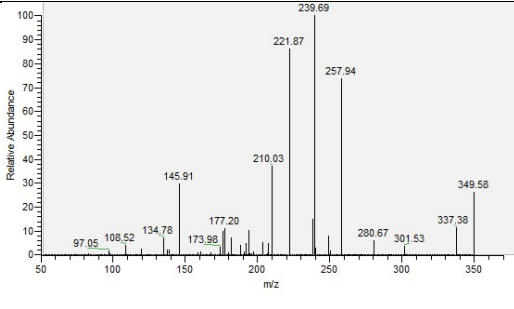
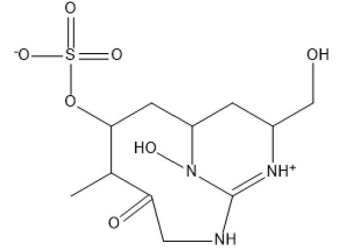
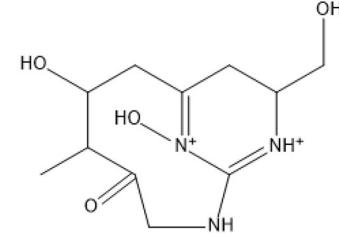
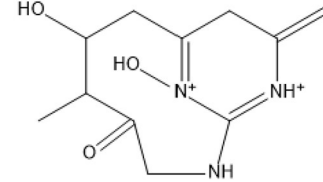


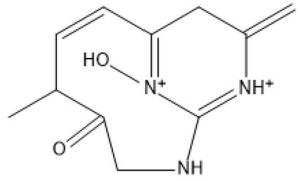
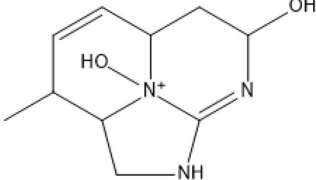
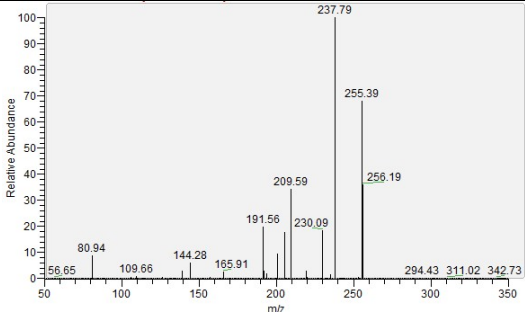
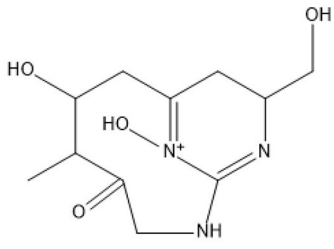
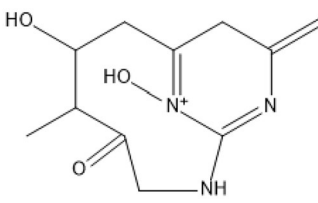
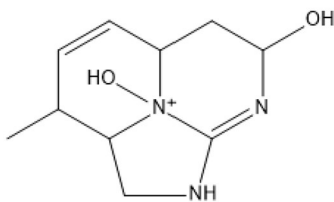
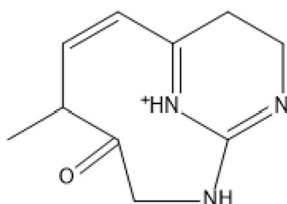
Figure A-3: Spectrum of the degraded COU after several sonication times (1 mM COU 5mL, 250 mL surrounding water, 100% nominal sonication power).

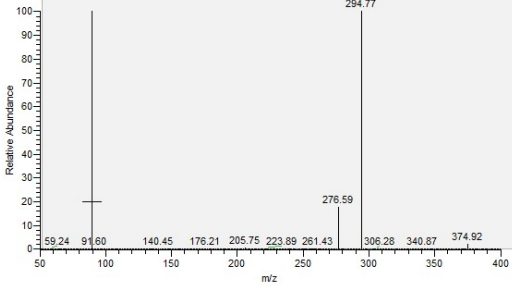
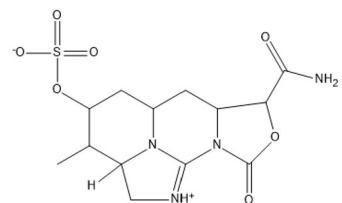
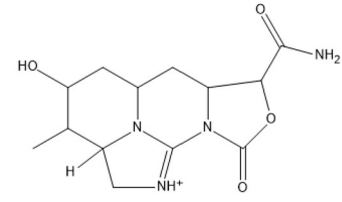
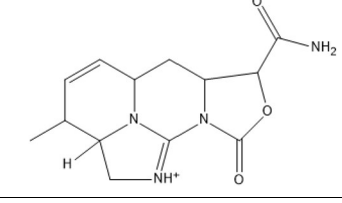
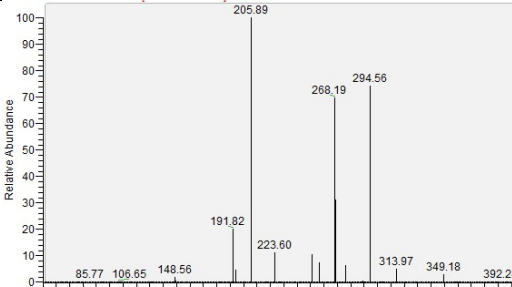
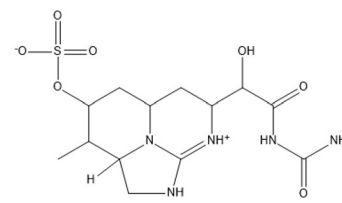
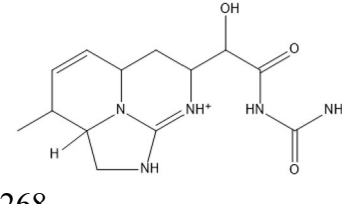
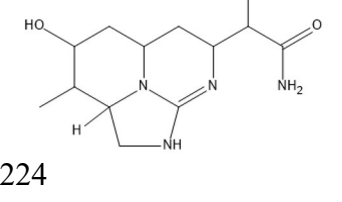
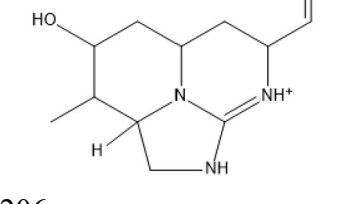
Table A-8-1: MS MS fragments and proposed structures.

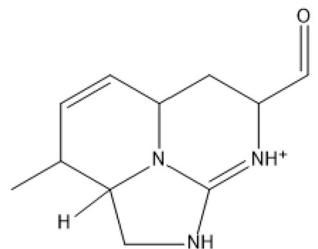
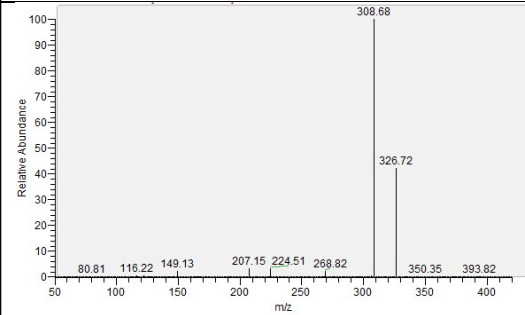
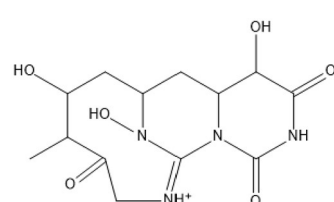
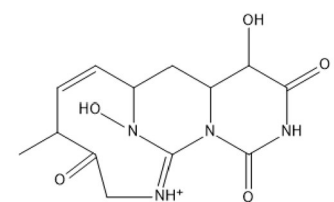
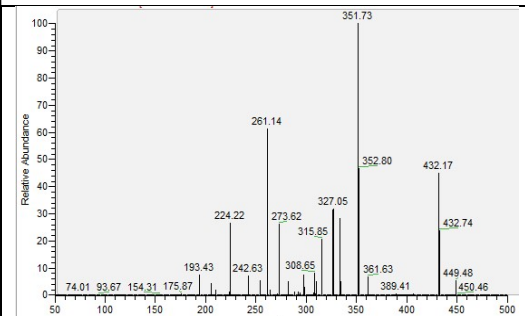
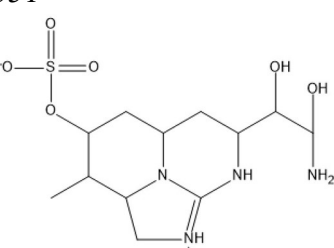
TP	m/z	Rt (min)	MS MS spectrum	m/z Fragment ions
291	292	5.3		<p>292</p> <p>212</p> <p>194</p>

				176	
321	322	4.1		322	
				242	
				224	
				206	

335	336	2.9		<p>256</p>  <p>238</p>  <p>210</p> 
337	338	2.99		<p>338</p>  <p>257</p>  <p>239</p>  <p>221</p>

				 <p>210</p> 
365	366	2.9		<p>256</p>  <p>238</p>  <p>210</p>  <p>192</p> 

374	375	7.98	 <p>Mass spectrum showing relative abundance versus m/z. The base peak is at m/z 294.77. Other significant peaks are labeled at m/z 59.24, 91.60, 140.45, 176.21, 205.75, 223.89, 261.43, 276.59, 306.28, 340.87, and 374.92.</p>	<p>375</p>  <p>Chemical structure of compound 375, a complex heterocyclic molecule with a sulfonamide group and an amide group.</p> <p>295</p>  <p>Chemical structure of compound 295, a complex heterocyclic molecule with a hydroxyl group and an amide group.</p> <p>277</p>  <p>Chemical structure of compound 277, a complex heterocyclic molecule with an amide group.</p>
391	392	5.5	 <p>Mass spectrum showing relative abundance versus m/z. The base peak is at m/z 205.89. Other significant peaks are labeled at m/z 85.77, 106.65, 148.56, 191.82, 223.60, 268.19, 294.56, 313.97, 349.18, and 392.24.</p>	<p>392</p>  <p>Chemical structure of compound 392, a complex heterocyclic molecule with a sulfonamide group, a hydroxyl group, and an amide group.</p> <p>295</p>  <p>Chemical structure of compound 295, a complex heterocyclic molecule with a hydroxyl group and an amide group.</p> <p>268</p>  <p>Chemical structure of compound 268, a complex heterocyclic molecule with a hydroxyl group and an amide group.</p> <p>224</p>  <p>Chemical structure of compound 224, a complex heterocyclic molecule with a hydroxyl group and an aldehyde group.</p> <p>206</p>

				
406	407	2.87		<p>327</p> 
				<p>309</p> 
449	450	2.8		<p>351</p> 

9 References

- [1] G. A. Codd, J. Meriluoto, and J. S. Metcalf, “Introduction,” *Handbook of Cyanobacterial Monitoring and Cyanotoxin Analysis*. pp. 1–8, Dec. 20, 2016, doi: doi:10.1002/9781119068761.ch1.
- [2] B. Whitton and M. Potts, “Introduction to the cyanobacteria,” *Ecol. Cyanobacteria II Their Divers. Sp. Time*, pp. 1–13, Jul. 2013, doi: 10.1007/978-94-007-3855-3_1.
- [3] Jutta Fastner and J. Humbert, “Handbook of Cyanobacterial Monitoring and Cyanotoxin Analysis,” in *Handbook of Cyanobacterial Monitoring and Cyanotoxin Analysis*, John Wiley and Sons, 2017.
- [4] S. Merel, D. Walker, R. Chicana, S. Snyder, E. Baurès, and O. Thomas, “State of knowledge and concerns on cyanobacterial blooms and cyanotoxins,” *Environ. Int.*, vol. 59, pp. 303–327, 2013, doi: <https://doi.org/10.1016/j.envint.2013.06.013>.
- [5] C. Christophoridis *et al.*, “Occurrence and diversity of cyanotoxins in Greek lakes,” *Sci. Rep.*, vol. 8, no. 1, p. 17877, Dec. 2018, doi: 10.1038/s41598-018-35428-x.
- [6] H. W. Paerl and J. Huisman, “Climate change: a catalyst for global expansion of harmful cyanobacterial blooms,” *Environ. Microbiol. Rep.*, vol. 1, no. 1, pp. 27–37, Feb. 2009, doi: 10.1111/j.1758-2229.2008.00004.x.
- [7] R. El-Shehawy, E. Gorokhova, F. Fernández-Piñas, and F. F. del Campo, “Global warming and hepatotoxin production by cyanobacteria: What can we learn from experiments?,” *Water Res.*, vol. 46, no. 5, pp. 1420–1429, 2012, doi: <https://doi.org/10.1016/j.watres.2011.11.021>.
- [8] H. Paerl and T. Otten, “Harmful Cyanobacterial Blooms: Causes, Consequences, and Controls,” *Microb. Ecol.*, vol. 65, Jan. 2013, doi: 10.1007/s00248-012-0159-y.
- [9] D. J. Conley *et al.*, “Controlling Eutrophication: Nitrogen and Phosphorus,” *Science (80-.)*, vol. 323, no. 5917, pp. 1014 LP – 1015, Feb. 2009, doi: 10.1126/science.1167755.

- [10] F. Montecchiario and M. Giordano, "Effect of prolonged dark incubation on pigments and photosynthesis of the cave-dwelling cyanobacterium *Phormidium autumnale* (Oscillatoriales, Cyanobacteria)," *Phycologia*, vol. 45, no. 6, pp. 704–710, Nov. 2006, doi: 10.2216/06-15.1.
- [11] M. Antonopoulou, E. Evgenidou, D. Lambropoulou, and I. Konstantinou, "A review on advanced oxidation processes for the removal of taste and odor compounds from aqueous media," *Water Res.*, vol. 53, pp. 215–234, 2014, doi: <https://doi.org/10.1016/j.watres.2014.01.028>.
- [12] J. Huisman, G. A. Codd, H. W. Paerl, B. W. Ibelings, J. M. H. Verspagen, and P. M. Visser, "Cyanobacterial blooms," *Nat. Rev. Microbiol.*, vol. 16, no. 8, pp. 471–483, 2018, doi: 10.1038/s41579-018-0040-1.
- [13] World Health Organization, "Toxic Cyanobacteria in Water: A guide to their public health consequences, monitoring and management." p. 400, 1999.
- [14] I. Chorus and J. Bartram, "Toxic cyanobacteria in water : a guide to their public health consequences, monitoring and management / edited by Ingrid Chorus and Jamie Bertram." World Health Organization, Geneva PP - Geneva, [Online]. Available: <https://apps.who.int/iris/handle/10665/42827>.
- [15] H. U. Wolf and C. Frank, "Toxicity assessment of cyanobacterial toxin mixtures," *Environ. Toxicol.*, vol. 17, no. 4, pp. 395–399, Jan. 2002, doi: 10.1002/tox.10066.
- [16] K. L. Rinehart, M. Namikoshi, and B. W. Choi, "Structure and biosynthesis of toxins from blue-green algae (cyanobacteria)," *J. Appl. Phycol.*, vol. 6, no. 2, pp. 159–176, 1994, doi: 10.1007/BF02186070.
- [17] E. J. Schantz *et al.*, "Structure of saxitoxin," *J. Am. Chem. Soc.*, vol. 97, no. 5, pp. 1238–1239, Mar. 1975, doi: 10.1021/ja00838a045.
- [18] I. Ohtani, R. E. Moore, and M. T. C. Runnegar, "Cylindrospermopsin: a potent hepatotoxin from the blue-green alga *Cylindrospermopsis raciborskii*," *J. Am. Chem. Soc.*, vol. 114, no. 20, pp. 7941–7942, Sep. 1992, doi: 10.1021/ja00046a067.
- [19] V. Messineo, S. Melchiorre, A. Di Corcia, P. Gallo, and M. Bruno, "Seasonal succession of *Cylindrospermopsis raciborskii* and *Aphanizomenon ovalisporum* blooms with cylindrospermopsin occurrence in the volcanic Lake Albano, Central Italy," *Environ. Toxicol.*, vol. 25, no. 1, pp. 18–27, Feb. 2010, doi: 10.1002/tox.20469.

- [20] A. A. de la Cruz *et al.*, “A review on cylindrospermopsin: the global occurrence, detection, toxicity and degradation of a potent cyanotoxin,” *Environ. Sci. Process. Impacts*, vol. 15, no. 11, pp. 1979–2003, 2013, doi: 10.1039/C3EM00353A.
- [21] A. T. C. Bourke, R. B. Hawes, A. Neilson, and N. D. Stallman, “An outbreak of hepato-enteritis (the Palm Island mystery disease) possibly caused by algal intoxication,” *Toxicon*, vol. 21, pp. 45–48, 1983, doi: [https://doi.org/10.1016/0041-0101\(83\)90151-4](https://doi.org/10.1016/0041-0101(83)90151-4).
- [22] A. D. THOMAS, M. L. SAKER, J. H. NORTON, and R. D. OLSEN, “Cyanobacterium *Cylindrospermopsis raciborskii* as a probable cause of death in cattle in northern Queensland,” *Aust. Vet. J.*, vol. 76, no. 9, pp. 592–594, Sep. 1998, doi: 10.1111/j.1751-0813.1998.tb10233.x.
- [23] R. Banker, S. Carmeli, M. Werman, B. Teltsch, R. Porat, and A. Sukenik, “Uracil Moiety is Required for Toxicity of the Cyanobacterial Hepatotoxin Cylindrospermopsin,” *J. Toxicol. Environ. Heal. Part A*, vol. 62, no. 4, pp. 281–288, Feb. 2001, doi: 10.1080/009841001459432.
- [24] R. E. Looper, M. T. C. Runnegar, and R. M. Williams, “Synthesis of the Putative Structure of 7-Deoxycylindrospermopsin: C7 Oxygenation Is Not Required for the Inhibition of Protein Synthesis,” *Angew. Chemie Int. Ed.*, vol. 44, no. 25, pp. 3879–3881, Jun. 2005, doi: 10.1002/anie.200500520.
- [25] R. K. Chiswell *et al.*, “Stability of cylindrospermopsin, the toxin from the cyanobacterium, *Cylindrospermopsis raciborskii*: Effect of pH, temperature, and sunlight on decomposition,” *Environ. Toxicol.*, vol. 14, no. 1, pp. 155–161, Feb. 1999, doi: 10.1002/(SICI)1522-7278(199902)14:1<155::AID-TOX20>3.0.CO;2-Z.
- [26] C. Moreira, J. Azevedo, A. Antunes, and V. Vasconcelos, “Cylindrospermopsin: occurrence, methods of detection and toxicology,” *J. Appl. Microbiol.*, vol. 114, no. 3, pp. 605–620, Mar. 2013, doi: 10.1111/jam.12048.
- [27] S. Pichardo, M. A. Cameán, and A. Jos, “In Vitro Toxicological Assessment of Cylindrospermopsin: A Review,” *Toxins*, vol. 9, no. 12, 2017, doi: 10.3390/toxins9120402.
- [28] A. A. Seawright *et al.*, “The oral toxicity for mice of the tropical cyanobacterium *Cylindrospermopsis raciborskii* (Woloszynska),” *Environ. Toxicol.*, vol. 14, no. 1, pp.

- 135–142, Feb. 1999, doi: 10.1002/(SICI)1522-7278(199902)14:1<135::AID-TOX17>3.0.CO;2-L.
- [29] J.-F. Briand, S. Jacquet, C. Bernard, and J.-F. Humbert, “Health hazards for terrestrial vertebrates from toxic cyanobacteria in surface water ecosystems,” *Vet. Res.*, vol. 34, no. 4, pp. 361–377, Jul. 2003, [Online]. Available: <https://doi.org/10.1051/vetres:2003019>.
- [30] C. Cartmell *et al.*, “Synthetic analogues of cyanobacterial alkaloid cylindrospermopsin and their toxicological activity,” *Toxicol. Vitro.*, vol. 44, pp. 172–181, 2017, doi: <https://doi.org/10.1016/j.tiv.2017.07.007>.
- [31] R. Sinha, L. A. Pearson, T. W. Davis, M. A. Burford, P. T. Orr, and B. A. Neilan, “Increased incidence of *Cylindrospermopsis raciborskii* in temperate zones – Is climate change responsible?,” *Water Res.*, vol. 46, no. 5, pp. 1408–1419, 2012, doi: <https://doi.org/10.1016/j.watres.2011.12.019>.
- [32] G. B. McGregor and L. D. Fabbro, “Dominance of *Cylindrospermopsis raciborskii* (Nostocales, Cyanoprokaryota) in Queensland tropical and subtropical reservoirs: Implications for monitoring and management,” *Lakes Reserv. Sci. Policy Manag. Sustain. Use*, vol. 5, no. 3, pp. 195–205, Sep. 2000, doi: 10.1046/j.1440-1770.2000.00115.x.
- [33] S. Everson, L. Fabbro, S. Kinnear, G. Eaglesham, and P. Wright, “Distribution of the cyanobacterial toxins cylindrospermopsin and deoxycylindrospermopsin in a stratified lake in north-eastern New South Wales, Australia,” *Mar. Freshw. Res.*, vol. 60, pp. 25–33, Jan. 2009, doi: 10.1071/MF08115.
- [34] D. J. Stirling and M. A. Quilliam, “First report of the cyanobacterial toxin cylindrospermopsin in New Zealand,” *Toxicon*, vol. 39, no. 8, pp. 1219–1222, 2001, doi: [https://doi.org/10.1016/S0041-0101\(00\)00266-X](https://doi.org/10.1016/S0041-0101(00)00266-X).
- [35] J. Fastner, R. Heinze, A. R. Humpage, U. Mischke, G. K. Eaglesham, and I. Chorus, “Cylindrospermopsin occurrence in two German lakes and preliminary assessment of toxicity and toxin production of *Cylindrospermopsis raciborskii* (Cyanobacteria) isolates,” *Toxicon*, vol. 42, no. 3, pp. 313–321, 2003, doi: [https://doi.org/10.1016/S0041-0101\(03\)00150-8](https://doi.org/10.1016/S0041-0101(03)00150-8).
- [36] C. Wiedner, J. Rucker, J. Fastner, I. Chorus, and B. Nixdorf, “Seasonal dynamics of

- cylindrospermopsin and cyanobacteria in two German lakes,” *Toxicon*, vol. 52, no. 6, pp. 677–686, 2008, doi: <https://doi.org/10.1016/j.toxicon.2008.07.017>.
- [37] L. Brient, M. Lengronne, M. Bormans, and J. Fastner, “First occurrence of cylindrospermopsin in freshwater in France,” *Environ. Toxicol.*, vol. 24, no. 4, pp. 415–420, Aug. 2009, doi: [10.1002/tox.20439](https://doi.org/10.1002/tox.20439).
- [38] V. Messineo *et al.*, “Cyanobacterial toxins in Italian freshwaters,” *Limnologica*, vol. 39, no. 2, pp. 95–106, 2009, doi: <https://doi.org/10.1016/j.limno.2008.09.001>.
- [39] L. Spoof *et al.*, “First observation of cylindrospermopsin in *Anabaena lapponica* isolated from the boreal environment (Finland),” *Environ. Toxicol.*, vol. 21, no. 6, pp. 552–560, Dec. 2006, doi: [10.1002/tox.20216](https://doi.org/10.1002/tox.20216).
- [40] M. Kokociński *et al.*, “*Aphanizomenon gracile* (Nostocales), a cylindrospermopsin-producing cyanobacterium in Polish lakes,” *Environ. Sci. Pollut. Res.*, vol. 20, no. 8, pp. 5243–5264, 2013, doi: [10.1007/s11356-012-1426-7](https://doi.org/10.1007/s11356-012-1426-7).
- [41] L. Bláhová, P. Babica, O. Adamovský, J. Kohoutek, B. Maršálek, and L. Bláha, “Analyses of cyanobacterial toxins (microcystins, cylindrospermopsin) in the reservoirs of the Czech Republic and evaluation of health risks,” *Environ. Chem. Lett.*, vol. 6, no. 4, pp. 223–227, 2008, doi: [10.1007/s10311-007-0126-x](https://doi.org/10.1007/s10311-007-0126-x).
- [42] A. Quesada *et al.*, “Toxicity of *Aphanizomenon ovalisporum* (Cyanobacteria) in a Spanish water reservoir,” *Eur. J. Phycol.*, vol. 41, no. 1, pp. 39–45, Feb. 2006, doi: [10.1080/09670260500480926](https://doi.org/10.1080/09670260500480926).
- [43] C. Moreira, R. Mendes, J. Azevedo, V. Vasconcelos, and A. Antunes, “First occurrence of cylindrospermopsin in Portugal: a contribution to its continuous global dispersal,” *Toxicon*, vol. 130, pp. 87–90, 2017, doi: <https://doi.org/10.1016/j.toxicon.2017.02.024>.
- [44] S. Gkelis and N. Zaoutsos, “Cyanotoxin occurrence and potentially toxin producing cyanobacteria in freshwaters of Greece: A multi-disciplinary approach,” *Toxicon*, vol. 78, pp. 1–9, 2014, doi: <https://doi.org/10.1016/j.toxicon.2013.11.010>.
- [45] R. Li *et al.*, “Isolation and identification of the cyanotoxin cylindrospermopsin and deoxy-cylindrospermopsin from a Thailand strain of *Cylindrospermopsis raciborskii* (Cyanobacteria),” *Toxicon*, vol. 39, no. 7, pp. 973–980, 2001, doi: [https://doi.org/10.1016/S0041-0101\(00\)00236-1](https://doi.org/10.1016/S0041-0101(00)00236-1).

- [46] K. Harada *et al.*, “Isolation of cylindrospermopsin from a cyanobacterium *Umezakia natans* and its screening method,” *Toxicon*, vol. 32, no. 1, pp. 73–84, 1994, doi: [https://doi.org/10.1016/0041-0101\(94\)90023-X](https://doi.org/10.1016/0041-0101(94)90023-X).
- [47] R. Li *et al.*, “FIRST REPORT OF THE CYANOTOXINS CYLINDROSPERMOPSIN AND DEOXYCYLINDROSPERMOPSIN FROM RAPHIDIOPSIS CURVATA (CYANOBACTERIA),” *J. Phycol.*, vol. 37, no. 6, pp. 1121–1126, Dec. 2001, doi: [10.1046/j.1529-8817.2001.01075.x](https://doi.org/10.1046/j.1529-8817.2001.01075.x).
- [48] L. Lei, L. Peng, X. Huang, and B.-P. Han, “Occurrence and dominance of *Cylindrospermopsis raciborskii* and dissolved cylindrospermopsin in urban reservoirs used for drinking water supply, South China,” *Environ. Monit. Assess.*, vol. 186, no. 5, pp. 3079–3090, 2014, doi: [10.1007/s10661-013-3602-8](https://doi.org/10.1007/s10661-013-3602-8).
- [49] J. P. Berry and O. Lind, “First evidence of ‘paralytic shellfish toxins’ and cylindrospermopsin in a Mexican freshwater system, Lago Catemaco, and apparent bioaccumulation of the toxins in ‘tegogolo’ snails (*Pomacea patula catemacensis*),” *Toxicon*, vol. 55, no. 5, pp. 930–938, 2010, doi: <https://doi.org/10.1016/j.toxicon.2009.07.035>.
- [50] C. D. Williams, M. T. Aubel, A. D. Chapman, and P. E. D’Aiuto, “Identification of cyanobacterial toxins in Florida’s freshwater systems,” *Lake Reserv. Manag.*, vol. 23, no. 2, pp. 144–152, Jun. 2007, doi: [10.1080/07438140709353917](https://doi.org/10.1080/07438140709353917).
- [51] L. Vidal and C. Kruk, “*Cylindrospermopsis raciborskii* (Cyanobacteria) extends its distribution to Latitude 34°53’S: Taxonomical and ecological features in Uruguayan eutrophic lakes,” *Panam J Aquat Sci*, vol. 3, Aug. 2008.
- [52] M. Pelaez *et al.*, “Sources and Occurrence of Cyanotoxins Worldwide BT - Xenobiotics in the Urban Water Cycle: Mass Flows, Environmental Processes, Mitigation and Treatment Strategies,” D. Fatta-Kassinos, K. Bester, and K. Kümmerer, Eds. Dordrecht: Springer Netherlands, 2010, pp. 101–127.
- [53] W. H. Organization, “Guidelines for safe recreational water environments. Volume 1, Coastal and fresh waters.” World Health Organization, Geneva PP - Geneva, [Online]. Available: <https://extranet.who.int/iris/restricted/handle/10665/42591>.
- [54] C. Svrcek and D. Smith, “Cyanobacteria toxins and the current state of knowledge on water treatment options: A review,” *J. Environ. Eng. Sci.*, vol. 3, pp. 155–185, May

2004, doi: 10.1139/s04-010.

- [55] W. H. Organization, *Guidelines for drinking-water quality: fourth edition incorporating first addendum*, 4th ed + 1. Geneva PP - Geneva: World Health Organization.
- [56] NHMRC, *Australian Drinking Water Guidelines 6: National Water Quality Management Strategy / National Health and Medical Research Council, National Resource Management Ministerial Council*. Commonwealth of Australia, 2011.
- [57] M. of Health, *Guidelines for Drinking-water Quality Management for New Zealand (3rd edn)*. Wellington: Ministry of Health, 2017.
- [58] AFSSA, “NoEvaluation des risques liés à la présence de cyanobactéries et de leurs toxines dans les eaux destinées à l’alimentation, à la baignade et autres activités récréatives,” 2006.
- [59] EPA, “Drinking Water Health Advisory for the Cyanobacterial Toxin Cylindrospermopsin,” Washington, DC, 2015.
- [60] I. R. Falconer and A. R. Humpage, “Health risk assessment of cyanobacterial (blue-green algal) toxins in drinking water,” *Int. J. Environ. Res. Public Health*, vol. 2, no. 1, pp. 43–50, Apr. 2005, doi: 10.3390/ijerph2005010043.
- [61] D. Farrer, M. Counter, R. Hillwig, and C. Cude, “Health-Based Cyanotoxin Guideline Values Allow for Cyanotoxin-Based Monitoring and Efficient Public Health Response to Cyanobacterial Blooms,” *Toxins*, vol. 7, no. 2. 2015, doi: 10.3390/toxins7020457.
- [62] M. B. Dixon, C. Falconet, L. Ho, C. W. K. Chow, B. K. O’Neill, and G. Newcombe, “Removal of cyanobacterial metabolites by nanofiltration from two treated waters,” *J. Hazard. Mater.*, vol. 188, no. 1, pp. 288–295, 2011, doi: <https://doi.org/10.1016/j.jhazmat.2011.01.111>.
- [63] S. J. Hoeger, G. Shaw, B. C. Hitzfeld, and D. R. Dietrich, “Occurrence and elimination of cyanobacterial toxins in two Australian drinking water treatment plants,” *Toxicon*, vol. 43, no. 6, pp. 639–649, 2004, doi: <https://doi.org/10.1016/j.toxicon.2004.02.019>.
- [64] E. Rodríguez, A. Sordo, J. S. Metcalf, and J. L. Acero, “Kinetics of the oxidation of cylindrospermopsin and anatoxin-a with chlorine, monochloramine and permanganate,” *Water Res.*, vol. 41, no. 9, pp. 2048–2056, 2007, doi: <https://doi.org/10.1016/j.watres.2007.01.033>.

- [65] R. Andreozzi, V. Caprio, A. Insola, and R. Marotta, "Advanced oxidation processes (AOP) for water purification and recovery," *Catal. Today*, vol. 53, no. 1, pp. 51–59, 1999, doi: [https://doi.org/10.1016/S0920-5861\(99\)00102-9](https://doi.org/10.1016/S0920-5861(99)00102-9).
- [66] J. L. WANG and L. E. J. I. N. XU, "Advanced Oxidation Processes for Wastewater Treatment: Formation of Hydroxyl Radical and Application," *Crit. Rev. Environ. Sci. Technol.*, vol. 42, no. 3, pp. 251–325, Feb. 2012, doi: 10.1080/10643389.2010.507698.
- [67] J. Wang and J. Wang, "Application of radiation technology to sewage sludge processing: A review," *J. Hazard. Mater.*, vol. 143, no. 1, pp. 2–7, 2007, doi: <https://doi.org/10.1016/j.jhazmat.2007.01.027>.
- [68] L. Wojnárovits and E. Takács, "Irradiation treatment of azo dye containing wastewater: An overview," *Radiat. Phys. Chem.*, vol. 77, no. 3, pp. 225–244, 2008, doi: <https://doi.org/10.1016/j.radphyschem.2007.05.003>.
- [69] G. V Buxton, C. L. Greenstock, W. P. Helman, and A. B. Ross, "Critical Review of rate constants for reactions of hydrated electrons, hydrogen atoms and hydroxyl radicals ($\cdot\text{OH}/\cdot\text{O}^-$ in Aqueous Solution)," *J. Phys. Chem. Ref. Data*, vol. 17, no. 2, pp. 513–886, Apr. 1988, doi: 10.1063/1.555805.
- [70] K. Azrague *et al.*, "Hydrogen peroxide evolution during V-UV photolysis of water," *Photochem. Photobiol. Sci.*, vol. 4, no. 5, pp. 406–408, 2005, doi: 10.1039/B500162E.
- [71] T. Garoma and M. D. Gurol, "Degradation of tert-butyl alcohol in dilute aqueous solution by an O₃/UV process," *Environ. Sci. Technol.*, vol. 38, no. 19, pp. 5246–5252, Oct. 2004, doi: 10.1021/es0353210.
- [72] N. Azbar, T. Yonar, and K. Kestioglu, "Comparison of various advanced oxidation processes and chemical treatment methods for COD and color removal from a polyester and acetate fiber dyeing effluent," *Chemosphere*, vol. 55, no. 1, pp. 35–43, 2004, doi: <https://doi.org/10.1016/j.chemosphere.2003.10.046>.
- [73] V. Sharma *et al.*, *Destruction of microcystins by conventional and advanced oxidation processes: A review*, vol. 91. 2012.
- [74] D. S. Bhatkhande, V. G. Pangarkar, and A. A. C. M. Beenackers, "Photocatalytic degradation for environmental applications – a review," *J. Chem. Technol. Biotechnol.*, vol. 77, no. 1, pp. 102–116, Jan. 2002, doi: 10.1002/jctb.532.
- [75] H. Al-Ekabi and N. Serpone, "Kinetics studies in heterogeneous photocatalysis. I.

- Photocatalytic degradation of chlorinated phenols in aerated aqueous solutions over titania supported on a glass matrix,” *J. Phys. Chem.*, vol. 92, no. 20, pp. 5726–5731, Oct. 1988, doi: 10.1021/j100331a036.
- [76] W. G. BARB, J. H. BAXENDALE, P. GEORGE, and K. R. HARGRAVE, “Reactions of Ferrous and Ferric Ions with Hydrogen Peroxide,” *Nature*, vol. 163, no. 4148, pp. 692–694, 1949, doi: 10.1038/163692a0.
- [77] S.-M. Kim and A. Vogelpohl, “Degradation of Organic Pollutants by the Photo-Fenton-Process,” *Chem. Eng. Technol.*, vol. 21, no. 2, pp. 187–191, Feb. 1998, doi: 10.1002/(SICI)1521-4125(199802)21:2<187::AID-CEAT187>3.0.CO;2-H.
- [78] J. Hoigné and H. Bader, “Rate constants of reactions of ozone with organic and inorganic compounds in water—I: Non-dissociating organic compounds,” *Water Res.*, vol. 17, no. 2, pp. 173–183, 1983, doi: [https://doi.org/10.1016/0043-1354\(83\)90098-2](https://doi.org/10.1016/0043-1354(83)90098-2).
- [79] T. E. Agustina, H. M. Ang, and V. K. Vareek, “A review of synergistic effect of photocatalysis and ozonation on wastewater treatment,” *J. Photochem. Photobiol. C Photochem. Rev.*, vol. 6, no. 4, pp. 264–273, 2005, doi: <https://doi.org/10.1016/j.jphotochemrev.2005.12.003>.
- [80] S. Yan *et al.*, “Ozonation of Cyndrospermopsin (Cyanotoxin): Degradation Mechanisms and Cytotoxicity Assessments,” *Environ. Sci. Technol.*, vol. 50, no. 3, pp. 1437–1446, Feb. 2016, doi: 10.1021/acs.est.5b04540.
- [81] C.-C. Wu, W.-J. Huang, and B.-H. Ji, “Degradation of cyanotoxin cyndrospermopsin by TiO₂-assisted ozonation in water,” *J. Environ. Sci. Heal. Part A*, vol. 50, no. 11, pp. 1116–1126, Sep. 2015, doi: 10.1080/10934529.2015.1047664.
- [82] L. Chen, C. Zhao, D. D. Dionysiou, and K. E. O’Shea, “TiO₂ photocatalytic degradation and detoxification of cyndrospermopsin,” *J. Photochem. Photobiol. A Chem.*, vol. 307–308, pp. 115–122, 2015, doi: <https://doi.org/10.1016/j.jphotochem.2015.03.013>.
- [83] T. Fotiou, T. Triantis, T. Kaloudis, and A. Hiskia, “Photocatalytic degradation of cyndrospermopsin under UV-A, solar and visible light using TiO₂. Mineralization and intermediate products,” *Chemosphere*, vol. 119, pp. S89–S94, 2015, doi: <https://doi.org/10.1016/j.chemosphere.2014.04.045>.
- [84] G. Zhang *et al.*, “Degradation of cyndrospermopsin by using polymorphic titanium

- dioxide under UV–Vis irradiation,” *Catal. Today*, vol. 224, pp. 49–55, 2014, doi: <https://doi.org/10.1016/j.cattod.2013.10.072>.
- [85] W. Song, S. Yan, W. J. Cooper, D. D. Dionysiou, and K. E. O’Shea, “Hydroxyl Radical Oxidation of Cyindrospermopsin (Cyanobacterial Toxin) and Its Role in the Photochemical Transformation,” *Environ. Sci. Technol.*, vol. 46, no. 22, pp. 12608–12615, Nov. 2012, doi: 10.1021/es302458h.
- [86] P.-J. Senogles, J. A. Scott, G. Shaw, and H. Stratton, “Photocatalytic Degradation of the Cyanotoxin Cyindrospermopsin, using Titanium Dioxide and UV Irradiation,” *Water Res.*, vol. 35, no. 5, pp. 1245–1255, 2001, doi: [https://doi.org/10.1016/S0043-1354\(00\)00372-9](https://doi.org/10.1016/S0043-1354(00)00372-9).
- [87] B. Bakheet, M. A. Islam, J. Beardall, X. Zhang, and D. McCarthy, “Electrochemical inactivation of *Cyindrospermopsis raciborskii* and removal of the cyanotoxin cyindrospermopsin,” *J. Hazard. Mater.*, vol. 344, pp. 241–248, 2018, doi: <https://doi.org/10.1016/j.jhazmat.2017.10.024>.
- [88] X. He, G. Zhang, A. A. de la Cruz, K. E. O’Shea, and D. D. Dionysiou, “Degradation Mechanism of Cyanobacterial Toxin Cyindrospermopsin by Hydroxyl Radicals in Homogeneous UV/H₂O₂ Process,” *Environ. Sci. Technol.*, vol. 48, no. 8, pp. 4495–4504, Apr. 2014, doi: 10.1021/es403732s.
- [89] S. Pilli, P. Bhunia, S. Yan, R. J. LeBlanc, R. D. Tyagi, and R. Y. Surampalli, “Ultrasonic pretreatment of sludge: A review,” *Ultrason. Sonochem.*, vol. 18, no. 1, pp. 1–18, 2011, doi: <https://doi.org/10.1016/j.ultsonch.2010.02.014>.
- [90] D. Chen, S. Sharma, and A. Mudhoo, *Handbook on Applications of Ultrasound: Sonochemistry for Sustainability*. 2011.
- [91] T. Y. Wu, N. Guo, C. Y. Teh, and J. X. W. Hay, “Theory and Fundamentals of Ultrasound BT - Advances in Ultrasound Technology for Environmental Remediation,” T. Y. Wu, N. Guo, C. Y. Teh, and J. X. W. Hay, Eds. Dordrecht: Springer Netherlands, 2013, pp. 5–12.
- [92] A. Henglein, “Sonochemistry: Historical developments and modern aspects,” *Ultrasonics*, vol. 25, no. 1, pp. 6–16, 1987, doi: [https://doi.org/10.1016/0041-624X\(87\)90003-5](https://doi.org/10.1016/0041-624X(87)90003-5).
- [93] H. Nomura and S. Koda, “Chapter 1 - What Is Sonochemistry?,” F. Grieser, P.-K.

- Choi, N. Enomoto, H. Harada, K. Okitsu, and K. B. T.-S. and the A. B. Yasui, Eds. Amsterdam: Elsevier, 2015, pp. 1–9.
- [94] R. A. Torres-Palma and E. A. Serna-Galvis, “Chapter 7 - Sonolysis,” S. C. Ameta and R. B. T.-A. O. P. for W. W. T. Ameta, Eds. Academic Press, 2018, pp. 177–213.
- [95] P. Riesz, T. Kondo, and C. M. Krishna, “Sonochemistry of volatile and non-volatile solutes in aqueous solutions: e.p.r. and spin trapping studies,” *Ultrasonics*, vol. 28, no. 5, pp. 295–303, 1990, doi: [https://doi.org/10.1016/0041-624X\(90\)90035-M](https://doi.org/10.1016/0041-624X(90)90035-M).
- [96] V. Mišík and P. Riesz, “EPR study of free radicals induced by ultrasound in organic liquids II. Probing the temperatures of cavitation regions,” *Ultrason. Sonochem.*, vol. 3, no. 1, pp. 25–37, 1996, doi: [https://doi.org/10.1016/1350-4177\(95\)00036-4](https://doi.org/10.1016/1350-4177(95)00036-4).
- [97] A. Henglein, “Chemical Effects of Continuous and Pulsed Ultrasound in Aqueous Solutions,” *Ultrason. Sonochem.*, vol. 2, Dec. 1995, doi: [10.1016/1350-4177\(95\)00022-X](https://doi.org/10.1016/1350-4177(95)00022-X).
- [98] C. Sehgal, T. J. Yu, R. G. Sutherland, and R. E. Verrall, “Use of 2,2-diphenyl-1-picrylhydrazyl to investigate the chemical behavior of free radicals induced by ultrasonic cavitation,” *J. Phys. Chem.*, vol. 86, no. 15, pp. 2982–2986, Jul. 1982, doi: [10.1021/j100212a034](https://doi.org/10.1021/j100212a034).
- [99] E. Fuchs and H. Heusinger, “Sonolysis and radiolysis of glyceraldehyde in deaerated aqueous solution,” *Ultrason. Sonochem.*, vol. 2, no. 2, pp. S105–S109, 1995, doi: [https://doi.org/10.1016/1350-4177\(94\)00014-J](https://doi.org/10.1016/1350-4177(94)00014-J).
- [100] W. Song, T. Teshiba, K. Rein, and K. E. O’Shea, “Ultrasonically Induced Degradation and Detoxification of Microcystin-LR (Cyanobacterial Toxin),” *Environ. Sci. Technol.*, vol. 39, no. 16, pp. 6300–6305, Aug. 2005, doi: [10.1021/es048350z](https://doi.org/10.1021/es048350z).
- [101] E. A. Neppiras, “Acoustic cavitation,” *Phys. Rep.*, vol. 61, no. 3, pp. 159–251, 1980, doi: [https://doi.org/10.1016/0370-1573\(80\)90115-5](https://doi.org/10.1016/0370-1573(80)90115-5).
- [102] G. Cum, R. Gallo, A. Spadaro, and G. Galli, “Effect of static pressure on the ultrasonic activation of chemical reactions. Selective oxidation at benzylic carbon in the liquid phase,” *J. Chem. Soc. Perkin Trans. 2*, no. 3, pp. 375–383, 1988, doi: [10.1039/P29880000375](https://doi.org/10.1039/P29880000375).
- [103] G. Cum, R. Gallo, A. Spadaro, and G. Galli, “Temperature effects in ultrasonically activated chemical reactions,” *Nuovo Cim. D*, vol. 12, no. 10, pp. 1423–1430, 1990,

doi: 10.1007/BF02452109.

- [104] M. Gutierrez and A. Henglein, "Chemical action of pulsed ultrasound: observation of an unprecedented intensity effect.," *J. Phys. Chem.*, vol. 94, no. 9, pp. 3625–3628, May 1990, doi: 10.1021/j100372a048.
- [105] G. O. H. Whillock and B. F. Harvey, "Ultrasonically enhanced corrosion of 304L stainless steel II: The effect of frequency, acoustic power and horn to specimen distance," *Ultrason. Sonochem.*, vol. 4, no. 1, pp. 33–38, 1997, doi: [https://doi.org/10.1016/S1350-4177\(96\)00015-6](https://doi.org/10.1016/S1350-4177(96)00015-6).
- [106] M. H. Entezari, P. Kruus, and R. Otson, "The effect of frequency on sonochemical reactions III: dissociation of carbon disulfide," *Ultrason. Sonochem.*, vol. 4, no. 1, pp. 49–54, 1997, doi: [https://doi.org/10.1016/S1350-4177\(96\)00016-8](https://doi.org/10.1016/S1350-4177(96)00016-8).
- [107] C. Petrier, A. Jeunet, J. L. Luche, and G. Reverdy, "Unexpected frequency effects on the rate of oxidative processes induced by ultrasound," *J. Am. Chem. Soc.*, vol. 114, no. 8, pp. 3148–3150, Apr. 1992, doi: 10.1021/ja00034a077.
- [108] S. Merouani, O. Hamdaoui, Y. Rezgui, and M. Guemini, "Effects of ultrasound frequency and acoustic amplitude on the size of sonochemically active bubbles – Theoretical study," *Ultrason. Sonochem.*, vol. 20, no. 3, pp. 815–819, 2013, doi: <https://doi.org/10.1016/j.ultsonch.2012.10.015>.
- [109] L. A. Crum, "Comments on the evolving field of sonochemistry by a cavitation physicist," *Ultrason. Sonochem.*, vol. 2, no. 2, pp. S147–S152, 1995, doi: [https://doi.org/10.1016/1350-4177\(95\)00018-2](https://doi.org/10.1016/1350-4177(95)00018-2).
- [110] L. H. Thompson and L. K. Doraiswamy, "Sonochemistry: Science and Engineering," *Ind. Eng. Chem. Res.*, vol. 38, no. 4, pp. 1215–1249, Apr. 1999, doi: 10.1021/ie9804172.
- [111] D. V. P. Naidu, R. Rajan, R. Kumar, K. S. Gandhi, V. H. Arakeri, and S. Chandrasekaran, "Modelling of a batch sonochemical reactor," *Chem. Eng. Sci.*, vol. 49, no. 6, pp. 877–888, 1994, doi: [https://doi.org/10.1016/0009-2509\(94\)80024-3](https://doi.org/10.1016/0009-2509(94)80024-3).
- [112] M. Ibsi and B. Brown, "Variation of the Relative Intensity of Cavitation with Temperature," *J. Acoust. Soc. Am.*, vol. 41, no. 3, pp. 568–572, Mar. 1967, doi: 10.1121/1.1910381.
- [113] C. M. Sehgal and S. Y. Wang, "Threshold intensities and kinetics of sonoreaction of

- thymine in aqueous solutions at low ultrasonic intensities,” *J. Am. Chem. Soc.*, vol. 103, no. 22, pp. 6606–6611, Nov. 1981, doi: 10.1021/ja00412a013.
- [114] K. J. Moulton, S. Koritala, and E. N. Frankel, “Ultrasonic hydrogenation of soybean oil,” *J. Am. Oil Chem. Soc.*, vol. 60, no. 7, pp. 1257–1258, 1983, doi: 10.1007/BF02702094.
- [115] K. J. Moulton, S. Koritala, K. Warner, and E. N. Frankel, “Continuous ultrasonic hydrogenation of soybean oil. II. Operating conditions and oil quality,” *J. Am. Oil Chem. Soc.*, vol. 64, no. 4, pp. 542–547, 1987, doi: 10.1007/BF02636391.
- [116] T. Leong, S. Wu, S. Kentish, and M. Ashokkumar, “Growth of Bubbles by Rectified Diffusion in Aqueous Surfactant Solutions,” *J. Phys. Chem. C*, vol. 114, no. 47, pp. 20141–20145, Dec. 2010, doi: 10.1021/jp107731j.
- [117] J. P. Lorimer and T. J. Mason, “Sonochemistry. Part 1—The physical aspects,” *Chem. Soc. Rev.*, vol. 16, no. 0, pp. 239–274, 1987, doi: 10.1039/CS9871600239.
- [118] P. Sathishkumar, R. V. Mangalaraja, and S. Anandan, “Review on the recent improvements in sonochemical and combined sonochemical oxidation processes – A powerful tool for destruction of environmental contaminants,” *Renew. Sustain. Energy Rev.*, vol. 55, pp. 426–454, 2016, doi: <https://doi.org/10.1016/j.rser.2015.10.139>.
- [119] R. J. Wood, J. Lee, and M. J. Bussemaker, “A parametric review of sonochemistry: Control and augmentation of sonochemical activity in aqueous solutions,” *Ultrason. Sonochem.*, vol. 38, pp. 351–370, 2017, doi: <https://doi.org/10.1016/j.ultsonch.2017.03.030>.
- [120] K. Yasui, T. Tuziuti, and Y. Iida, “Dependence of the characteristics of bubbles on types of sonochemical reactors,” *Ultrason. Sonochem.*, vol. 12, no. 1, pp. 43–51, 2005, doi: <https://doi.org/10.1016/j.ultsonch.2004.06.003>.
- [121] P. Anastas and N. Eghbali, “Green Chemistry: Principles and Practice,” *Chem. Soc. Rev.*, vol. 39, no. 1, pp. 301–312, 2010, doi: 10.1039/B918763B.
- [122] M. Kida, S. Ziembowicz, and P. Koszelnik, “Removal of organochlorine pesticides (OCPs) from aqueous solutions using hydrogen peroxide, ultrasonic waves, and a hybrid process,” *Sep. Purif. Technol.*, vol. 192, pp. 457–464, 2018, doi: <https://doi.org/10.1016/j.seppur.2017.10.046>.
- [123] A. Hiskia, M. Ecke, A. Troupis, A. Kokorakis, H. Hennig, and E. Papaconstantinou,

- “Sonolytic, Photolytic, and Photocatalytic Decomposition of Atrazine in the Presence of Polyoxometalates,” *Environ. Sci. Technol.*, vol. 35, no. 11, pp. 2358–2364, Jun. 2001, doi: 10.1021/es000212w.
- [124] A. Lianou, Z. Frontistis, E. Chatzisyneon, M. Antonopoulou, I. Konstantinou, and D. Mantzavinos, “Sonochemical oxidation of piroxicam drug: effect of key operating parameters and degradation pathways,” *J. Chem. Technol. Biotechnol.*, vol. 93, no. 1, pp. 28–34, Jan. 2018, doi: 10.1002/jctb.5346.
- [125] R. Xiao, Z. He, D. Diaz-Rivera, G. Y. Pee, and L. K. Weavers, “Sonochemical degradation of ciprofloxacin and ibuprofen in the presence of matrix organic compounds,” *Ultrason. Sonochem.*, vol. 21, no. 1, pp. 428–435, 2014, doi: <https://doi.org/10.1016/j.ultsonch.2013.06.012>.
- [126] E. A. Serna-Galvis *et al.*, “Sonochemical degradation of antibiotics from representative classes-Considerations on structural effects, initial transformation products, antimicrobial activity and matrix,” *Ultrason. Sonochem.*, vol. 50, pp. 157–165, 2019, doi: <https://doi.org/10.1016/j.ultsonch.2018.09.012>.
- [127] M. P. Rayaroth, U. K. Aravind, and C. T. Aravindakumar, “Degradation of pharmaceuticals by ultrasound-based advanced oxidation process,” *Environ. Chem. Lett.*, vol. 14, no. 3, pp. 259–290, 2016, doi: 10.1007/s10311-016-0568-0.
- [128] H. Fu, R. P. S. Suri, R. F. Chimchirian, E. Helmig, and R. Constable, “Ultrasound-Induced Destruction of Low Levels of Estrogen Hormones in Aqueous Solutions,” *Environ. Sci. Technol.*, vol. 41, no. 16, pp. 5869–5874, Aug. 2007, doi: 10.1021/es0703372.
- [129] P. Rajasekhar, L. Fan, T. Nguyen, and F. A. Roddick, “A review of the use of sonication to control cyanobacterial blooms,” *Water Res.*, vol. 46, no. 14, pp. 4319–4329, 2012, doi: 10.1016/j.watres.2012.05.054.
- [130] P. Li, Y. Song, S. Yu, and H.-D. Park, “The effect of hydrodynamic cavitation on *Microcystis aeruginosa*: Physical and chemical factors,” *Chemosphere*, vol. 136, pp. 245–251, 2015, doi: <https://doi.org/10.1016/j.chemosphere.2015.05.017>.
- [131] J. Park, J. Church, Y. Son, K.-T. Kim, and W. H. Lee, “Recent advances in ultrasonic treatment: Challenges and field applications for controlling harmful algal blooms (HABs),” *Ultrason. Sonochem.*, vol. 38, pp. 326–334, 2017, doi:

<https://doi.org/10.1016/j.ultsonch.2017.03.003>.

- [132] M. Lüring, D. Meng, and J. E. Faassen, “Effects of Hydrogen Peroxide and Ultrasound on Biomass Reduction and Toxin Release in the Cyanobacterium, *Microcystis aeruginosa*,” *Toxins*, vol. 6, no. 12, 2014, doi: 10.3390/toxins6123260.
- [133] W. Song, A. A. de la Cruz, K. Rein, and K. E. O’Shea, “Ultrasonically Induced Degradation of Microcystin-LR and -RR: Identification of Products, Effect of pH, Formation and Destruction of Peroxides,” *Environ. Sci. Technol.*, vol. 40, no. 12, pp. 3941–3946, Jun. 2006, doi: 10.1021/es0521730.
- [134] W. Song and K. E. O’Shea, “Ultrasonically induced degradation of 2-methylisoborneol and geosmin,” *Water Res.*, vol. 41, no. 12, pp. 2672–2678, 2007, doi: <https://doi.org/10.1016/j.watres.2007.02.041>.
- [135] J. W. Boag, E. Epp, E. M. Fielden, and R. P. Parker, “3. Chemical Dosimetry,” *J. Int. Comm. Radiat. Units Meas.*, vol. os18, no. 1, pp. 14–21, Apr. 2016, doi: 10.1093/jicru/os18.1.14.
- [136] Y. Iida, K. Yasui, T. Tuziuti, and M. Sivakumar, “Sonochemistry and its dosimetry,” *Microchem. J.*, vol. 80, no. 2, pp. 159–164, 2005, doi: <https://doi.org/10.1016/j.microc.2004.07.016>.
- [137] M. Náfrádi *et al.*, “Application of coumarin and coumarin-3-carboxylic acid for the determination of hydroxyl radicals during different advanced oxidation processes,” *Radiat. Phys. Chem.*, vol. 170, p. 108610, 2020, doi: <https://doi.org/10.1016/j.radphyschem.2019.108610>.
- [138] K. Hirano and T. Kobayashi, “Coumarin fluorometry to quantitatively detectable OH radicals in ultrasound aqueous medium,” *Ultrason. Sonochem.*, vol. 30, pp. 18–27, 2016, doi: <https://doi.org/10.1016/j.ultsonch.2015.11.020>.
- [139] H. Czili and A. Horváth, “Applicability of coumarin for detecting and measuring hydroxyl radicals generated by photoexcitation of TiO₂ nanoparticles,” *Appl. Catal. B Environ.*, vol. 81, pp. 295–302, Jun. 2008, doi: 10.1016/j.apcatb.2008.01.001.
- [140] V. Leandri, J. M. Gardner, and M. Jonsson, “Coumarin as a Quantitative Probe for Hydroxyl Radical Formation in Heterogeneous Photocatalysis,” *J. Phys. Chem. C*, vol. 123, no. 11, pp. 6667–6674, Mar. 2019, doi: 10.1021/acs.jpcc.9b00337.
- [141] G. Louit *et al.*, “The reaction of coumarin with the OH radical revisited: Hydroxylation

- product analysis determined by fluorescence and chromatography,” *Radiat. Phys. Chem.*, vol. 72, pp. 119–124, Feb. 2005, doi: 10.1016/j.radphyschem.2004.09.007.
- [142] A. K. Jana and S. N. Chatterjee, “Estimation of hydroxyl free radicals produced by ultrasound in Fricke solution used as a chemical dosimeter,” *Ultrason. Sonochem.*, vol. 2, no. 2, pp. S87–S91, 1995, doi: [https://doi.org/10.1016/1350-4177\(95\)00025-2](https://doi.org/10.1016/1350-4177(95)00025-2).
- [143] X. Fang, G. Mark, and C. von Sonntag, “OH radical formation by ultrasound in aqueous solutions Part I: the chemistry underlying the terephthalate dosimeter,” *Ultrason. Sonochem.*, vol. 3, no. 1, pp. 57–63, 1996, doi: [https://doi.org/10.1016/1350-4177\(95\)00032-1](https://doi.org/10.1016/1350-4177(95)00032-1).
- [144] R. W. Matthews, “The Radiation Chemistry of the Terephthalate Dosimeter,” *Radiat. Res.*, vol. 83, no. 1, pp. 27–41, Jan. 1980, doi: 10.2307/3575256.
- [145] D. A. Skoog, S. R. Crouch, and F. J. Holler, *Principles of instrumental analysis*. Belmont, CA: Thomson Brooks/Cole, 2007.
- [146] P. Joseph C. Arsenault; Patrick D. McDonald, *Beginners Guide to Liquid Chromatography*. Waters Corporation, 2007.
- [147] D. A. Skoog, D. M. West, F. J. Holler, and S. R. Crouch, *Fundamentals of analytical chemistry*. 2014.
- [148] U. D. Neue, “CHROMATOGRAPHY: LIQUID | Mechanisms: Reversed Phases,” I. D. B. T.-E. of S. S. Wilson, Ed. Oxford: Academic Press, 2007, pp. 1–7.
- [149] V. R. Meyer, *Practical high-performance liquid chromatography*. United States: John Wiley and Sons, New York, NY, 1988.
- [150] Waters Corporation, “2998 Photodiode Array Detector Operator’s guide,” .
- [151] “Mass Spectrometry,” *Liquid Chromatography – Mass Spectrometry: An Introduction*. pp. 33–74, Feb. 14, 2003, doi: [doi:10.1002/0470867299.ch3](https://doi.org/10.1002/0470867299.ch3).
- [152] M. Welker, H. Bickel, and J. Fastner, “HPLC-PDA detection of cylindrospermopsin—opportunities and limits,” *Water Res.*, vol. 36, no. 18, pp. 4659–4663, 2002, doi: [https://doi.org/10.1016/S0043-1354\(02\)00194-X](https://doi.org/10.1016/S0043-1354(02)00194-X).
- [153] R. Guzmán-Guillén, A. I. Prieto, A. G. González, M. E. Soria-Díaz, and A. M. Cameán, “Cylindrospermopsin determination in water by LC-MS/MS: Optimization and validation of the method and application to real samples,” *Environ. Toxicol.*

- Chem.*, vol. 31, no. 10, pp. 2233–2238, Oct. 2012, doi: 10.1002/etc.1954.
- [154] J. S. Metcalf, K. A. Beattie, M. L. Saker, and G. A. Codd, “Effects of organic solvents on the high performance liquid chromatographic analysis of the cyanobacterial toxin cylindrospermopsin and its recovery from environmental eutrophic waters by solid phase extraction,” *FEMS Microbiol. Lett.*, vol. 216, no. 2, pp. 159–164, Nov. 2002, doi: 10.1111/j.1574-6968.2002.tb11430.x.
- [155] G. K. Eaglesham *et al.*, “Use of HPLC-MS/MS to monitor cylindrospermopsin, a blue–green algal toxin, for public health purposes,” *Environ. Toxicol.*, vol. 14, no. 1, pp. 151–154, Feb. 1999, doi: 10.1002/(SICI)1522-7278(199902)14:1<151::AID-TOX19>3.0.CO;2-D.
- [156] S. Bogialli, M. Bruno, R. Curini, A. Di Corcia, C. Fanali, and A. Laganà, “Monitoring Algal Toxins in Lake Water by Liquid Chromatography Tandem Mass Spectrometry,” *Environ. Sci. Technol.*, vol. 40, no. 9, pp. 2917–2923, May 2006, doi: 10.1021/es052546x.
- [157] S.-K. Zervou, C. Christophoridis, T. Kaloudis, T. M. Triantis, and A. Hiskia, “New SPE-LC-MS/MS method for simultaneous determination of multi-class cyanobacterial and algal toxins,” *J. Hazard. Mater.*, vol. 323, pp. 56–66, 2017, doi: <https://doi.org/10.1016/j.jhazmat.2016.07.020>.
- [158] C. Dell’Aversano, G. K. Eaglesham, and M. A. Quilliam, “Analysis of cyanobacterial toxins by hydrophilic interaction liquid chromatography–mass spectrometry,” *J. Chromatogr. A*, vol. 1028, no. 1, pp. 155–164, 2004, doi: <https://doi.org/10.1016/j.chroma.2003.11.083>.
- [159] H. Ferkous, S. Merouani, O. Hamdaoui, Y. Rezgui, and M. Guemini, “Comprehensive experimental and numerical investigations of the effect of frequency and acoustic intensity on the sonolytic degradation of naphthol blue black in water,” *Ultrason. Sonochem.*, vol. 26, pp. 30–39, 2015, doi: <https://doi.org/10.1016/j.ultsonch.2015.02.004>.
- [160] F. Méndez-Arriaga, R. A. Torres-Palma, C. Pétrier, S. Esplugas, J. Gimenez, and C. Pulgarin, “Ultrasonic treatment of water contaminated with ibuprofen,” *Water Res.*, vol. 42, no. 16, pp. 4243–4248, 2008, doi: <https://doi.org/10.1016/j.watres.2008.05.033>.

- [161] Z. Wei, R. Spinney, R. Ke, Z. Yang, and R. Xiao, "Effect of pH on the sonochemical degradation of organic pollutants," *Environ. Chem. Lett.*, vol. 14, no. 2, pp. 163–182, 2016, doi: 10.1007/s10311-016-0557-3.
- [162] E. Villaroel, J. Silva-Agredo, C. Petrier, G. Taborda, and R. A. Torres-Palma, "Ultrasonic degradation of acetaminophen in water: Effect of sonochemical parameters and water matrix," *Ultrason. Sonochem.*, vol. 21, no. 5, pp. 1763–1769, 2014, doi: <https://doi.org/10.1016/j.ultsonch.2014.04.002>.
- [163] C. Pétrier, R. Torres-Palma, E. Combet, G. Sarantakos, S. Baup, and C. Pulgarin, "Enhanced sonochemical degradation of bisphenol-A by bicarbonate ions," *Ultrason. Sonochem.*, vol. 17, no. 1, pp. 111–115, 2010, doi: <https://doi.org/10.1016/j.ultsonch.2009.05.010>.
- [164] J. V Goldstone, M. J. Pullin, S. Bertilsson, and B. M. Voelker, "Reactions of Hydroxyl Radical with Humic Substances: Bleaching, Mineralization, and Production of Bioavailable Carbon Substrates," *Environ. Sci. Technol.*, vol. 36, no. 3, pp. 364–372, Feb. 2002, doi: 10.1021/es0109646.
- [165] G. Mark *et al.*, "OH-radical formation by ultrasound in aqueous solution – Part II: Terephthalate and Fricke dosimetry and the influence of various conditions on the sonolytic yield," *Ultrason. Sonochem.*, vol. 5, no. 2, pp. 41–52, 1998, doi: [https://doi.org/10.1016/S1350-4177\(98\)00012-1](https://doi.org/10.1016/S1350-4177(98)00012-1).
- [166] A. Tauber, G. Mark, H.-P. Schuchmann, and C. von Sonntag, "Sonolysis of tert-butyl alcohol in aqueous solution," *J. Chem. Soc. Perkin Trans. 2*, no. 6, pp. 1129–1136, 1999, doi: 10.1039/A901085H.